



**Guilherme Alexandre dos Santos Espadanal Ramos**

Bachelor of Science in Biomedical Engineering

## **EMG Signal Processing in Amateur and Professional Sports with Performance Evaluation and Injury Prevention**

Dissertation submitted in partial fulfillment  
of the requirements for the degree of

Master of Science in  
**Biomedical Engineering**

Adviser: Prof. Dr. Hugo Filipe Gamboa, Auxiliar Professor,  
Faculty of Sciences and Technology,  
NOVA University of Lisbon

Co-adviser: Prof. Dr. Carla Maria Quintão, Auxiliar Professor,  
Faculty of Sciences and Technology,  
NOVA University of Lisbon

Examination Committee

Chairperson: Prof. Dr. Célia Maria Henriques  
Rapporteur: Prof. Dr. Pedro Manuel Vieira  
Members: Prof. Dr. Hugo Filipe Gamboa  
Prof. Dr. Carla Maria Quintão



FACULDADE DE  
CIÊNCIAS E TECNOLOGIA  
UNIVERSIDADE NOVA DE LISBOA

**March, 2018**



## **EMG Signal Processing in Amateur and Professional Sports with Performance Evaluation and Injury Prevention**

Copyright © Guilherme Alexandre dos Santos Espadanal Ramos, Faculdade de Ciências e Tecnologia, Universidade NOVA de Lisboa.

A Faculdade de Ciências e Tecnologia e a Universidade NOVA de Lisboa têm o direito, perpétuo e sem limites geográficos, de arquivar e publicar esta dissertação através de exemplares impressos reproduzidos em papel ou de forma digital, ou por qualquer outro meio conhecido ou que venha a ser inventado, e de a divulgar através de repositórios científicos e de admitir a sua cópia e distribuição com objetivos educacionais ou de investigação, não comerciais, desde que seja dado crédito ao autor e editor.





*To my Grandfather and my Parents,  
who accompanied me on this  
and in so many other adventures*



## Acknowledgements

Curiosities lie in most, or even all, individual recollections and are, very often, what allow us to keep our memories alive.

One curiosity in this document can be found in this very section, in which the first words to be seen by the reader were in fact the last ones to be written.

An acknowledgement is a simple gesture, but, an extremely important one, considering that it represents a recognition of the personal or professional contribution made by certain individuals.

As I come to the end of my academic studies, I feel the need to utter a few words of thanks to the various people who supported me on this path that is life, where the journey, not the destination, is what counts.

I will start by praising the role played by the Faculty of Sciences and Technology of NOVA University of Lisbon, specifically the welcome it provided, the atmosphere it promotes on its campus, and the working conditions it offers.

A place of learning is characterised not only by its students but also by its teachers.

All the teaching staff with whom I had the opportunity to interact deserve a sincere word of thanks, for their capacity to transfer the knowledge I acquired and the cordial relationships they establish with the students.

I should highlight the role of Prof. Dr. Hugo Gamboa and Prof. Dr. Carla Quintão, who, as my mentors, supported, stimulated and challenged me constantly, removing obstacles that arose during the investigative process, while establishing themselves as huge sources of knowledge and experience.

In addition, Prof. Dr. Cláudia Quaresma gave me some essential tips during the process of submitting the experimental protocol to the Ethical Council, and I am most grateful for her time.

Along with my mentors, Engineer João Rodrigues was always present and available to help me steer my work in the right direction, establishing a very warm relationship that enabled a vast amount of learning, particularly during the data-processing stages of the project.

Furthermore, the close partnership with *Plux Wireless Biosignals* proved to be extremely useful, allowing me to develop in many ways and to experience a business environment, something which students typically only have access once their course has ended.

---

I must thank all the staff at *Plux* for the healthy environment that is typical of a normal working day at this company, for all their prompt answers to my questions and for the lessons they taught me.

In particular, I wish to thank André Lemos, who was the trigger for this project, and from whom I received, with a contagious liking, constant guidance and important updates about the world of recreational and top-level sport.

I would also like to mention the various members of the *software* team, consisting of Engineers Rui Freixo, Maria Magalhães, Gonçalo Telo and Carlos Azevedo, and the specialist in the clinical field Catarina Oliveira, for their availability to help me.

In the second half of the project I had the opportunity to work with Miquel Alfaras and Miguel Thomas. This interaction had a significant impact on my final results, both because of the work and advice they shared with me and because of the constructive conversations we had. I hope this word of thanks is only the beginning of my retribution.

The partnership established with the Laboratory of Motor Behaviour of the Faculty of Human Kinetics of the University of Lisbon, through his coordinator Prof. Dr. Pedro Pezarat and members Prof. Dr. Gonçalo Mendonça and Dr. João Vaz, was extremely important for the physiological perspective included in my thesis, enhancing my knowledge.

I am also very grateful for the pilot acquisitions that were ceded by these elements, constituting a contribute with inestimable value for the development of the project.

However, the academic and professional side of day-to-day life only functions well if supported by a rewarding and comforting personal side. I must therefore pay tribute to the individuals who have been instrumental to my happiness today and who have given me the hope that I will continue to be so in their company.

From a chronological point of view, everything has a beginning and, in this case, the beginning starts with my four grandparents, that I have always remembered fondly and from whom I received positive lessons.

Fortunately, I still have the chance to keep learning from my grandfather Joaquim, who, at the age of 90, is a source of inspiration and vitality. I would even go so far as to say that he has displayed more joviality than me in my 24 years.

The generational journey continues with my parents. They, more than anyone, put up with my uncertainty and supported me unconditionally, teaching me that sometimes we need to fall in order to learn how to get up, although with my mother and father all of my falls were controlled, just like a child's first bike ride.

Both fought quite to ensure that I was always well, and I am happy to know that I can continue to receive their care and advice in the future, because come what may, I know that I will always be able to count on them “to infinity and beyond”.

Also in terms of family, I should stress the role which my godfather, Luís, played and continues to play, by giving me two great joys during my time at the faculty, with the birth of my cousins Gonzalo and Tiago. I hope that through them I can repay him for what he has done for me.

---

With regard to friends, which I genuinely consider to be an extension of family, I must recall my oldest and most recent ones, with whom I hope my friendship lasts forever, or, given my age and average life expectancy, for at least more fifty years.

A huge thank you to João, Pedro and Manuel. I am always yearning for our cinema trips, board games and memorable conversations, because they allow me to remember the good times we have spent together over fourteen years and plan the future.

In respect of my more recent friends, I should say that all the people I had the pleasure of meeting in my years at the faculty meant a lot to me on a personal level, and unfortunately I cannot list them all here.

In the early (and turbulent) phase, I formed a quartet with Ana Duarte, Beatriz Valpradinhos and Helena Piteira. Our friendships began on the very first day and I hope to preserve them as time goes on.

There was a transitional period between the turbulence and academic stability, having some persons been particularly important for initiating or at least contributing towards the paradigm shift: Inês Barros and Filipa Correia, with whom I had the opportunity to work, and who helped me settle in, for which I am grateful.

I have one special mention left for Bilena Almeida and Sara Russo, with whom I established incredible friendships of an exponential nature, since they started slowly and grew at an uncontrollable pace. Sometimes I am quite slow person, but in this respect, I will do everything I can to keep up with this pace.

Finally, leaving behind the human world, I would like to make one final acknowledgement. I hope readers don't consider it belittling to those mentioned above, but I could not forget my four-legged friends. Unfortunately, many of them have already left us, but they live on my memory: Pluto, Pânico, Tareca, Buster and Gala – lots of petting for all the happy and unexpected moments they gave me.



*I have not failed.*  
*I've just found 10 000 ways that won't work.*  
**Thomas A. Edison**





## Abstract

---

Physical activity is a constant in life, prolonging since the primordial times until now as an intrinsic element of human condition, though his character have suffered a transmutation, going from a need, by the predatory nature of the human being, for an option in escaping sedentary habits of contemporary society.

Despite the enormous benefits of sports practice, there are also some negative consequences associated, namely the emergence of muscular injuries provided by the installation of fatigue, due to an overload on time or in the intensity of training.

The consequences of an injury are drastic, conditioning the quotidian of the injured and carrying high costs for the health system, establishing this problem as the starting point of the present work.

Although investigations on this subject have recently appeared, yet is not common to find commercial solutions for evaluating fatigue and with the capability of warning the user about the risk of injury.

In order to avoid the fatigue consequences, is proposed the implementation of a computational system for physiological signal processing - Electromyographic (EMG) and Electrocardiographic (ECG) - extracting multiple indexes with informative potential at fatigue level.

There is provided an automatic evaluation of the state of fatigue assured by the definition of a **Global Fatigue Index** that synthesises information from distinct individual fatigue indexes and implementation of a **Classification System**, with the capability of giving to the user the indication if the physical activity is originating the approximation or deviation from fatigue state.

The computer system was built for a future integration as a *plugin* on a signal acquisition *software*. This framework is a specialized tool for acquiring and processing of the physiological signals collected in equipments such as *bitalino* and *biosignalsplux*, being directed to the practice of *indoor* cycling.

**Keywords:** Online Processing; Offline Processing; Biosignals; Monitoring of Fatigue Levels; Machine-Learning; Global Fatigue Index; Cycling;

---



## Resumo

---

A atividade física é uma constante da vida, prolongando-se desde os tempos primordiais até à atualidade como um elemento intrínseco à condição humana, embora o seu caráter tenha sofrido uma transmutação, passando de uma necessidade, pela natureza predatória do ser-humano, para uma opção na fuga aos hábitos sedentários da sociedade contemporânea.

Apesar dos enormes benefícios da prática desportiva também existem consequências negativas associadas, nomeadamente o surgimento de lesões musculares pela instalação de fadiga, em virtude de uma sobrecarga no tempo ou na intensidade do treino.

As consequências de uma lesão são drásticas, condicionando o quotidiano do lesado e acarretando custos elevados para o próprio e para o sistema de saúde, estabelecendo-se esta problemática como o ponto de partida do presente trabalho.

Apesar de recentemente terem surgido investigações sobre esta temática, ainda não são comuns as soluções comerciais para avaliação da fadiga e com a capacidade de alertar o utilizador sobre o risco de lesão.

De modo a procurar evitar as consequências da fadiga, apresenta-se a implementação de um sistema informático de processamento de sinais fisiológicos - Eletromiográficos (EMG) e Eletrocardiográficos (ECG) - recorrendo à extração de múltiplos índices com potencial informativo do nível de fadiga.

Disponibiliza-se uma avaliação automática do estado de fadiga, assegurada pela definição de um **Índice Global da Fadiga** que sumariza a informação de múltiplos índices individuais e por um **Sistema de Classificação Binário**, que indica ao utilizador se a atividade física está a originar uma aproximação ou afastamento do estado de fadiga.

O sistema informático foi construído de modo a ser integrado como um *plugin* num *software* de aquisição de sinais, que se estabelece como uma solução especializada para aquisição e processamento dos sinais fisiológicos recolhidos por equipamentos como o *bitalino* e *biosignalsflux*, sendo direcionado para a prática de ciclismo *indoor*.

**Palavras-chave:** Processamento Online; Processamento Offline; Biosinais; Monitorização dos Níveis de Fadiga; Machine Learning; Índice Global de Fadiga; Ciclismo;

---



# Contents

<b>List of Figures</b>	<b>xix</b>
<b>List of Tables</b>	<b>xxiii</b>
<b>Glossary</b>	<b>xxv</b>
<b>Acronyms and Initialisms</b>	<b>xxvii</b>
<b>List of Symbols</b>	<b>xxix</b>
<b>1 Introduction</b>	<b>1</b>
1.1 Motivation . . . . .	1
1.2 Objectives to be Achieved . . . . .	3
1.3 Thesis Overview . . . . .	4
<b>2 Theoretical Background</b>	<b>7</b>
2.1 Physiological Signals . . . . .	7
2.1.1 EMG - Origin and Comments . . . . .	7
2.1.2 ECG - Origin and Comments . . . . .	9
2.2 Signal Processing Methods . . . . .	10
2.2.1 Event Detection - TKEO Algorithm . . . . .	10
2.2.2 Event Detection - Pan-Tompkins Algorithm . . . . .	11
2.3 Extracted Features . . . . .	15
2.4 Fatigue State . . . . .	15
2.4.1 Fatigue Definition . . . . .	15
2.4.2 Types of Fatigue . . . . .	15
2.4.3 Muscular Fatigue Causes . . . . .	18
2.4.4 Literature Review . . . . .	19
2.5 Acquisition and Monitoring System . . . . .	24
2.6 Classification Systems - <i>Support Vector Machines</i> . . . . .	25
<b>3 Methods Used</b>	<b>27</b>
3.1 Induction of Fatigue - Experimental Protocol . . . . .	28
3.1.1 Submission to the Ethical Council of NMS . . . . .	29

## CONTENTS

---

3.1.2	Reformulation of the Submitted Documents . . . . .	30
3.1.3	Calibration Protocol . . . . .	30
3.2	Identification of Fatigue Indexes . . . . .	31
3.2.1	Assumptions . . . . .	31
3.2.2	Empirical Method . . . . .	33
3.2.3	Method Based on a Meta-Analysis . . . . .	36
3.3	Definition of a Global Fatigue Index . . . . .	39
3.3.1	Formal Specification . . . . .	39
3.3.2	Fatigue by Levels . . . . .	40
3.4	Classifiers . . . . .	41
<b>4</b>	<b>Presentation of Results</b>	<b>47</b>
4.1	Indexes with Information Potential . . . . .	47
4.2	Typical Evolution of the Global Index . . . . .	49
4.3	Classification Systems - Comparative Study . . . . .	50
4.4	Fatigue Analysis Plugin - Foundations . . . . .	53
4.4.1	EMG Plugin . . . . .	54
4.4.2	HRV Plugin . . . . .	58
4.4.3	Computational Restrictions . . . . .	60
4.5	Fatigue Analysis Plugin - <i>Offline</i> . . . . .	61
<b>5</b>	<b>Discussion of Results and Expectations for the Future</b>	<b>67</b>
5.1	Discussion of Results . . . . .	67
5.2	Future Expectations . . . . .	69
	<b>Bibliography</b>	<b>71</b>
<b>A</b>	<b>List of Features (Figures)</b>	<b>83</b>
<b>B</b>	<b>Experimental Protocol</b>	<b>89</b>
B.1	Protocol of Day 1 . . . . .	89
B.2	Protocol of Day 2 . . . . .	93
<b>C</b>	<b>Processing Results for Tendency Evaluation</b>	<b>97</b>
<b>D</b>	<b>Report Generated by the <i>Offline</i> Fatigue Monitoring Plugin</b>	<b>105</b>
<b>E</b>	<b>Publications and Other Initiatives</b>	<b>115</b>

## List of Figures

1.1	Breakdown of the content of each chapter . . . . .	4
2.1	Illustration of the various phases of the mechanism by which the muscle fibre contracts . . . . .	8
2.2	Evolution of the membrane potential for the generation of action potentials and conduction system . . . . .	9
2.3	Results of applying each step of the algorithm for detecting periods of activity using the TKEO operator . . . . .	12
2.4	Delimiting periods of muscular activation through the binary signal . . . . .	12
2.5	Partial results of each phase of the Pan-Tompkins algorithm (Part 1) . . . . .	13
2.6	Partial results of each phase of the Pan-Tompkins algorithm (Part 2) . . . . .	13
2.7	Graphical representation of the evolution of the content of the list of R peaks over the various phases included in the <i>Python</i> implementation of the Pan-Tompkins algorithm . . . . .	14
2.8	Time series showing the evolution of the duration of RR intervals during the acquisition (Tachogram) . . . . .	14
2.9	List of features extracted from the EMG and ECG signals, grouped into their respective categories . . . . .	15
2.10	Sub-division of Fatigue by Type and Origin . . . . .	18
2.11	Explanation of the set of physiological signals with the potential to provide information on the fatigue state . . . . .	20
2.12	Cause-effect structure relating to the impact that a change in <i>pH</i> and lactate concentration has on the functioning of the muscle fibre . . . . .	23
2.13	Illustration of the <i>hardware</i> and <i>software</i> component used to acquire and monitor the physiological signals . . . . .	25
2.14	Geometric illustration of the concepts taken into account in an SVM of the binary type . . . . .	26
3.1	Appearance of the matrix summarising the parameters of the linear regression applied to the processing results . . . . .	34
3.2	Process of validating the empirical method for identifying trends . . . . .	36
3.3	<i>Forest Plots</i> graphically synthesising the results of the meta-analysis . . . . .	37

3.4	Diagram summarising the mechanism for determining a sample of the global fatigue index . . . . .	40
3.5	Graphical correspondence between the thresholds defining the fatigue zones and their origin in the <i>box plot</i> . . . . .	41
3.6	Graphic summary of the procedure from the initial population sample of 14 subjects up to the 22 examples for extracting features . . . . .	43
3.7	Graphic summary of the procedure for extracting features from the evolution time series of each fatigue index . . . . .	44
4.1	Typical evolution of the global fatigue index during the fatigue induction phase	49
4.2	Evolution of the global fatigue index during the fatigue induction phase for the 11 subjects . . . . .	50
4.3	Results of applying the <b>RFECV</b> function with the scores obtained in each iteration . . . . .	51
4.4	Evolution of the classification decision over the course of the acquisition . . .	52
4.5	Evolution of the classification decision over the course of the acquisition for each subject of the population sample . . . . .	53
4.6	Results shown by the first of the two <i>plugins</i> for processing the EMG signal .	54
4.7	Results shown in the second <i>plugin</i> for processing the EMG signal . . . . .	54
4.8	Functions of the EMG <i>plugin</i> for real-time processing, from the point of view of the user and the programmer . . . . .	55
4.9	Configurable elements in the interface of the <i>plugin</i> for monitoring the evolution of EMG parameters in real-time, as well as processing results . . . . .	56
4.10	Correlation coefficients between the rectified EMG signal and the binarised signal of activations presented in the form of a graph . . . . .	57
4.11	Presentation of the processing results of the <i>plugin</i> for <i>offline</i> heart rate variability analysis . . . . .	58
4.12	Interface of the HRV <i>plugin</i> for real-time processing, together with its internal operating logic . . . . .	59
4.13	Comparison of the tachograms obtained in the <i>plugin</i> for <i>offline</i> analysis and the <i>plugin</i> for real-time analysis . . . . .	60
4.14	View of the interface of the <i>plugin</i> for monitoring the fatigue state . . . . .	62
4.15	Focused view of the tab in the interface for specifying the device and channel associated with each type of signal . . . . .	62
4.16	File importation options for calibrating the system, and the sequence of steps	63
4.17	Alert message stating that classification of the fatigue state is not possible, given that some indexes have not been extracted . . . . .	63
4.18	Section of the interface for configuring algorithms and methods used in the processing phase . . . . .	64
4.19	View of the various processing results arising from the analysis of the EMG and ECG fatigue indexes . . . . .	65



A.1	Illustration of the median frequency concept . . . . .	83
A.2	Description of the proposed logic for determination of the median frequency in the scalogram . . . . .	84
A.3	Identification of the position of the centroid by graphically highlighting the correspondence with the parameters <i>Major Frequency</i> and <i>Major Time</i> . . .	84
A.4	Illustration of the convex area concept . . . . .	84
A.5	Presentation of the temporal and frequency dispersion . . . . .	85
A.6	Graphical identification of the average value of the duration of the RR intervals for the processing window under analysis . . . . .	85
A.7	Representation of the statistical dispersion of the results around the mean value	86
A.8	Detachment of modal <i>bin</i> of the histogram associated with the duration of RR intervals . . . . .	86
A.9	Presentation of the <i>Poincaré</i> plot . . . . .	87
A.10	Power bands typically used for analysing cardiac variability through the tachogram power spectrum . . . . .	87
B.1	Ternary Model defining the training zones in cardiorespiratory terms . . . . .	92
B.2	Graphical illustration of the value of $VO_{2max}$ . . . . .	92
B.3	Graphical illustration of the value of $VT1$ . . . . .	93



## List of Tables

2.1	List and description of the various EMG indexes studied . . . . .	16
2.2	List and description of the various ECG indexes studied . . . . .	17
2.3	Failure points and causes/consequences of fatigue setting in . . . . .	18
2.4	Summary of the results from one study contained in the bibliography . . . . .	21
3.1	Pre-defined values of Maximum Power Output by gender . . . . .	30
3.2	Properties of the population sample formed by 14 subjects . . . . .	32
4.1	List of indexes with fatigue information potential . . . . .	48
4.2	Presentation of the ideal window size and time-step combination for extracting each fatigue index . . . . .	49
4.3	Success rates of the classifier using the Cross-Layer Estimation and Leave One Out methods . . . . .	51
C.1	EMG processing results generated during the iterative application of the empirical method . . . . .	98
C.2	ECG processing results (Time-Domain features) generated during the iterative application of the empirical method . . . . .	99
C.3	ECG processing results (Frequency-Domain features) generated during the iterative application of the empirical method . . . . .	100
C.4	EMG processing results generated during the iterative application of the meta-analysis . . . . .	101
C.5	ECG processing results (Time-Domain features) generated during the iterative application of the meta-analysis . . . . .	102
C.6	ECG processing results (Frequency-Domain features) generated during the iterative application of the meta-analysis . . . . .	103



## Glossary

Convex Hull	Corresponds to an area (2D space) or a volume (3D space) that includes all the points in analysis. It has the particularity that any pair of these points, can be connected to each other by a line totally contain inside the area/volume.
Dygraph	A <i>JavaScript</i> charting library. At the present work, this word, is also used for referring the object produced by the constructor contained in this library.
Ergometer	A device structurally similar to a bicycle, ideal to execute <i>indoor</i> training programs and stress tests, considering that is possible to increase or decrease the pedal resistance (and consequently the difficulty of the exercise) by digitally specifying the load and the target power.
Goniometer	A measure instrument for determination of the angle formed between two lines. Specifically, in biomechanics, it is used to measure the range of motion at a joint.
Scalogram	Bidimensional structure that synthesizes the process of signal decomposition, using the Wavelet Transform. Has dimensions of time, frequency and intensity of each wavelet (through a color scale).
Tachogram	Defines a time-series that describes the evolution of RR interval duration along the electrocardiographic (ECG) data acquisition. With this resource, the analyser can interpret the ECG data in a higher level of abstraction, by studying only the periodicity of the cardiac signal.



## Acronyms and Initialisms

ANS	Autonomic Nervous System.
CNPD	Comissão Nacional de Proteção de Dados.
ECG	Electrocardiogram, Electrocardiography or Electrocardiographic.
EMG	Electromyogram, Electromyography or Electromyographic.
FFT	Fast Fourier Transform.
FMH	Faculdade de Motricidade Humana ( <i>Faculty of Human Kinetics</i> - University of Lisbon).
GFI	Global Fatigue Index.
HCN	Hyperpolarisation-Activated Cyclic Nucleotide-Gated Channels.
HF	High Frequency Band.
HRV	Heart Rate Variability.
IFI	Individual Fatigue Index.
LF	Low Frequency Band.
MAV	Mean Absolute Value.
MMG	Mechanomyography.
MPO	Maximum Power Output.
MVC	Maximal Voluntary Contraction.
NIRS	Near-Infrared Spectroscopy.
NMS	NOVA Medical School.

## ACRONYMS AND INITIALISMS

---

PSD	Power Spectral Density.
RMS	Root Mean Square.
RPM	Rotations Per Minute.
SAN	Sinoatrial Node.
SMG	Sonomyography.
STFT	Short-Time Fourier Transform.
SVM	Support Vector Machine(s).
TOI	Tissue Oxygenation Index.
ULF	Ultra-Low Frequency Band.
VLF	Very-Low Frequency Band.



## List of Symbols

$VCO_2$	Rate of carbon dioxide released in breath (volume/time).
$VO_2$	Rate of oxygen consumed by the organism (volume/time).
$VO_{2max}$	Represents the maximum rate of oxygen consumption when the subject is exposed to an intense physical activity. It is determined in a trial where the difficulty of the task is gradually incremented.
$VT1$	Like $VO_{2max}$ , this parameter can be determined during an incremental test and defines the imbalance point where the ventilation rate become bigger than the rate of oxygen consumption. It is achieved before $VO_{2max}$ .



# Introduction

## 1.1 Motivation

Scientific advances observed throughout history have, to a large extent, stemmed from human curiosity and the ability to accept challenges whose solutions define the boundaries of what is possible.

The development that has taken place in the field of medicine is one of these examples, corroborated by the increase in average life expectancy and in the quality of life itself, not only in the Western world, where every European citizen tends to live for around 80.6 years on average [1], but also at a global level, with the differences between developed and developing countries becoming smaller and smaller. A prime example of this is India, where average life expectancy has increased from 23 years to 68 years over the last century [2].

Going only a few decades back, it is possible to see that there were considerable obstacles to clinical practice, which were partly caused by the difficulties associated with observing the inside of a living body. Knowledge of this environment was therefore essentially obtained through *post-mortem* examinations.

As a result of the developments that took place at the end of the 19<sup>th</sup> century and during the 20<sup>th</sup> century [3–6], with the creation of medical imaging systems, the inside of the body ceased to be *terra incognita*.

In parallel, signal acquisition systems were developed on the basis of internal physiological phenomena, namely Electrocardiographic (ECG) and Electromyographic (EMG) systems, spurred on by the essential work of Willem Einthoven and Louis Lapicque in the early 20<sup>th</sup> century [7, 8].

Both procedures make it possible to record and monitor the electrical activity generated and transmitted by the human body, this activity being essential for the communication of information between organ systems by means of the nerve network that makes up the nervous system.

However, ECG and EMG systems have gradually ceased to apply exclusively to clinical contexts, and have started to be used in people's day-to-day lives, particularly in occupational and sports settings, enabling the reaction displayed by the body in physically demanding situations to be understood through preventive and not so reactive monitoring.

Some may believe that there is a behavioural tendency, on the part of amateur and professional sports-people, to find physiological monitoring solutions which ultimately allow their physical performance to be analysed.

There are good indicators of the growth potential of these systems on the intelligent monitoring device market [9].

By way of example, is expected that a considerable increase in revenue linked to wearable products take place, which include physiological monitoring devices: the number of devices should increase from 335 million in 2016 to around 835 million in 2020 [10], owing to the recent investment on the part of technology companies in smartwatches, which include many of the features of conventional fitness trackers [11].

In terms of revenue by 2021, the current 30 660 million dollars may increase to 37 280 million dollars, with a growth of approximately 21% [12], the market of smart-clothes becoming increasingly dominant [13].

All of these facts give a substantial boost to research and innovation into physiological monitoring systems, and it is within this context that this thesis falls.

In addition to commercial appeal, which is an important factor in the sustainability of technological projects, there is one key motivation which is decidedly more in line with the duties and ethics of biomedical engineering.

Despite the fact that practising sport has clear reported benefits, it can also cause problems, such as muscular lesions, preventing training from continuing and leading to intervals which considerably hinder the athlete's progress [14].

Fatigue is thought to be one of the mechanisms that contribute to injury [15], and therefore monitoring devices with the capacity to predict and quantify this state may be the next step in the evolution of physiological monitoring systems.

Scientists have been trying to evaluate this state for some decades now and a number of studies exist in this area [16–26], however, it is still uncommon for this research to be applied to sports contexts, particularly as part of real-time monitoring or processing, and the studies essentially end up serving academic purposes, meaning that commercial opportunities are virtually unexplored [16].

The *BSX Insight*<sup>TM</sup> device may be considered to be a recent example of this type of solution. It determines the athlete's lactate threshold based on an optical near-infrared spectroscopy system (NIRS) and infers the level of muscle oxygenation using a specific model, giving it high future potential in terms of quantifying the development of muscular fatigue over the course of the exercise session [27, 28].

The current environment may be conducive to the development of devices for evaluating fatigue, stimulating scientists to propose a solution that combines information (fatigue indexes) from multiple types of physiological signals, like EMG and ECG.

A fatigue monitoring system may have an incredibly beneficial impact, in terms of sport, if it has the capacity to alert the user when he or she is experiencing problematic levels of fatigue.

This preventive potential will reduce the number of injuries being, therefore, a major motivation prior to and during this project implementation.

## 1.2 Objectives to be Achieved

The main objective of this project is to implement a computer system with the capacity to objectively evaluate fatigue in a sports context.

However, it became necessary to reduce the abstraction of this objective, which has been broken down into the following specific objectives:

- Preparation of an experimental protocol, for the isolated study of the “fatigue” variable and corresponding approval by an external body (Ethical Council);
- Implementation of an algorithm for processing the analysed signals, with the capacity to extract multiple features;
- Identification of trends and patterns which may be related to the fatigue state and which consequently become the feature in an indicator relating to this state (time, frequency and time-frequency domains);
- Incorporation of the algorithm into a *plugin* for *offline* evaluation of the identified fatigue indexes, designed for the *OpenSignals software*;
- Inclusion of a classifier for automatically detecting the user’s type of fatigue (“**Positive Fatigue**” or “**Negative Fatigue**”, which refer to the installation and recovery from fatigue, respectively);
- Definition of a global fatigue index (GFI) for characterising the fatigue state, combining the information supplied by multiple features into a single value;
- Switching of the *offline* algorithm to a real-time analysis system.

### 1.3 Thesis Overview

The body of the thesis is divided into 5 chapters with a varying number of sub-chapters. Figure 1.1 shows the underlying topics of each chapter, which are described in greater detail in the following paragraphs.



Figure 1.1: Breakdown of the content of each chapter

This first chapter is intended to describe the context of the project. It explains the problem situation, its relevance and the objectives that must be achieved to solve it.

**Chapter 2** goes on to present some relevant definitions, in particular regarding the concept of “fatigue”, the different types and the possible causes, and contains a literature review of studies in this area.

This chapter also includes a brief description of the *biosignalsplux* acquisition system and the *OpenSignals software*, into which the processing features for monitoring the fatigue state were incorporated, along with a description of some of the algorithms and methods used in the computer implementation of the proposed system.

This section ends with a summary of the concepts and the “mechanics” associated with classification systems of the *Support Vector Machine* (SVM) type.

**Chapter 3** sets out the experimental protocol designed to induce fatigue and explains how the methods described in **Chapter 2**, namely processing techniques and algorithms used in data analysis, were applied, as well as the steps followed in the identification of trends.

**Chapter 4** contains the results that were obtained and specifies which EMG and ECG indexes have the potential to provide information about fatigue. It also addresses the efficiency of the trained classification system.

Said chapter also describes the *plugins* for extracting parameters from the EMG and ECG signals in real-time and the final *plugin* for monitoring the fatigue state in an *offline* context.

Finally, the last chapter contains a discussion of the results and presents the conclusions and expectations for the future.

The annexes set out some activities carried out in parallel with the thesis project, but within its scope, which played an important part in the final project design.

There were also included additional images and tables to complement some of the information given in the various chapters.





## Theoretical Background

### 2.1 Physiological Signals

Despite the fact that fatigue monitoring has been explored in various studies using a wide range of signals, as may be seen in section 2.4.4, in the current version of the system the monitoring was carried out by limiting the signals in question to EMG and ECG signals<sup>1</sup>. A brief description of the physiological origin of each of the signals and the instrumentation used to record them is provided in the sections that follow.

#### 2.1.1 EMG - Origin and Comments

Muscular contraction is the result of the coordinated action of the nervous system and the muscle, and there are various steps between the generation of the nerve impulse and the joint contraction of the muscle fibres.

The action potential is generated at the neuron, propagating along the axon through multiple depolarisations and repolarisations of the membrane, caused by the opening of voltage-sensitive sodium and potassium channels which are activated in sequence as they are reached by the wave of potential.

When the action potential reaches the axon terminal, it is transmitted to the next neuron across chemical synapses, with the release of neurotransmitters into the synaptic cleft (neuron-neuron interface).

The neurotransmitters bind to sodium channels which are activated by molecular stimuli, allowing this ion to enter the intracellular environment and thus disrupt the membrane potential, recreating the action potential.

The mechanism, whereby the action potential is transmitted from neuron to neuron, will be repeated at the interface between the neuron and the muscle fibre.

---

<sup>1</sup>The choice of these signals gives us information of the local and global effects of fatigue

When it reaches the muscle fibre, the action potential propagates along its membrane (sarcolemma), which contains small invaginations (T-tubules) surrounded by calcium cisternae.

The stimulation of the calcium cisternae causes this ion to be released to the intracellular environment, triggering the translational movement between actin and myosin myofilaments as a result of the bond established with troponin.

This connection generates a change in the shape of the tropomyosin, exposing the sites where actin and the myosin heads (myofilaments) can bind, allowing them to make contact.

The interaction between myofilaments releases the ADP molecule bound to the myosin, causing its head to move, dragging the actin and culminating in the contraction of the muscle fibre. This dynamic is maintained as there are calcium ions bound to troponin, that is, for the period during which the calcium cisternae are stimulated (Figure 2.1).

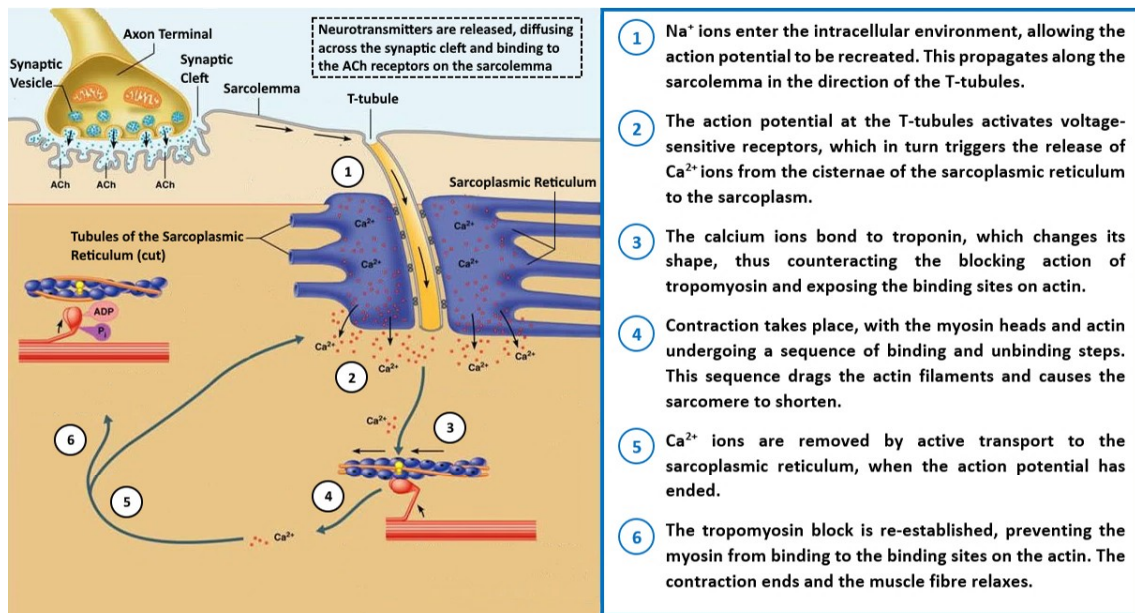


Figure 2.1: Illustration of the various phases of the mechanism by which the muscle fibre contracts (from the point at which the nerve impulse reaches the synaptic cleft) [29]

As it propagates over the sarcolemma, the potential wave spills over to the most superficial layer of the skin, making it possible to record the electromyographic signal<sup>2</sup>, captured by a system of electrodes. A certain degree of attenuation occurs, which explains the reduced amplitude of the EMG signals and the need for amplification.

The electromyographic information may be considered to fall within a frequency band of between 10 and 400 Hz, although this interval may be relaxed slightly to include components with frequencies of between 5 and 10 Hz and between 400 and 450 Hz [30].

<sup>2</sup>Sum of the action potentials of the multiple motor units determining the characteristics of the EMG signal, giving rise to an anarchic appearance as observed in Figure 2.3a

### 2.1.2 ECG - Origin and Comments

In contrast with the skeletal muscle, the contraction of the cardiac muscle (myocardium) does not occur voluntarily, instead being coordinated by the sympathetic and parasympathetic components of the autonomic nervous system (ANS).

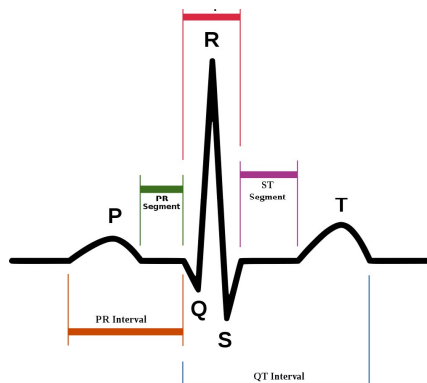
The cardiac action potential is generated by specialised structures in the heart characterised by auto-excitability, which are known as pacemakers.

The sinoatrial node (SAN) is considered to be the heart's "natural pacemaker", because it ensures that the heart's rhythm is regular. It does so by virtue of channels in the membrane of its cells which behave in a special way, known as *hyperpolarisation activated cyclic nucleotide gated channels* (HCN).

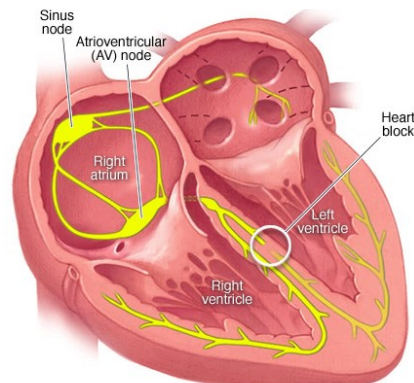
The distinctive characteristic of these channels is that they open for very low membrane potentials, reopening almost immediately after phase 3 of the previous action potential. This ensures that a permanent current of positive ions can enter the SAN cells, allowing the membrane potential to gradually increase until it reaches the activation threshold and generates a new action potential, in an endless cycle.

Once generated, the action potential propagates along the cardiac conduction system, formed by the atrioventricular node, the bundle of His and the branches of the Purkinje fibres which span the various sections of the myocardium (Figure 2.2b).

Along this journey, the following steps occur in sequence: the atrial region is depolarised (atrial systole – P wave), repolarised (atrial diastole), ventricular depolarisation takes place almost simultaneously (ventricular systole – QRS complex), followed by ventricular repolarisation (ventricular diastole – ST segment and T wave), giving rise to the events illustrated in Figure 2.2a.



a Electrical events characterising the ECG signal [31]



b Action potential conduction system [32]

Figure 2.2: Evolution of the membrane potential for the generation of action potentials and conduction system

In terms of instrumentation, there are many similarities between ECG sensors and EMG sensors, given that the signals they record originate from events with shared characteristics based on the contraction of a muscle (cardiac or skeletal).

The frequency band of electrocardiographic signals is more limited than that of EMG signals, being between 0.05 and 40 Hz [33]. However, in clinical terms (with new-born children in particular) it is common for the upper cut-off frequency to be extended to 150 or 250 Hz, because it can still contain relevant information [34].

The passband of EMG signals contains that of ECG signals, which is why the positioning of the electrodes is extremely important for avoiding *cross-talk*.

## 2.2 Signal Processing Methods

Despite having a similar origin associated with the depolarisation wave responsible for the contraction of skeletal and cardiac muscles, EMG and ECG signals are very different when viewed graphically.

ECG signals are regular, and have very well defined “structures” that are easy to identify. In contrast, EMG signals are not naturally regular, given that they are generated voluntarily, and are characterised by a binary divide between regions of muscular activation and inactivation.

For efficient processing, it is important to restrict the study to specific events of each signal.

In the case of the ECG signal, the aim is to observe the way in which heart rate variability (HRV) changes as fatigue sets in. It is therefore necessary to evaluate periodicity by detecting the R peaks and the respective time differences between them.

In the case of the EMG signal, the regions of inactivity are not relevant, considering that they only contain noise. It is therefore necessary to isolate the regions of muscular activation in the EMG signal, restricting the study to the samples contained in the various periods of activation.

To ensure that these events (detection of R peaks and detection of the start and finish of periods of muscular activation) are identified, two scientifically well-established algorithms have been used. The implementation logic is set out in the sections that follow.

### 2.2.1 Event Detection - TKEO Algorithm

The logic of this algorithm is based on the establishment of a threshold and the capacity to distinguish between signal and noise. The EMG signal is subsequently converted into a binary format, that is, all the samples with a value above the threshold acquire the value of 1 and all the samples under the threshold are considered to be zero.

However, owing to the extremely unstable nature of the EMG signal, where very sudden and marked transitions take place, there is a high probability that if a static threshold is established it will be exceeded multiple times during the period of muscular activity.

In normal conditions for each period of muscular activation, the threshold must be exceeded once in the upward direction and once in the downward direction, defining the start and finish of the event.

Implementing this logic directly is therefore not feasible and some processing steps are needed before the EMG signal can be “binarised”.

There are some extremely successful methods for identifying periods of activity, such as the statistical algorithm proposed by Bonato [35].

Despite the robustness of the method, given its nature it may not be appropriate for the real-time analysis system we intend to develop later on. Another approach has therefore been chosen which combines simplicity with detection efficiency, involving an algorithm that uses a single threshold and applies a filter to smooth the signal.

The method is based on that proposed by Hodges [36] and improved by Pimentel with the introduction of the TKEO operator for increasing efficiency in the detection of periods of muscular activation [37].

The algorithm encompasses the following steps:

- ① Filtering of the EMG signal to minimise the effect of noise (Figure 2.3b);
- ② Application of the TKEO operator to each sample of the filtered signal (Figure 2.3c);  

$$TKEO[i] = EMG_{filt}[i]^2 - (EMG_{filt}[i+1] \times EMG_{filt}[i-1])$$
- ③ Rectification and Smoothing of the TKEO signal using a sliding average, which cannot be configured by the user (Figures 2.3d and 2.3e);
- ④ Additional level of smoothing, which the user can configure by defining the size of the smooth window (Figure 2.3f);
- ⑤ Definition of the threshold, established as a function of the average value and standard deviation of the population of samples of the original EMG signal, and a variable  $h$  defined by the user, corresponding to the level of the threshold ( $Threshold = \mu + h \times \sigma$ );
- ⑥ Binarisation through signal scanning, to compare each sample with the established threshold, converting all the samples above the threshold to 1 and all the samples below the threshold to 0 (Figure 2.4);
- ⑦ The starts of the periods of activity correspond to all the upward transitions  $0 \rightarrow 1$ , while the ends correspond to downward transitions  $1 \rightarrow 0$ .

### 2.2.2 Event Detection - Pan-Tompkins Algorithm

This algorithm proves to be very robust and efficient, with correct detection rates of over 90% [38].

The ECG signal will be exposed to a **filtration**, **differentiation** and **integration** sequence, and undergo a final step in which false R peaks are excluded.

The first three steps of the sequence are intended to “simplify” the format of the signal in such a way that only the transitions (like the R peaks) stand out, minimising secondary

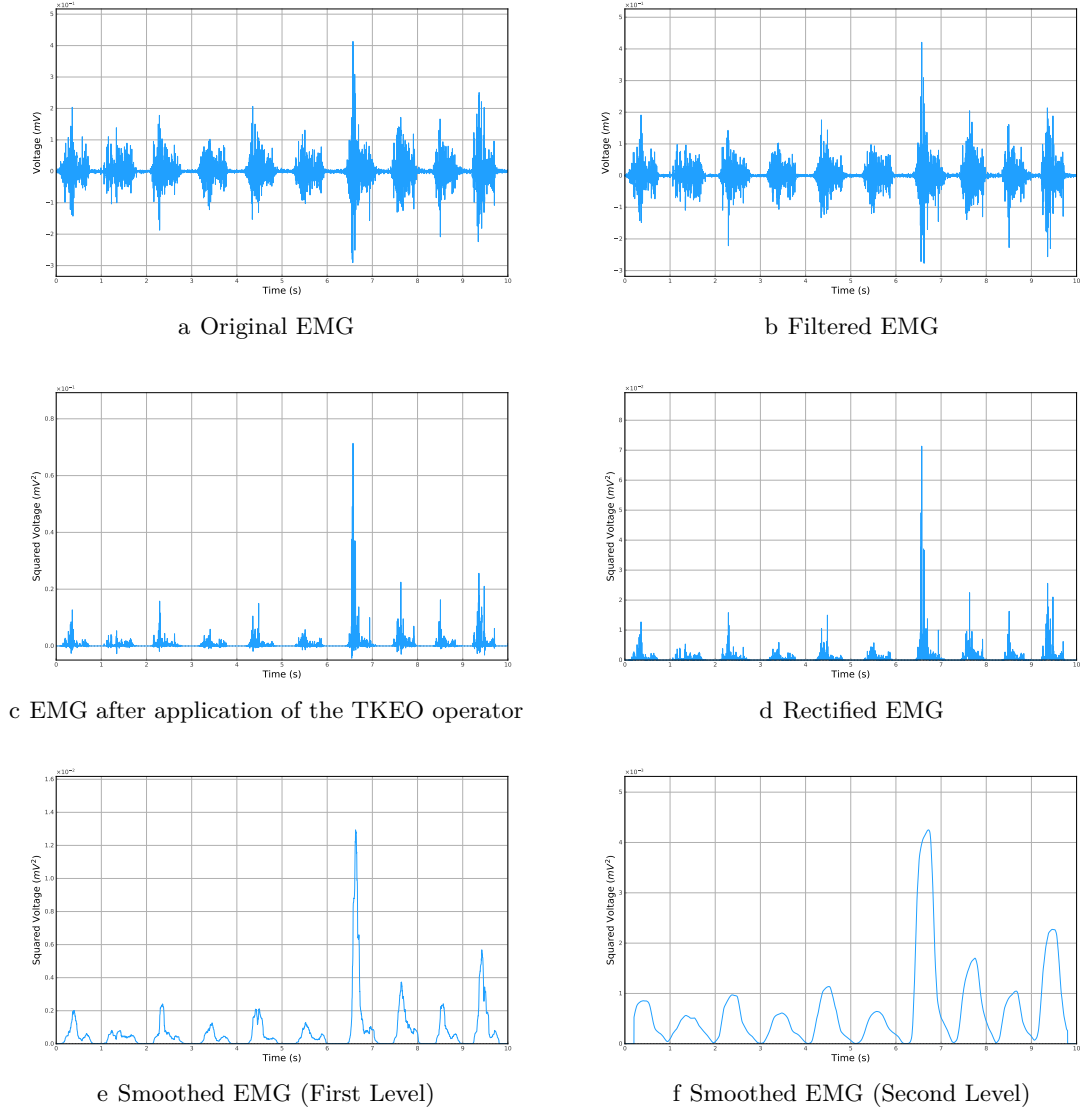


Figure 2.3: Results of applying each step of the algorithm for detecting periods of activity using the TKEO operator

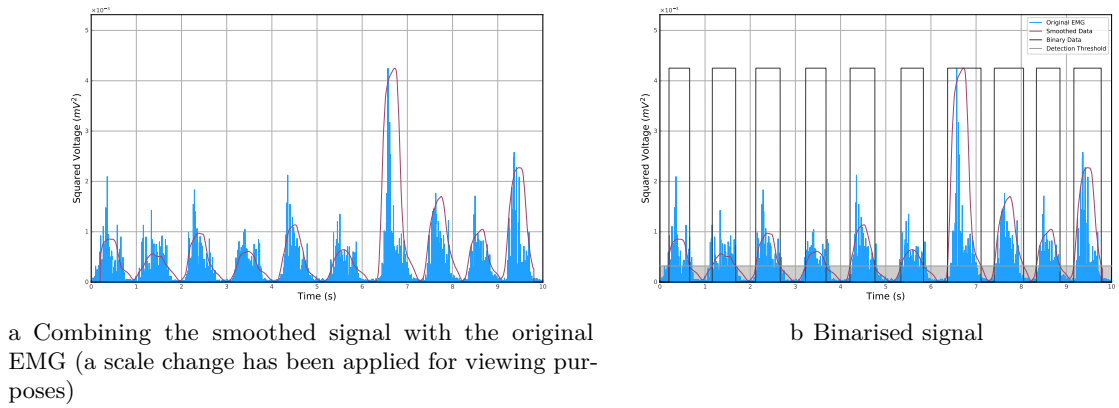


Figure 2.4: Delimiting periods of muscular activation through the binary signal

events which could potentially lead to incoherence for the algorithm, thus increasing the efficiency of the R peak detection.

In the filtration step, the signal is applied to the input of a second-order Butterworth passband filter, with a passband located between **5** and **15 Hz**, corresponding to the typical frequencies at which the R peak forms (Figure 2.5b).

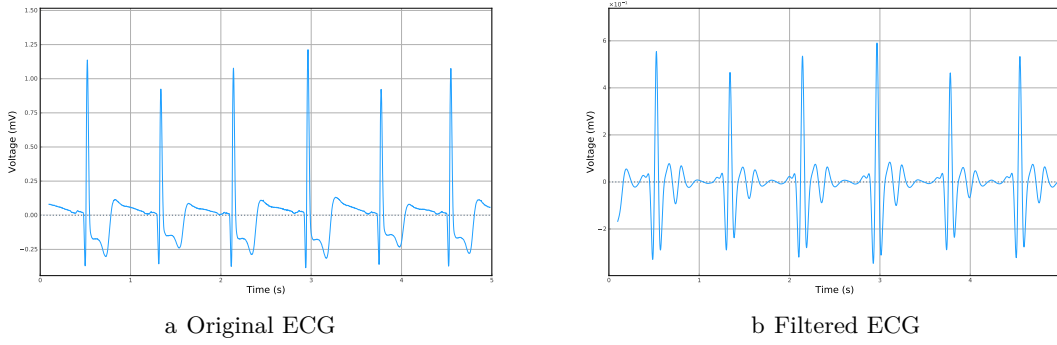


Figure 2.5: Partial results of each phase of the Pan-Tompkins algorithm (Part 1)

The filtered signal then undergoes differentiation, which involves the sequential subtraction of consecutive inputs, where the input  $i$  of the differentiated vector will be equal to the difference between the values contained in the inputs  $i+1$  and  $i$  of the filtered vector (Figure 2.6a).

The differentiated signal suffers, subsequently, a “rectification”, where each sample is raised to the power of 2 (Figure 2.6b).

Once these steps are complete, the signal is integrated using a sliding window of size  $N = 0.080 \times f_{sampling}$ . This size was chosen to be similar to the maximum duration (in physiological terms) that the QRS complex may have, in this case around 0.080 s, half the value suggested by J. Pan and W. Tompkins [38] (Figure 2.6c).

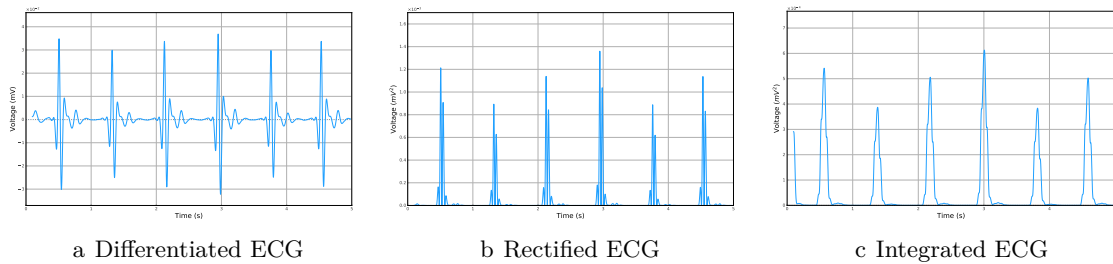


Figure 2.6: Partial results of each phase of the Pan-Tompkins algorithm (Part 2)

These preparatory steps to isolate the R peaks, in order to make it easier to detect them in programming terms, are followed by a sequence of steps included in the original Pan-Tompkins algorithm [38], transposed to the *Python* format by Raja Selvaraj. A description of this can be found in the Position Paper prepared over the course of the project, which is available in Appendix E.



Figure 2.7 shows the evolution in the detection of R peaks, from the moment a list of possible peaks is available, followed by the list of probable peaks and finally showing the definitive R peaks in the various implementation phases proposed by Pan and Tompkins.

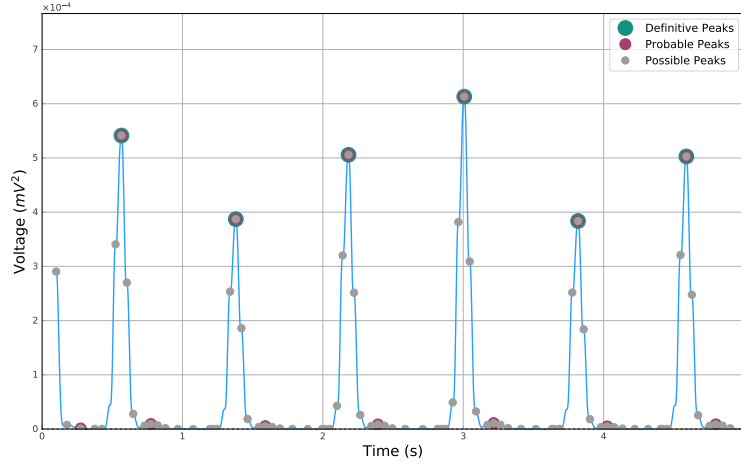


Figure 2.7: Graphical representation of the evolution of the content of the list of R peaks over the various phases included in the *Python* implementation of the Pan-Tompkins algorithm

At this point the system has the provisional list of R peaks, and the tachogram can be generated (Figure 2.8). This is a derivation of the ECG signal which makes it possible to centre the analysis on the periodic component of the cardiac signal. It is the source of information from which different indexes will be extracted in order to evaluate heart rate variability, as illustrated in section 2.3.

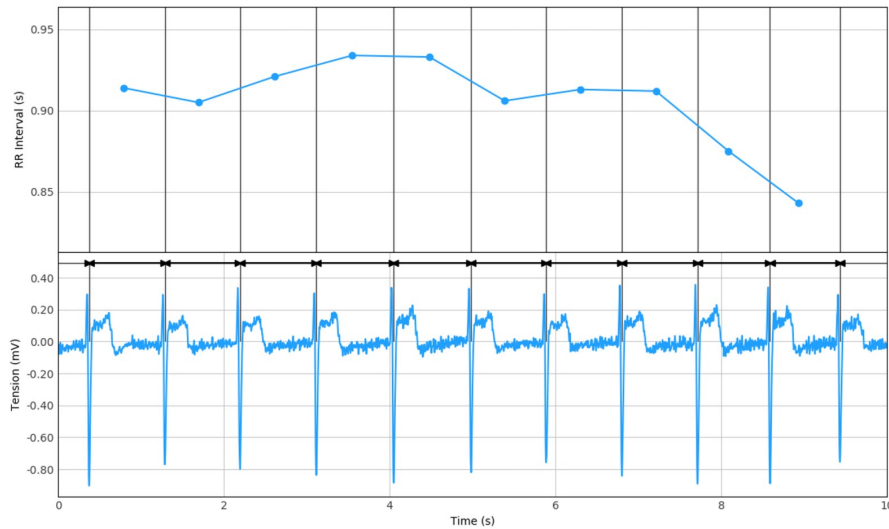


Figure 2.8: Time series showing the evolution of the duration of RR intervals during the acquisition (Tachogram)

However, before this determination process, the tachogram must pass through a filtration level to remove ectopic beats.



## 2.3 Extracted Features

The set of features that may be extracted from the EMG and ECG signals is vast, so a more limited set has been selected for analysis in this project, as shown in the diagram of Figure 2.9.

EMG			ECG	
Time	Frequency	Time-Frequency	Time	Frequency
<ul style="list-style-type: none"> <li>• RMS</li> </ul>	<ul style="list-style-type: none"> <li>• Median Frequency</li> <li>• Total Power</li> </ul>	<ul style="list-style-type: none"> <li>• Median Frequency</li> <li>• Major Frequency</li> <li>• Major Time</li> <li>• Mean Power</li> <li>• Area</li> <li>• Volume</li> <li>• Time Dispersion</li> <li>• Frequency Dispersion</li> </ul>	<ul style="list-style-type: none"> <li>• Maximum RR Interval</li> <li>• Minimum RR Interval</li> <li>• Average RR Interval</li> <li>• SDNN</li> <li>• rmsSD</li> <li>• Triangular Index</li> <li>• SD1</li> <li>• SD2</li> <li>• SD1/SD2</li> </ul>	<ul style="list-style-type: none"> <li>• Power inside ULF Band</li> <li>• Power inside VLF Band</li> <li>• Power inside LF Band</li> <li>• Power inside HF Band</li> <li>• Median Frequency</li> </ul>

Figure 2.9: List of features extracted from the EMG and ECG signals, grouped into their respective categories

It is, therefore, worth providing a brief introduction about each of the indexes studied and, where possible, a graphical correspondence. This is the purpose of Tables 2.1 and 2.2, the graphical examples being included in Appendix A.

## 2.4 Fatigue State

### 2.4.1 Fatigue Definition

Fatigue may be described as a gradual phenomenon which develops over time and which is caused by continuous physical or mental effort. From the point of view of the muscles, it is characterised by an inability to maintain an effort and depends on the muscle in question and the physique of the patient [43]. It has different causes and mechanisms, as indicated by Cifrek:

*“Muscle fatigue represents a complex phenomenon encompassing various causes, mechanisms and forms of manifestation. It develops as a result of a chain of metabolic, structural and energetic changes in muscles due to insufficient oxygen and nutritive substances supply through blood circulation, as well as a result of changes in the efficiency of the nervous system”* [16].

The various causes and types of fatigue, which are implicit in the above definition, will be described in greater detail in the following sections.

### 2.4.2 Types of Fatigue

Because of its diverse manifestations the fatigue state has been sub-divided into types, although the classification of the fatigue state is not entirely standardised, as highlighted by Shen [44], and depends on the type of base model used to study it.

Table 2.1: List and description of the various EMG indexes studied

Feature	Definition	Comments	Figure
Median Frequency	Frequency allowing the spectrum to be divided into two regions of equal power [39]	Enables the degree of compression of the power spectrum to be evaluated	A.1 and A.2
RMS	$\sqrt{\frac{1}{N} \sum_{i=1}^N x_i^2}$	This will be an estimator of the amplitude of the signal, that is, its intensity	-
Total Power	Corresponds to the whole power contained in spectrum of analogical/digital signals, determined by the integral/sum	Evaluates the strength of the signal, equivalent to the RMS to a certain extent	A.1
Major Frequency	Coordinate of the centroid in the frequency dimension of the scalogram	Function equivalent to Median Frequency	A.3
Major Time	Coordinate of the centroid in the time dimension of the scalogram	Indicates the phase of the contraction cycle where the intensity of the signal is highest	A.3
Mean Power	Mean power in the components included in the scalogram	-	-
Area	Number of pixels in the post-segmentation convex-hull of the scalogram	-	A.4
Volume	Convex volume from including the power dimension in the (two-dimensional) pixels	Similarities with Total Power	-
Time (Frequency) Dispersion	Length (Height) of the convex-hull	Degree of compression of the information in the time and frequency dimension	A.5

However, taking into account the sub-divisions made in the references consulted [16, 17, 24, 45], a possible sub-division is shown in Figure 2.10.

There are two main types of fatigue: **Subjective Fatigue** and **Objective Fatigue**.

In the first case, the physical incapacity is caused by psychological factors, such as a loss of motivation or concentration [24].

In the second case (Objective Fatigue), there is a change in physiological processes, namely a loss of efficiency in relation to standard function or the production of metabolic waste which disrupts the normal sequence of events. This is the type of fatigue being studied and the one for which the projected system is intended.

Table 2.2: List and description of the various ECG indexes studied

Feature	Definition	Comments	Figure
maxRR, minRR and avgRR	Maximum, minimum and average duration of the RR intervals contained in the tachogram	Intended for evaluating heart rate (inverse)	A.6
SDNN	Standard deviation of the duration of RR intervals	Evaluates the degree of dispersion of the duration of RR intervals in relation to the average value ( $\propto$ HRV)	A.7
rmsSD	Average quadratic deviation of the difference in duration between consecutive RR intervals	-	-
Triangular Index	Fraction between the total number of RR intervals and the number of RR intervals in the modal <i>bin</i> of the histogram [40]	Equivalent to SDNN but less susceptible to outliers	A.8
SD1	Parameter extracted from the Poincaré plot in a non-linear analysis of HRV	Describes short-term heart rate variability [40]	-
SD2	<i>Identical to SD1</i>	Describes long-term heart rate variability [40]	A.9
SD1/SD2	Proportion between short- and long-term heart rate variability	-	-
ULF VLF LF HF Power	Power contained in the tachogram power spectrum frequency bands [0;0.003] Hz (ULF), [0.003;0.040] Hz (VLF), [0.040;0.150] Hz (LF), [0.150;0.400] Hz (HF)	Reflecting thermoregulatory mechanisms (VLF), sympathetic modulation (LF) and parasympathetic modulation (HF) of HRV [41, 42]	A.10

Fatigue can be further divided into two branches, depending on the source of the physiological “disturbance”: **Central Fatigue** and **Peripheral Fatigue** [45].

Fatigue is classified as peripheral when the cause occurs in the muscle tissue and is triggered by changes in ionic concentrations in the intracellular environment (sarcoplasm) [45].

Central fatigue is associated with changes at a neuronal level which ultimately influence the nerve impulse responsible for muscle contraction, affecting ability to exert a force.

There is another possible source of physiological fatigue, which is a breakdown of activity at the neuromuscular junction [17].

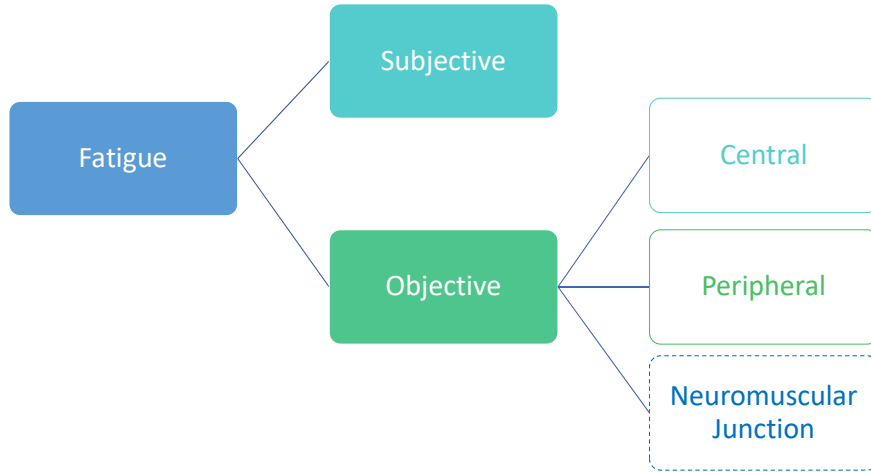


Figure 2.10: Sub-division of Fatigue by Type and Origin

### 2.4.3 Muscular Fatigue Causes

Section 2.4.2 covered how fatigue is classified based on its origin, but the causes have not been explicitly mentioned: that is the purpose of this section.

However, before proceeding to a list of the causes, it is necessary to understand the mechanism that precedes the voluntary contraction of skeletal muscle, considering that any of the possible causes of fatigue is rooted in the failure of one of the links in this fascinating mechanism.

If one considers the physiological framework for the muscular contraction mechanism (section 2.1.1), one can gain a more intuitive understanding of the causes of fatigue, that is, what leads one of the steps in the mechanism to fail [25].

The failure points (which refer to the origins of fatigue defined in section 2.4.2) may lie in the **Central Nervous System**, in the **Neuromuscular Junction** or in the **Muscle Fibre** itself [46] (Table 2.3).

Table 2.3: Failure points and causes/consequences of fatigue setting in

Central Nervous System
- Decrease in the recruitment of motor units
- Change in the rate at which muscle fibres are fired/stimulated by motor neurons
Neuromuscular Junction
- Influencing of the transmission of the chemical signal in this region
Muscle Fibre
- Variation in the conduction velocity of the nerve impulse in the Sarcolemma and in the T-tubules
- Failure in the release of $Ca^{2+}$ by the sarcoplasmic reticulum
- Inability of $Ca^{2+}$ and troponin C to bond, causing the binding sites on actin to close

The causes originating in the central nervous system may result from a blocking effect affecting the transmission of the nerve impulse, known as neuromuscular blocking [46] at the acetylcholine receptors in the neuromuscular junction and in the membrane of the motor neurons, before the neuromuscular junction.

Some drugs have this effect by causing the channels in the membrane of the muscle fibre to lose their sensitivity to the chemical message contained in the neurotransmitters, making it impossible for the action potential to propagate along the sarcolemma and, ultimately, for the muscle to contract [47].

The causes originating in the neuromuscular junction, meanwhile, may lie in the pre-synaptic region owing to a high rate of stimulation of the terminal branches of the nerve, or in the post-synaptic region owing to reduced receptor excitability [46].

In terms of causes intrinsic to the muscle fibre, these are caused by a deficit in energy production (glycolysis and aerobic respiration) or an imbalance in electrolyte gradients, responsible for the input of nutrients and the output of metabolic waste [46].

Nutrients are essential for maintaining stability at the cellular level, so a deficit in supply can have a considerable effect on the vital functions of the muscle cell.

With regard to metabolic waste, this may be harmless, but, in some cases, if it accumulates, it can affect the cell. Lactic acid, for example, plays a role in decreasing the intracellular  $pH$ .

Nevertheless, we should finish this section with a brief comment, because we refer to muscular fatigue causes, which, in a first perspective, could include the skeletal and cardiac muscle.

However it only covers the skeletal muscle, considering that the cardiac muscle does not enter in fatigue, due to the mitochondria overpopulation and the higher density of capillaries that bring the required nutrients for myocardium cells to produce energy.

So with HRV analysis, when we mention (section 2.1) that can give us information of fatigue in a global perspective is because of the fact that the same physical activity, that locally affects the muscle function, can also have impact in cardiopulmonary terms, and since the skeletal muscle is dependent of the blood supply, so the muscle is indirectly affected by the non-local (global) effect of physical activity that induces fatigue.

#### 2.4.4 Literature Review

The literature reviewed, as part of the project, revealed a wide range of approaches to evaluating fatigue (Figure 2.11), enabling this state to be observed from multiple perspectives and supporting the idea that fatigue is a phenomenon with repercussions at various physiological levels.

This chapter will therefore provide a summary of the conclusions reached in other studies.

Particular attention will be given to studies based on EMG and ECG signals, considering that they correspond to the signals investigated as part of this thesis.

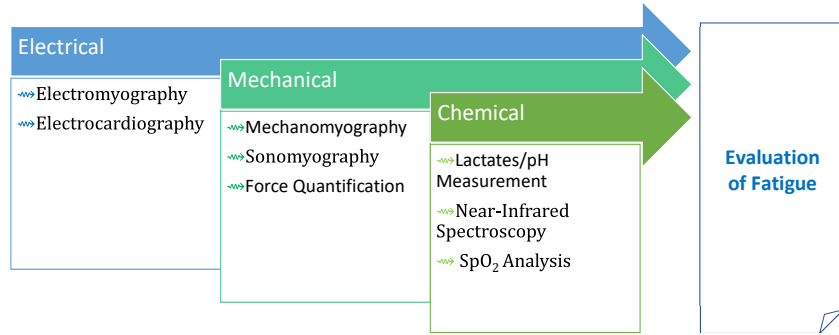


Figure 2.11: Explanation of the set of physiological signals with the potential to provide information on the fatigue state

#### 2.4.4.1 Studies Based on EMG

Given the electrical nature of the nerve impulse which reaches the muscle fibres and causes them to contract, Electromyography is a logical means of analysing fatigue, through the consequences and effects that are produced in the EMG signal.

The work conducted by Carlo De Luca and Roberto Merletti, among other investigators, in the evaluation of muscular fatigue contributed towards a significant advance in fatigue monitoring, with the EMG signal processing techniques residing in the time domain and the frequency domain.

Analysis in these domains produced very consistent results which are considered to be well established, namely the fact that the amplitude of the EMG signal, described by the *Root Mean Square* (RMS) and *Mean Absolute Value* (MAV) estimators, increases when fatigue arises and the median frequency decreases considerably, with the spectrum being compressed in the region of low frequencies owing to the decrease in the conduction velocity of the nerve impulse in the muscle fibres [16, 17].

It should be highlighted that the increase in amplitude occurs in surface EMG, since at a depth the filtering effect of the skin (which acts as a low-pass filter) ceases to apply and the amplitude does not display the same relationship with regard to fatigue [48].

The EMG signal is analysed in frequency domain by applying the Fourier Transform or methods which combine time and frequency, such as Short-Time Fourier Transform (STFT) and Wavelet Transform, with the latter method producing the best results [49].

Transposing the EMG signal to the time-frequency domain using the Wavelet Transform frees the investigator from constraints relating to the criterion of stationarity, making the technique rather appealing.

However, unlike the Fourier Transform, in this case the decomposition of the EMG signal will be synthesised in the form of an image (scalogram), in such a way as to reflect the information from the time dimension and the frequency dimension simultaneously.

Each pixel of the scalogram is associated with a frequency and time pair  $(f, \Delta t)$ , allowing the analyser to see the frequency composition of the signal in a given time window, something that was not explicit in the Fourier Analysis.

Given the robustness of the method, characterised by lower variability and greater statistical meaning in the parameters established [50], it is increasingly being exploited in studies aimed at evaluating muscle fatigue.

With this method is possible to extract a range of indexes that are typically applied to images, such as the determination of the centroid or the convex area.

Once the image has been segmented, to select regions with a greater quantity of information, using the Otsu method [18, 51], the processing can be limited to the components of the scalogram with the most information.

One of the reference studies [18] measures the effects that changing the exercise intensity (resistance offered by the cycle ergometer) has on the scalogram and the degree to which the “Wavelet Indexes” vary over time.

In this study, the following indexes were extracted: **Work Rate**, **Area**, **Mean Power**, **Main Frequency** and **Median Power Frequency**. Only **Work Rate**, **Area** and **Mean Power** are shown to undergo consistent changes, in the direction of growth, when exercise intensity is increased.

In addition, over time (and therefore as fatigue is acquired), these indexes evolve, with different trends depending on the exercise intensity (73%, 100% and 133%), as shown in Table 2.4.

Table 2.4: Summary of the results from the study [18]

Intensity	Work Rate	Area	Mean Power	Median Power Frequency
73%	↑	↓	↑↑	↓
100%	↓	↑	↑	↓
133%	↓↓	↑↑	↓	↓↓

Owing to the fact that **Median Power Frequency** is the parameter with the most consistent evolution (decrease due to the emergence of fatigue) for the various exercise intensities, this index is promising in this Wavelet Analysis, as already demonstrated in the Fourier Analysis.

In another study [50], it is observed that in specific frequency bands of the scalogram there is a well-defined increase in its power, partially corroborating the global evolution trend of **Mean Power** in [18].

#### 2.4.4.2 Studies Based on ECG

The need for the muscles to produce more energy during their activity means that the nervous system must increase blood flow in order to supply more oxygen to the tissues. This necessarily causes an increase in the heart rate as fatigue sets in [52].

In a recent analysis, L. Schmitt et al. identified four fatigue patterns in sportspeople (skiers).

It was observed, with greater prevalence, that the power of the signal which describes heart rate variability (comparison of heart rate variability – RR interval – in fatigue conditions with the median value of multiple tests in non-fatigue conditions) over time decreases with the fatigue state, a change which is accompanied by an increase in the heart rate identified in other studies [19].

Heart rate variability may be evaluated using multiple indexes, as demonstrated in section 2.3.

However, despite the diversity of HRV indexes, only a small number are included as potential fatigue indexes.

In the vast majority of literature references gathered on the evaluation of fatigue state using HRV analysis, processing is centred on the extraction of parameters from the frequency domain, there being one case where the non-linear indexes SD1 and SD2 are included [20].

To extract frequency parameters, a power spectral analysis (PSD) of the signal is required. The transposition can take place using non-parametric means, which despite being less precise are more efficient in computational terms, namely Fast Fourier Transform (FFT) or parametric methods which are more sensitive but also computationally demanding [53].

In any of the approaches, the spectrum obtained may be sub-divided into the four bands (ULF, VLF, LF and HF), as shown in Table 2.2.

Fatigue of a neurological origin is the most studied, which makes sense considering that heart rate variability is caused by the overall action of the autonomic nervous system, and can be triggered by the integration of multiple factors at the same time.

Even though intense muscular activity produces a response in the ANS (variations in the sympathetic component) [54] and a resulting change in the heart rate and heart rate variability, this isolated origin is only one contribution to the decision-making process of the ANS, which receives stimuli from other organic systems (which could lead to a contradictory change in the sympathetic component) [55].

The conclusions drawn for the skiers were partially validated in top-level swimmers, and once again various fatigue patterns were recorded (three, in this particular case), where the most common trend was that of a decrease in the LF and HF components, followed by an increase in heart-rate [21].

However, this decrease in the sympathetic predominance of the ANS (represented by the LF band) is contradicted by other studies in which it is found to increase [56, 57].

The difference may be partly explained by the signal acquisition conditions before and after the exercise [21], or during prolonged conduction [57].

The position of the volunteer during the signal acquisition period may also be relevant, since this influences the activation of low-pressure baroreceptors (ANS inputs) and therefore their response and effects on heart rate [55].



### 2.4.4.3 Alternative Methods

As explained in Figure 2.11, the fatigue state can be monitored through physiological signals originating in chemical or mechanical events.

In mechanical terms, particular mention may be made of mechanomyography (MMG) and sonomyography (SMG), which record acceleration variations during muscle contraction and capture images with an ultrasound system.

Some of the studies consulted show consistent results in relation to isometric contractions, reporting the increase in the amplitude of the MMG signal [58–60]. This is in contrast to what is observed in dynamic contractions [23, 61].

Sonomyography is a technique whereby images are acquired using ultrasound, based on a principle similar to that of sonar: a device formed of an ultrasound transmitter and an ultrasound receiver is applied to the surface of the body, surrounding the muscle.

In one particular study, the authors concluded that the thickness of the muscle increased during contraction, that is, as the fatigue state began to set in, although in a non-linear way, with a more marked initial growth followed by a phase with growth at a lower rate [24].

In terms of methods for monitoring fatigue through phenomena that occur at a chemical level, particular mention may be made of Near-Infrared Spectroscopy (NIRS) and the measurement of  $pH$  or Lactates.

Owing to the accumulation of pyruvate in the intracellular environment (of the muscle fibre in conditions of intense activity), when its rate of production in glycolysis exceeds the rate of consumption in aerobic respiration, this molecule undergoes oxidation. Lactic acid forms and subsequently dissociates, releasing  $H^+$  ions into the intracellular environment and leading to a reduction in the  $pH$  (Figure 2.12).

This sequence indicates that in fatigue conditions there will be a decrease in  $pH$  and an accumulation of lactic acid [25].

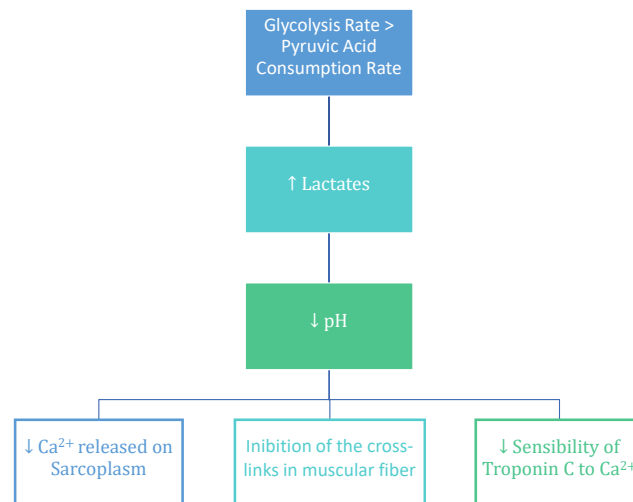


Figure 2.12: Cause-effect structure relating to the impact that a change in  $pH$  and lactate concentration has on the functioning of the muscle fibre [25]

Finally, the NIRS technique is very promising, and is already used in one of the existing commercial systems (*BSX Insight<sup>TM</sup>*).

This technique employs a coupled system comprising a point that emits electromagnetic radiation in the near-infrared region and a receiver.

This type of radiation can travel through tissue relatively easily, but ends up being absorbed by haemoglobin. The retransmission is then detected by the receptor, and the transmitted light shows characteristics and intensity different from those initially emitted.

The variation in the properties of the electromagnetic radiation (intensity) will make it possible to estimate, using a mathematical model, the proportion between the oxidised form of haemoglobin, which transports the oxygen to the tissues, and the reduced form (deoxyhaemoglobin), which changes over the course of the muscular activity [62, 63].

The mathematical relationships and models typically used for the final quantification of this parameter are the Modified Beer-Lambert Method [63] (estimate of the variation in the concentration of oxy-Hb and deoxy-Hb forms over time) together with the Tissue Oxygenation Index (TOI) [26] for estimating the oxygenation level in the muscular region, an increase in the oxidised form and a decrease in the reduced form of haemoglobin being observed.

## 2.5 Acquisition and Monitoring System

Before any signals can be processed, they must be acquired, and therefore the system for monitoring the fatigue state is dependent on an *hardware* component.

However, owing to the role played by *Plux* in the project, it was unnecessary to plan the acquisition system, considering the multiple and wide-ranging solutions commercialised by the company. One of the devices used in the project will be described in this section: *biosignalsplux*.

On its own, *biosignalsplux* has the capacity to acquire 4 to 8 signals simultaneously, using its digital channels.

The 8-channel hub has the capacity to pair to other hubs, thus increasing the number of channels available (Figure 2.13a).

After the acquisition, it is necessary to extract information from the collected signals, which can be achieved by processing them on a computer. *biosignalsplux* can communicate with the personal computer of the user by means of *Bluetooth* technology.

As soon as the file with the acquired signals is transmitted, the *software* component comes into play for the processing step.

*Plux's OpenSignals* (Figure 2.13b) platform for monitoring signals collected by its devices is available free of charge, and the user has the option of adding more functions with *plugins* for specialised processing of each type of signal.

The *plugins* work based on the interaction of three components or programming languages: *HTML*, *JavaScript* and *Python*.

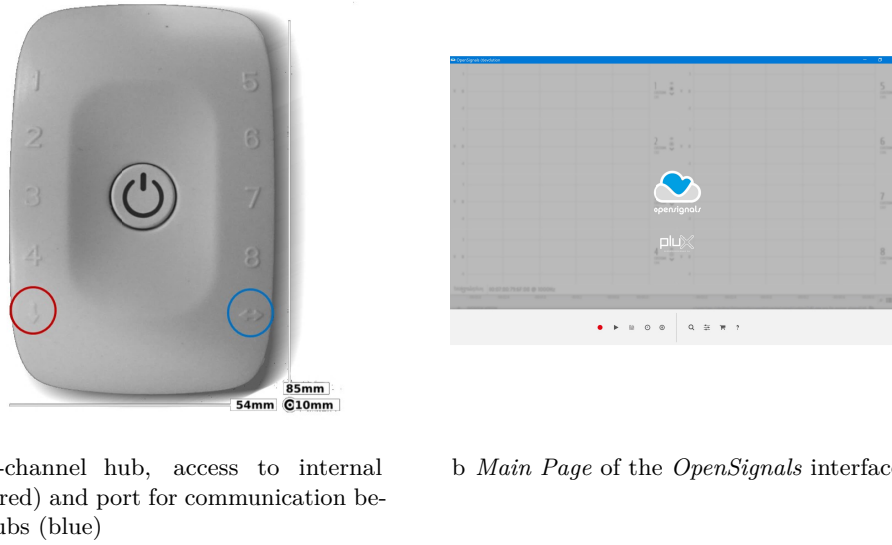


Figure 2.13: Illustration of the *hardware* and *software* component used to acquire and monitor the physiological signals

The *HTML* component is used to construct the interface, this static structure being made dynamic through the event management provided by the programming in *JavaScript*.

For its part, the *Python* component carries out all the processing functions, allowing for quick and efficient extraction of the features of each type of physiological signal.

The system envisaged for monitoring the fatigue state is based on this approach, and is a *plugin* of *OpenSignals*, that is, it is not an independent programme but rather a set of processing functions incorporated into the existing solution.

## 2.6 Classification Systems - *Support Vector Machines*

In this project, a binary classifier of the *Support Vector Machine* (SVM) type was implemented. The classifier returns a “**Positive Fatigue**” result when the fatigue is setting in and a “**Negative Fatigue**” result when the body is in the recovery phase and the level of fatigue is dropping.

By virtue of the above, it is possible to provide the user with objective and automatic information about the fatigue state.

A *Support Vector Machine* essentially works based on Cartesian logic, given that each example corresponds to a point with a number  $N$  of coordinates equivalent to the number of features analysed, that is, each feature defines a dimension of the space.

This type of classification algorithm falls within the hyperplanes class, the training phase taking place through a supervised method.

As Schölkopf states [64], in the training phase of a SVM, the objective is to find a function  $f$  generated from a given number of training examples, with the capacity to correctly classify any new testing example.

This type of classifier was initially intended for binary problems [65], but may be extended to studies with a greater number of classes using the *1-vs-All* method, although alternative approaches do exist [66].

A hyperplane is a generalisation of the notion of a “plane” typical of three-dimensional space, allowing any space to be divided into two closed and convex regions (binary classifier), like in Figure 2.14, or, in a problem with  $M$  classes, into  $M$  different regions by combining the various hyperplanes generated in the *1-vs-All* approach.

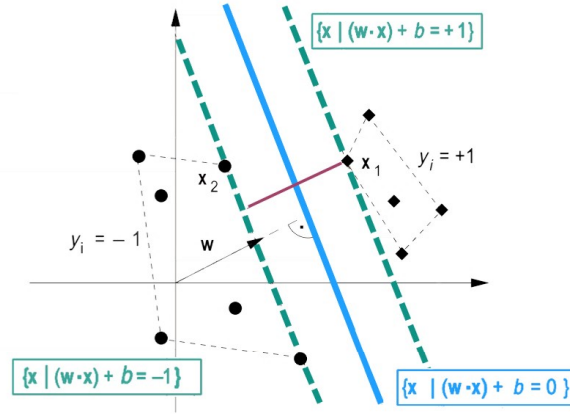


Figure 2.14: Geometric illustration of the concepts taken into account in an SVM of the binary type, showing the convex-hull containing the training points of each class (delimited by the black line), the auxiliary margins including the *support vectors*  $x_1$  and  $x_2$  (green dotted line) and the shortest segment linking the two convex-hulls (red) [64]

The training phase of an SVM will be geared towards the search for the hyperplane  $(\vec{w} \cdot \vec{x} + b = 0, \vec{w} \in R^N, b \in R)$ <sup>3</sup> that allows the distance or separation between the two classes under analysis to be maximised, giving rise to a decision function as follows:

$$f(\vec{x}) = \text{sign}(\vec{w} \cdot \vec{x} + b) \quad (2.1)$$

Geometrically, this maximisation of the separation between two classes corresponds to generating, for each class, the convex-hull that includes all the training examples.

Next is the determination of the smallest segment which links the boundaries of the two convex-hulls and consequently the optimum hyperplane, considering that they are perpendicular to each other and cross at the central point of the segment.

For each class, the point located at the shortest distance from the convex-hull of the other class is a *supporting vector*.

Objectively it will correspond to an optimisation problem where the aim is to find the hyperplane that allows the distance to be maximised in relation to the various training points [67].

<sup>3</sup> $\vec{x}$  being the vector with the value of the features associated with the testing example and  $\vec{w}$  and  $b$  being parameters determined during the classifier training phase

## Methods Used

In normal conditions the body is in a state of equilibrium and internal harmony. However, drawing an analogy with Newton's third law, for any disturbance (action), there is a reaction.

When studying a process at the physical or physiological level, one analyses the effect that a disturbance of certain variables has, with the aim of gaining a better understanding of the mechanism that takes place between “action” and “reaction”.

In order for the impact of the disturbance of a certain condition to have scientifically enlightening results, a methodical procedure must be followed. The key purpose of this procedure is to ensure that the only condition which varies between tests or over time is associated, ideally, with the variable being analysed.

An experimental protocol allows the investigator to come close to this objective, although it is not always possible to produce a result which is influenced exclusively by the variable under analysis.

In this project, the variable being studied is **Fatigue**. The aim is to induce it in order to record the impact in terms of muscle and heart activity, by means of the corresponding electrophysiological signals (EMG and ECG).

Taking into account this intention, an experimental protocol was prepared for conditions similar to those of indoor cycling. In this respect, mention should be made of the important collaboration with the Laboratory of Motor Behaviour (FMH), through his members Prof. Dr. Pedro Pezarat, Prof. Dr. Gonçalo Mendonça and Dr. João Vaz, which allowed the studies on fatigue conducted by both parties to converge.

With the data that were supplied, it was possible to evaluate the existence of trends related to the fatigue state by applying several different methods, which will be explained in this chapter.

### 3.1 Induction of Fatigue - Experimental Protocol

In the tests, signals of a physiological origin were collected (EMG and ECG), the procedure being split into two days separated by a minimum recovery period of 24 hours.

The study targets volunteers who regularly practise sport, aged between 20 and 35 years, because this corresponds to the period in which physiological functions and physical capacities reach maximum efficiency [68].

In addition, the protocol was aimed at male volunteers only, given the fluctuations in the rate of oxygen consumption in female individuals and their specific heart rate variability as a result of the menstrual cycle [69].

Including both genders in the sample would introduce entropy into the analysis of results, considering that the analyser would be exposed to a variable which he or she cannot control.

The procedure to be carried out on each protocol day comprises the following conditions:

- **Day 1 (30 minutes)**

- Practice of ergometric exercise (replicating the conditions of cycling) with an incremental level of difficulty, achieved by progressively increasing the power/resistance in the pedalling cycle;
- Collection/analysis of the gases exhaled during the expiratory process, with the aim of determining the volunteer's ventilation thresholds. This makes it possible to establish his profile and measure his physical condition, so that the test on "Day 2" can be adapted to these specific characteristics;
- The procedure is continued until exhaustion;

- **Day 2 (30 minutes)**

- Based on the power profile established on "Day 1", the volunteer must undergo a test on **Severe Domain** (defined as **Rigorous Effort** on the protocol). The test is made rigorous by setting the ergometer to the corresponding power level;
- The test ends when the volunteer stops being able to maintain a constant pedalling rhythm ( $60 \pm 5$  RPM);

The detailed description of the steps contained in the protocol can be consulted at Appendix B.

### 3.1.1 Submission to the Ethical Council of NMS

Given the extremely demanding nature of the tests for inducing fatigue, the protocol needed to be approved by an external and independent body. A request was therefore sent to the Ethical Council of Nova Medical School (NMS).

For the request for approval of the Experimental Protocol by the Ethical Council of NMS to be valid, various documents had to be prepared in order to comply with the requirements established in the guidelines provided by this body [70]. These documents are as follows:

- ① **Form for project submission<sup>1</sup>;**
- ② ***Curriculum Vitae* of the individuals involved in the research;**
- ③ **Declaration of Authorisation to use the infrastructure where the tests are being conducted (*LIBPHYS-UNL*);**
- ④ **Data Disclosure Policy Declaration;**  
The purpose of this was to formally record the authors' commitment to preserving the rights of the study participants and limit the disclosure of the collected data to the situations accepted by the volunteer and specified in the *Informed Consent Sheet*
- ⑤ **Informed Consent to be given to the volunteer;**
- ⑥ **Study Protocol;**  
The objectives of the project to which the protocol relates were set out and the repercussions for the scientific community and for society were explained.  
In addition, the period and site/infrastructure in which the tests took place/would take place were specified.
- ⑦ **State of the Art on the project topic;**
- ⑧ **Experimental Protocol;**
- ⑨ **Description of the Instruments used;**

All the documents were submitted for evaluation by the Ethical Council on 16 January 2018, and were allocated the identifier 02/2018/CEFCM.

Approval of the protocol will allow data to be acquired on a large scale in the future, thus complementing the pilot acquisitions (prior to the submission to the Ethical Council) analysed during the thesis project.

The pilot data were obtained as part of a series of acquisitions led on Laboratory of Motor Behaviour (FMH) by Prof. Dr. Pedro Pizarat, Prof. Dr. Gonalo Mendona and Dr. Joo Vaz during a PhD in the area of fatigue evaluation, with the particularly purpose of understanding its effects in the dynamic stability of biological systems.

---

<sup>1</sup>Available at [http://www.nms.unl.pt/main/alldoc/FCM/CEFCM\\_-\\_Formulrio\\_para\\_submisso\\_de\\_projectos\\_1.pdf](http://www.nms.unl.pt/main/alldoc/FCM/CEFCM_-_Formulrio_para_submisso_de_projectos_1.pdf)

### 3.1.2 Reformulation of the Submitted Documents

Following its first evaluation, the Ethical Council requested supplementary information in order to answer the following questions:

- ① Is the volunteers' health evaluated before the tests are carried out, or is it known by the recruitment site ?
- ② Does the laboratory chosen for the tests (LIBPHYS) have basic life support equipment and staff who are trained in using it ?

One additional document was also requested: a declaration from the National Data Protection Commission (CNPd) to approve the collection of the volunteers' personal data.

Thus, in order to ensure that the requirements underlying the above questions be met, the location where the tests take place have to changed and the respective declaration from the CNPD also need to be requested.

The resolution of these aspects is under development, and there are good prospects in fulfilling the requirements explained by the Ethical Council.

With the positive answer to these questions, the hypothesis that the protocol be approved, and therefore can be applied in the future phases of the project, remains.

### 3.1.3 Calibration Protocol

In order to define a global fatigue index (Section 3.3), the current version of the system requires a calibration protocol in which fatigue is induced in a controlled manner.

The protocol submitted for "Day 2" covers this function, consisting of an ergometric test at constant power, which would be determined in the procedure of "Day 1".

Given that the protocol of "Day 1" requires specialised instruments, it would not be feasible in the day-to-day, and it was proposed that pre-defined power values derived from an empirical measurement taken by Coggan be used [71].

Table 3.1 shows the median value of Maximum Power Output (MPO) during a 5-minute test<sup>2</sup> for volunteers who do not practise cycling professionally.

Table 3.1: Pre-defined values of Maximum Power Output (MPO) by gender

Males (W/kg)	Females (W/kg)
2.74	2.26

The power associated with the calibration test will be obtained by means of the expression:

$$Power(Day\ 2) = MPO(Gender) \times mass_{volunteer} \quad (3.1)$$

---

<sup>2</sup>Will be a relative value of power per unit of mass, corresponding in theory to the load per unit of mass that the volunteer manages to bear during a test of approximately 5 minutes, before reaching exhaustion



## 3.2 Identification of Fatigue Indexes

EMG and ECG signals were the means selected for achieving the goal of objectively evaluating the fatigue state. However, the data acquisition alone does not allow immediate conclusions to be drawn about this state.

Signals constitute a means with high information potential, and must be processed in a manner that is adapted to the specific characteristics of the problem to be solved.

Objectively, this process of extracting knowledge is carried out by analysing linear or non-linear parameters derived from the signals.

However, it is not always possible to make generalisations about the problem situation based on the absolute value of these parameters (also referred to as indexes or features), as is the case with fatigue.

The process of acquiring fatigue varies considerably from subject to subject and between muscles, depending additionally on the type of contraction [72, 73]. It is therefore necessary to find an alternative way that makes it possible not only to extract knowledge about this phenomenon but also to make generalisations about it.

One of the possible approaches, followed in this project, consisted in centring the analysis on the evaluation of the evolution trend of a given index over the course of the acquisition, that is, during the disturbance of the fatigue variable, by processing the data and extracting the indexes over a sliding window<sup>3</sup>. This chapter explains two methods used to identify trends related to the acquisition of fatigue.

### 3.2.1 Assumptions

In simple terms, a trend can be considered to be a binary concept in which the possible result will be growth or decline, mathematically inferred by generating the linear regression line which best fits the experimental data.

The generated line is characterised by a slope, where negative values are indicative of a declining trend while positive values relate to a growing trend.

Based on this principle, the indexes described in section 2.3 were extracted from the EMG and ECG signals acquired in the fourteen pilot tests (Table 3.2), and their evolution trend was evaluated using two methods, which are set out in the sections that follow.

The selection criterion of some of the indexes is because of the fact that were frequently referenced in the studies on fatigue and the rest were studied in a convergence logic, since they were already entered in the *Plux* EMG and HRV processing systems. It was therefore interesting to see whether they could be adapted to this new purpose.

---

<sup>3</sup>Each window includes a segment of the signal, and the value of the index under analysis is extracted by considering the samples contained in the window.

After the extraction, the window moves in such a way as to cover another segment of the signal. This is followed by another index extraction.

The process is repeated consecutively until the last sample of the signal is reached. The final result is a time series with a number of samples that matches the number of windows, and with a time coordinate that is the instant corresponding to the centre of the window and the value of the index

Table 3.2: Properties of the population sample formed by 14 subjects [74]

Variable	Value $\pm$ Standard Deviation
Age (years)	$24.5 \pm 3.6$
Body mass index ( $kg.m^{-2}$ )	$23.7 \pm 1.7$
$VO_{2max}$ ( $mL.kg^{-1}.min^{-1}$ )	$52.5 \pm 5.7$
Power at $VO_{2max}$ (W)	$204.5 \pm 33.7$

An index denoting a trend for a given subject in isolation is not of interest, but if this trend is observed in all or a large part of the sample, it may constitute a pattern in the EMG/ECG signals, relating to the “fatigue” variable, and the index will therefore be an indicator of this state.

It should be highlighted that the pilot acquisitions, where the two trend identification methods were applied, come with some constraints, given that the EMG and ECG signals were not recorded synchronously and there are errors in the acquisition of three subjects’ ECG data. This means that the sample of 14 subjects is reduced to 11 for the analysis of electrocardiographic data.

The EMG signal was collected for five muscles located in the lower limb: *Rectus Femoris*, *Vastus Lateralis*, *Vastus Medialis*, *Semitendinosus* and *Biceps Femoris*. This was done exclusively during the period in which the volunteer acquired fatigue.

The ECG signal, meanwhile, was acquired during and after the period in which fatigue was induced, which means that information was obtained about when the “fatigue” variable evolves in the additive direction and when it evolves in the subtractive direction, in the recovery phase.

To evaluate whether an index constitutes a fatigue index, it is necessary to consider its evaluation in opposing conditions, that is, when the “fatigue” variable arises and when it dissipates.

In the ECG signal, data were obtained in these two situations, unlike the EMG signal, considering no information exists about the recovery phase.

However, the setting-in of fatigue and the speed at which this takes place depends on the individual characteristics of each muscle and its level of activity during the task being monitored.

Some authors [75, 76] point out that in conditions similar to those of the protocol used, the *Vastus Medialis* muscle is quite resistant to the installation of fatigue. The decision was therefore made to classify the EMG signal from this muscle as a counterexample to the setting-in of fatigue.

Ideally fatigue should not be present, in order for the example to be robust. However, taking into account the specific characteristics of the data collected, this approach is the best approximation of the conditions in which the “fatigue” variable dissipates or at least does not set in.

Given that a sliding-windows system is used to extract the indexes, there are two methodological variables to be considered: the most suitable window size for analysing the trends and the respective time-step.

Thus, the two methods that follow were intended not only to produce a list of indexes with the potential to provide information about the fatigue state, but also to define the ideal conditions for transforming this potential into knowledge.

### 3.2.2 Empirical Method

The first method that was followed with the aim of identifying trends in the collected EMG and ECG signals was an empirical process based on a voting system [77, 78]. It was a simple and introductory approach intended to flag up indexes with the potential to provide information about the fatigue state.

While this list was not definitive, it provided useful indexes that were partially corroborated at the end by the second method applied (detailed in the next section).

During the processing, an analysis was conducted of the EMG signal in 14 subjects and of the ECG signal in 11 subjects, and various processing window sizes were combined with different time-steps (the processing was repeated for each combination of window size and time-step).

For each type of analysis, characterised by a window size ( $wind_{size}^i$ ) and by a time-step ( $wind_{step}^j$ ), forming a  $[wind_{size}^i, wind_{step}^j]$  pair, the evolution time series of each  $Ind^k$  index was obtained, and the linear regression line which best fitted the experimental data was then generated.

The slope and the correlation coefficient were stored in a text file, each line consisting of the fields:

```

subject_under_analysis | window_size | space_between_windows
name_of_parameter_under_analysis | correlation_coefficient_r2 | slope_m

```

The information was subsequently organised in a matrix format, using two matrixes.

In both matrixes, each cell had the following headings: the type of analysis ( $[wind_{size}^i, wind_{step}^j]$ ) to which relates and the name of the parameter (Figure 3.1).

The content of the cells in **Matrix A** is the average value of  $r^2$  (associated with the  $[wind_{size}^i, wind_{step}^j]$  combination), taking into account all the subjects.

In **Matrix B**, each cell contains a *score* calculated based on the polarity of the slope.

The *score* to be incorporated into the  $[wind_{size}^i, wind_{step}^j, Ind^k]$  cell of **Matrix B** is obtained by counting the number of positive slopes and the number of negative slopes, as demonstrated by the following expression:

$$score = \frac{\#m_+ \times 1 + \#m_- \times (-1)}{\#Subjects} \quad (3.2)$$

			Parameter				
			$Ind^1$	$Ind^2$	$Ind^3$	$Ind^4$	...
Type of Analysis	$wind_{size}^1$	$wind_{step}^1$					
	$wind_{size}^1$	$wind_{step}^2$					
	...	...					
	$wind_{size}^2$	$wind_{step}^1$					
	...	...					
	$wind_{size}^3$	$wind_{step}^1$					
	...	...					

Figure 3.1: Appearance of the matrix summarising the parameters of the linear regression applied to the processing results

A *score* very close to 1 indicates that the evolution trend of the  $Ind^k$  parameter, when fatigue arises, will be in the upward direction, with the evolution series of the index denoting an increase over the course of the acquisition in most or all of the subjects.

Inversely, a *score* close to -1 defines a downward trend for the population sample being studied, with a large number of subjects displaying an  $Ind^k$  evolution in the downward direction.

A *score* close to 0 represents incoherence, that is, some subjects display an evolution in the upward direction and others in the downward direction, with the “negative” votes cancelling out the “positive” votes in the numerator of expression 3.2.

In this situation, the index does not show a consistent evolution for the various subjects and therefore should not be considered to be a fatigue index.

Thus, the *score* in the  $[wind_{size}^i, wind_{step}^j, Ind^k]$  cell of **Matrix B** defines the dominant direction of the  $Ind^k$  evolution trend and how regular and consistent it is in the subject sample.

In contrast, the cell of **Matrix A**, with the same coordinates, provides an indication of the quality of the linear adjustment, establishing whether or not the evolution of the index denotes linear behaviour.

As mentioned, the *score* may assume values between -1 and 1, giving rise to the fundamental question of how to know whether a given score does or does not signify the existence of a trend in the data.

The criterion used was strictly empirical and was based on a probabilistic logic.

Essentially the aim was to evaluate the *score* on a new level of abstraction, that is, by establishing a correspondence between the domain  $D$  and the codomain  $CD$ :

$$\begin{aligned}
 D &\rightarrow CD \\
 [-1, 1] &\rightarrow \{Coherence\ Zone, Incoherence\ Zone\}
 \end{aligned}$$

In order to ensure that it is not more probable for the class “Coherence Zone” or “Incoherence Zone” to be attributed, the decision was made to divide the domain into two parts of equal size ( $[-1, -0.5] \cup [0.5, 1] \rightarrow$  “Coherence Zone” and  $] -0.5, 0.5[ \rightarrow$  “Incoherence Zone”).

An index  $Ind^k$  would be considered to be a potential indicator of the fatigue state if the two following conditions were met:

- ① The modulus of the average value of the *score*, including all the types of analysis, must be greater than 0.50 during the fatigue induction phase (falling within the “Coherence Zone”);
- ② Between the fatigue acquisition phase and the recovery phase, the average value of the *score* must invert the signal or switch to the “Incoherence Zone” characterised by an average modulus *score* of less than 0.50.

Despite being based on logical criteria, the method presented is empirical in nature and therefore carries with it some subjectivity.

In order to ensure certainty in the interpretation of the results produced, a validation process was carried out.

There was one relevant doubt relating to randomness, that is, it was necessary to know whether the *score* might denote values in the coherence zone when faced with a random set of samples.

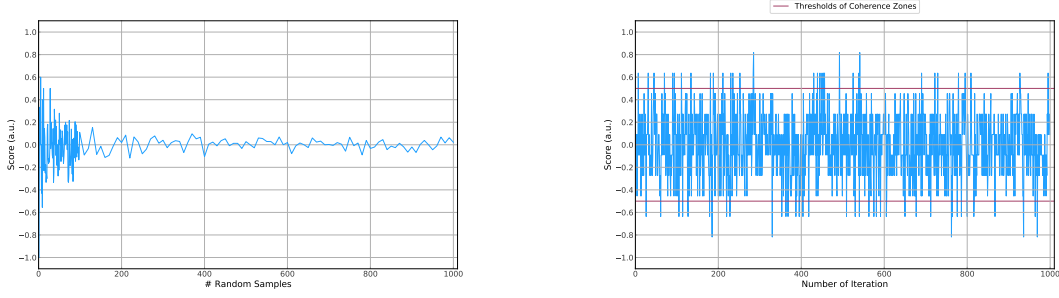
The most direct approach for resolving this doubt was by generating a set of  $N$  random slopes, the respective *score* being calculated as it was for the population sample.

Multiple generation cycles were carried out with varied set sizes (1, 10, 100, 1000 ... random slopes), to see whether the slope would converge to 0 when faced with a set of random events, that is, whether the method indicates that there is not a trend in a random universe.

The results (Figure 3.2a) made it possible to conclude that for reduced sample sizes, such as those in this study, there is a chance that high *scores* will emerge in relation to a set of random events. This is undesirable, and therefore trends need to be identified using another method.

Figure 3.2b illustrates this problem in more detail. The number of elements in the sample of random slopes is fixed at 11 (identical to the number of ECG signals available) and the calculation of the score is repeated in multiple iterations (in each iteration 11 new random slopes are generated).

However, it should be noted that as the size of the sample increases the *score* converges to 0, indicating that the empirical method is a promising approach for identifying trends in a test with multiple volunteers, provided that the sample has a reasonable size (tests of at least 50 volunteers).



a Convergence of the *score* when the empirical method of evaluating trends was applied in a successively greater population sample

b Demonstration of the weakness of the empirical model for small population samples (11 elements), where the *score* can assume high values highlighting trends in random events

Figure 3.2: Process of validating the empirical method for identifying trends

### 3.2.3 Method Based on a Meta-Analysis

The second method that was followed fell within the scope of a Meta-Analysis, an area which encompasses procedures for combining information in an objective way.

For this study, the objective would be to identify trends using the information contained in the slope of the linear regression line that best fitted the experimental data. There are literature references which describe approaches in this respect.

One method in particular, referred to in [79], made it possible to preserve the basic logic of the empirical method, that of generating the linear regression line, in order to deduce the evolution trend through the slope.

Once the linear regression line of the evolution of the  $Ind^k$  index had been generated for each subject, there were 11 to 14 slopes (for the ECG and EMG data, respectively). These were combined into a single slope, by calculating a weighted average of the individual slopes of each subject  $s$  (Expression 3.4), in which the weight corresponds to the inverse of the variance associated with the slope  $m_s$  (Expression 3.3).

$$w_s = \frac{1}{\sigma_{m_s}^2} \quad (3.3)$$

$$m_{comb} = \frac{\sum_{s=1}^N m_s w_s}{\sum_{s=1}^N w_s} \quad (3.4)$$

Greater variance means that the estimate of the individual slope  $m_s$  is less accurate and must therefore have less weight in the weighting, in contrast to subjects in which the variance is lower.

The combined slope has a variance associated with it, of a value equal to the inverse of the sum of the weights derived from the individual variances (Expression 3.5).

$$\sigma_{comb}^2 = \frac{1}{\sum_{s=1}^N w_s} \quad (3.5)$$

With this information (estimate of an average slope and its variance), it was possible to determine the 95% confidence interval.

By definition, the confidence interval is the interval in which there is 95% confidence that the true value of the estimated parameter (slope) will be found (defined by Expression 3.6).

$$IC_{(1-\alpha) \times 100\%}^{m_{comb}} = \left[ \hat{m}_{comb} - F_{t(n-2)}^{-1} \left(1 - \frac{\alpha}{2}\right) \sqrt{\hat{\sigma}_{m_{comb}}^2}; \hat{m}_{comb} + F_{t(n-2)}^{-1} \left(1 - \frac{\alpha}{2}\right) \sqrt{\hat{\sigma}_{m_{comb}}^2} \right] \quad (3.6)$$

$\hat{m}_{comb}$  and  $\hat{\sigma}_{m_{comb}}^2$  being the estimated values of the combined slope and of its variance and  $F_{t(n-2)}^{-1}$  reflecting the value of the  $t$ -student statistic for  $n - 2$  degrees of freedom, with  $n$  establishing the size of the population sample (in this case 11 or 14 subjects)

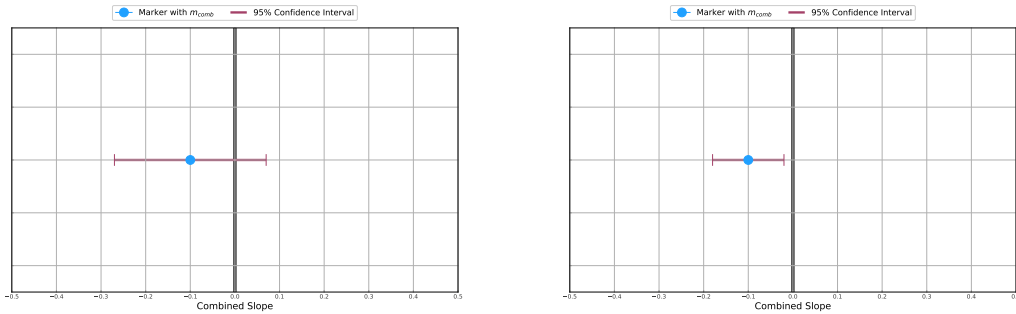
So, the “outputs” of this meta-analysis correspond to the combined slope and to the respective confidence interval in the calculation.

The greater the slope, in absolute value, the more well-defined the trend.

A smaller confidence interval reflects a more accurate estimate of the combined slope and less incoherence.

If the confidence interval only contained values with signs identical to the combined slope, it would be accepted that the evolution of the studied index followed a trend (Figure 3.3b).

Otherwise, the index would be excluded from the analysis since the uncertainty and incoherence associated with the combined slope would be high, and there would be a chance that the real value could be positive or negative [80, 81] (Figure 3.3a).



a Graphical result of the Meta-Analysis when no trend exists

b Graphical result of the Meta-Analysis when a trend exists

Figure 3.3: *Forest Plots* graphically synthesising the results of the meta-analysis, based on the estimate of the combined slope and the respective confidence interval

Ideally, the aim was to obtain a combined slope which was as high as possible (in absolute terms), demonstrating a marked pace of variation in the series and a reduced confidence interval/variance.

Thus, for an index considered to be a fatigue index since it denotes trend behaviour, according to the meta-analysis criterion, the most favourable analysis  $[wind_{size}^i, wind_{step}^j]$  for extracting it would be if it produced a combined slope and a variance which maximised the difference between the two magnitudes, or, equivalently, minimised the coefficient of variation (Expression 3.7) [82, 83].

$$CV[wind_{size}^i, wind_{step}^j] = \frac{\sigma_{comb}}{m_{comb}} \quad (3.7)$$

Considering that different analyses were carried out for each index, the criterion used for excluding ECG indexes was based on the following premises:

- ① Any index that does not meet the conditions defined in the meta-analysis (confidence interval associated with the combined slope contains positive and negative values), in the analysis which minimises the coefficient of variation in the segment of the signal relating to the fatigue induction phase, will be excluded;
- ② From the list of remaining indexes in step ①, the indexes which (i) denote an inversion of the combined slope (in the best analysis) between the fatigue induction segment and the recovery phase or (ii) where the confidence interval in the recovery phase contain positive and negative values (characteristic of undefined estimate) are considered to be fatigue indexes.

As mentioned in section 3.2.1, the EMG acquisitions relate exclusively to the fatigue acquisition phase, that is, electromyographic data were not collected in conditions of less demanding exercise that could represent a recovery phase.

Thus, there must be an adaptation in the premises used to identify fatigue indexes, and the new formulation must be based on the fact that signals from different muscles were acquired during the test, two of these being more exposed to the effects of fatigue during the cyclic movement of the lower limbs.

The two muscles in question are the *Rectus Femoris* and *Vastus Lateralis*, according to the literature review carried out [84, 85]. From the start, it was expected that the data collected from these muscles would show the most coherent trends in the EMG indexes (in particular in the *Rectus Femoris*), in contrast to the *Vastus Medialis* muscle, which would be less exposed to fatigue [75, 76].

The analysis of results was limited to the *Rectus Femoris* and *Vastus Medialis* muscles, given that these constitute the muscles in “extreme positions” in terms of susceptibility to fatigue acquisition (a fatigue index must display a well-defined evolution in the first and an indefinite evolution in the second).

Thus, the criteria used in this study to characterise an EMG index as an indicator of fatigue were as follows:

- ① Any index that does not meet the conditions defined in the meta-analysis (confidence interval associated with the combined slope contains positive and negative values),



for the analysis which minimises the coefficient of variation in the *Rectus Femoris* muscle, will be excluded;

- ② From the list of remaining indexes in step ①, the indexes which for the *Vastus Medialis* muscle in the reference analysis (identified in Premise ①) do not meet the validity criterion according to the conditions defined in the meta-analysis (confidence interval associated with the combined slope contains positive and negative values), or where there is inversion or incoherence in the evolution of the index, are considered to be fatigue indexes.

### 3.3 Definition of a Global Fatigue Index

As mentioned previously, the acquisition of fatigue is a complex phenomenon, not only in terms of how it originates but also in terms of how it manifests.

Although individually some EMG and ECG parameters evolve in parallel to this state, as indicated in section 2.4.4 and demonstrated in section 4.1, combining the information to conduct a global analysis of the phenomenon from different perspectives stood out as an interesting opportunity.

The appeal of this approach is not limited to the fact that information from several signals and therefore several indexes can be integrated. It is also possible, with a single value, to synthesise the information from multiple sources, making communication with the end user of the system more simple and intuitive, which is one of the objectives of the project.

#### 3.3.1 Formal Specification

The selected approach involved determining a weighted average. Thus the global fatigue index (GFI) at the instant  $i$  will have the sample  $i$  of each fatigue index as terms and the value of a parameter derived from the meta-analysis (coefficient of variation) as weights, as described in section 3.2.3.

It should be highlighted that all the input terms were normalised using the maximum value of each fatigue index, in the course of a calibration test.

The calibration test consists in applying the protocol of “Day 2”, set out in section B.2.

Each fatigue index  $Ind^k$  will have a window size and time-step ( $[wind_{size}^i, wind_{step}^j]$ ) that are ideal for analysing it and an associated coefficient of variation (Expression 3.7).

The weight of each individual fatigue index (IFI) in the calculation of the global index will thus be defined by the inverse coefficient of variation corresponding to the most favourable  $[wind_{size}^i, wind_{step}^j]$  combination as demonstrated on Expression 3.8 and Figure 3.4.

$$GFI[i] = \frac{\sum_{k=1}^N IFI_k[i] \times CV_k^{-1}}{\sum_{k=1}^N CV_k^{-1}} \quad (3.8)$$

$N$  being the number of fatigue indexes to be considered,  $IFI_k[i]$  being a sample of the fatigue index  $k$  and  $CV$  being the coefficient of variation for the most favourable window size and time-step combination for the extraction of the  $IFI_k$  index

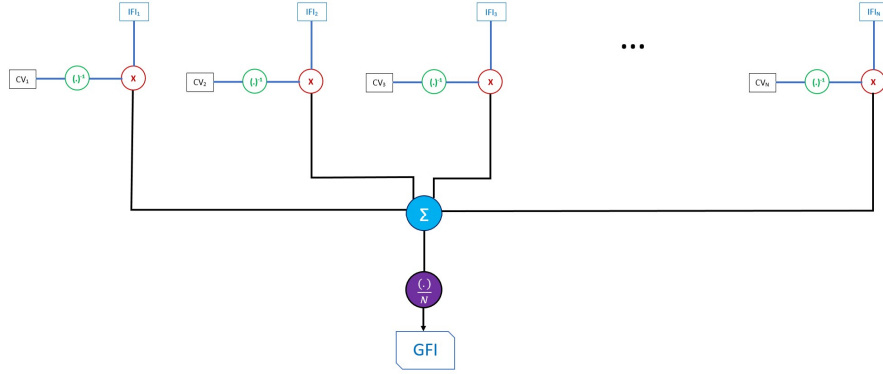


Figure 3.4: Diagram summarising the mechanism for determining a sample of the global fatigue index (GFI), based on a sample of each of the  $N$  individual indexes (IFI) and the coefficient of variation (CV) calculated during the trend identification phase

An index with a higher coefficient of variation has less weight in the definition of the global index, this being a logical option, so that each index is attributed a weight proportional to the degree of certainty in the identification of its evolution trend in fatigue conditions<sup>4</sup>.

### 3.3.2 Fatigue by Levels

In order to provide the user of the system with information at a higher level of abstraction, a ternary scale reflecting the severity of the fatigue state is depicted in addition to the evolution of the value of the global index.

The scale is characterised by “Green” zones associated with a low level of or no fatigue, “Yellow” zones indicating the marked setting-in of fatigue, and “Red” zones representing a problematic level of fatigue, with a high potential to cause lesions.

Considering that the global index has values between 0 and 1, owing to the fact that all the terms used in its determination are normalised, this interval needed to be divided into three zones, that is, through two thresholds.

<sup>4</sup>Recalling the definition of coefficient of variation in section 3.2.3, it was concluded that higher values illustrate situations in which the variance, in the determination of the combined slope for the evolution of a given index, is higher and therefore the determination of the combined slope is more uncertain

The choice of thresholds was based on an objective, albeit merely statistical, criterion. In the future it will be necessary to understand their physiological correspondence or possibly reformulate them.

Thus, after the calibration test is carried out, it is processed to extract the maximum values of each index and the thresholds. This information constitutes a “Volunteer Profile”, making it possible to carry out a subsequent personalised analysis that is adapted to the specific characteristics of the individual.

During the processing of the calibration test, the evolution of the global index over time is outlined and a *box plot* is then prepared, to provide a graphical illustration of the distribution of the samples.

The separation threshold between the “Green” and “Yellow” zones corresponds to the median while the separation threshold between the “Yellow” and “Red” zones is the 25<sup>th</sup> percentile (Figure 3.5).

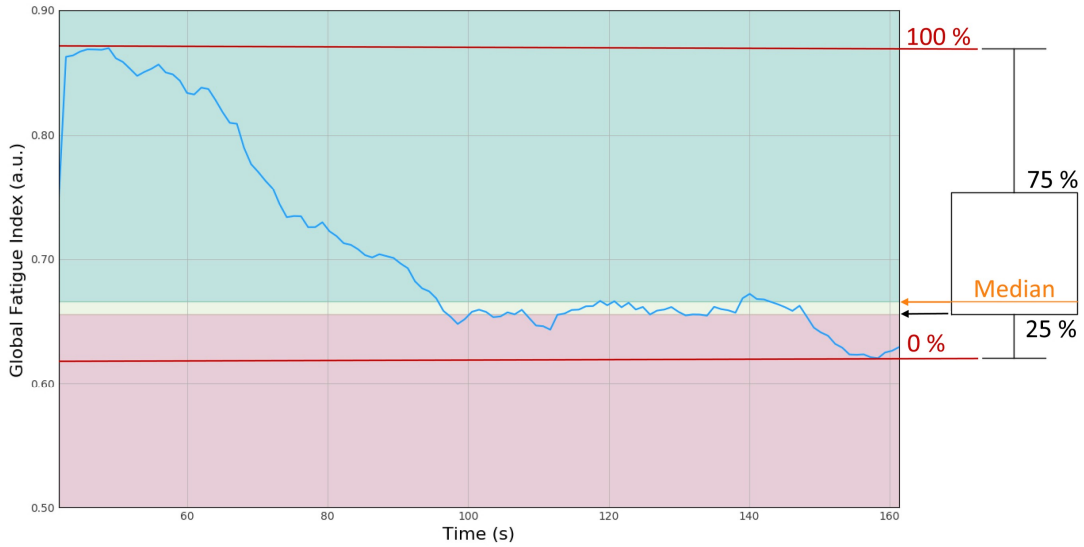


Figure 3.5: Graphical correspondence between the thresholds defining the fatigue zones and their origin in the *box plot*

### 3.4 Classifiers

Defining the global fatigue index was an interesting approach for synthesising and integrating information from several signals. However, despite the fact that the initial results show it to be viable, it is still only an attempt.

Thus, in order to supplement the information supplied by the global fatigue index, the decision was made to implement a binary classification system based on a *Support Vector Machine*.

In parallel, the classification results will be able to help validate those that exist for the global fatigue index.

The incentive of this option was the fact that it is a robust method with a scientific basis which can be easily incorporated into the processing given the existence of a number of *Python* libraries for this purpose.

One of these libraries is known as *scikit-learn* and provides numerous tools in the area of Machine Learning, making it a wide-ranging and extremely intuitive solution. It was for this reason that it was chosen to create the classifier.

As mentioned, the implemented classifier is a binary one, and returns the result of **“Positive Fatigue”** class when fatigue is setting in and **“Negative Fatigue”** class when the body is in the recovery phase and the level of fatigue is dropping.

As well as the class being attributed to the volunteer at a given instant of the test, the degree of certainty in this classification (“probability of accuracy”) is also given.

Considering the set of signals available (11 ECG signals and 14 EMG signals), the subjects for which ECG data were not acquired were excluded and the sample was limited to 11 subjects for classification purposes.

For these 11 subjects, the respective ECG and EMG signals were divided into two segments.

The first segment corresponds to the first half of the acquisition, while fatigue can be found in the body at low levels, reflecting the conditions covered by the **“Negative Fatigue”** class.

As for the second segment, given that it covers data from the more advanced phase of the test, it follows that there must already be significant levels of fatigue and it therefore fits the conditions intrinsic to the **“Positive Fatigue”** class.

In total, splitting the acquisitions from the 11 subjects into two parts resulted in 22 training examples, 11 of the examples relating to the **“Positive Fatigue”** class and the remaining 11 to the **“Negative Fatigue”** class. This made it possible to maintain equilibrium during the training phase and avoid biased behaviour later on, which could occur if the numbers of training examples in the two classes were very different.

To summarise, at the start there were 14 subjects, but ECG and EMG data were only simultaneously acquired for 11. The EMG and ECG acquisitions from each of these 11 subjects were segmented into two parts, giving rise to two training examples (one for each class), as shown on Figure 3.6.

Considering that we have an  $N$  number of EMG fatigue indexes and an  $M$  number of ECG fatigue indexes, for each of the training examples, characterised by the set of corresponding EMG and ECG data,  $N + M$  evolution series were generated (one per index) through the sliding-windows mechanism.

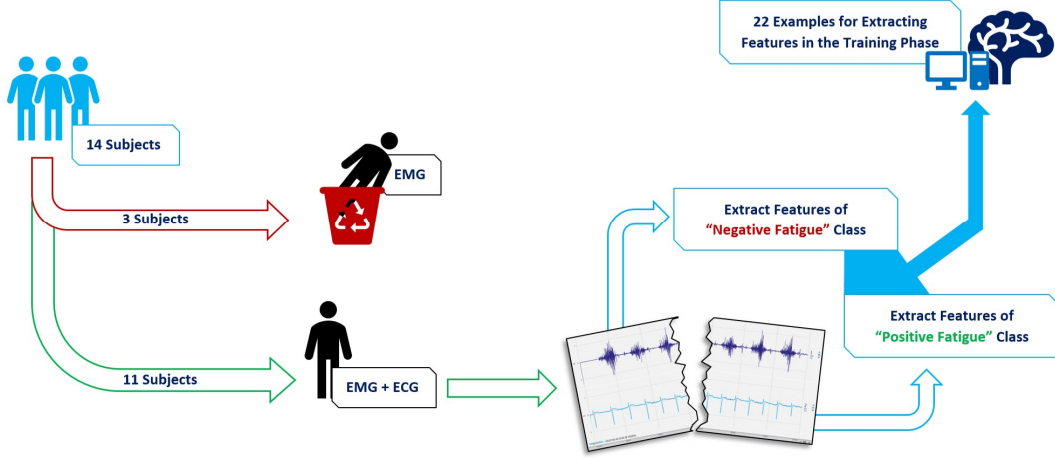


Figure 3.6: Graphic summary of the procedure from the initial population sample of 14 subjects up to the 22 examples for extracting features

The following two features were extracted per series:

- **Average value of the normalised series**

$$feature_1 = \frac{\sum_{j=1}^L \frac{Ind^i[j]}{\max_{Ind^i}}}{L} \quad (3.9)$$

$L$  being the number of samples of the index  $Ind^i$  extracted from the analysed segment of the EMG or ECG signal and  $\max_{Ind^i}$  functioning as a normalisation term defining the maximum value of the  $Ind^i$  index taking into account the entire acquisition, that is, the EMG or ECG signal before the segmentation

- **Relative Variation Rate**

$$feature_2 = \frac{\frac{Ind_{end}^i}{Ind_{start}^i} - 1}{t_{end} - t_{start}} \quad (3.10)$$

$Ind_{start}^i$  and  $Ind_{end}^i$  corresponding to the value of the  $Ind^i$  index in the first and last sample of the time series and  $t_{start}$  and  $t_{end}$  to the respective time instants

With these two features, the aim was to take account of, firstly, the information about the absolute value of the fatigue indexes (through  $feature_1$ ) and, secondly, the evolution trend (through  $feature_2$ , which defines the percentage of average variation between two samples).

A training example is thus reduced to a vector with  $2 \times (N + M)$  entries (Figure 3.7).

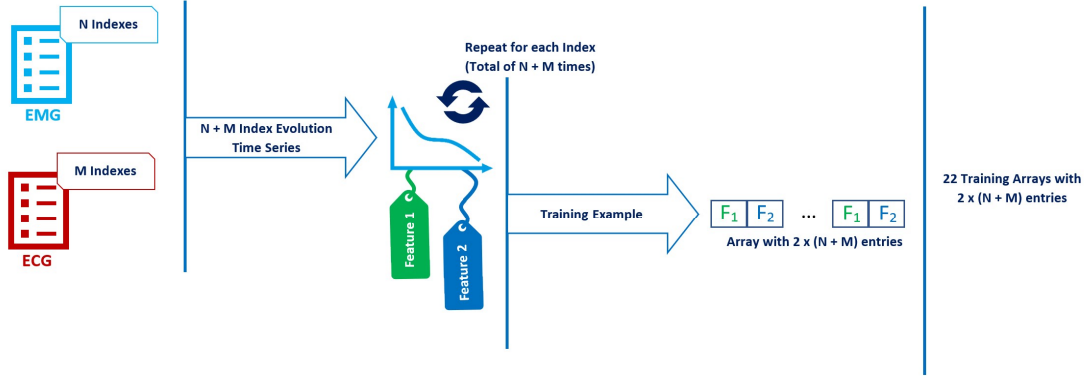


Figure 3.7: Graphic summary of the procedure for extracting features from the evolution time series of each fatigue index

The next phase of constructing the classifier was **Feature Selection**. The aim of this is to remove redundant or meaningless parameters which would increase the complexity of the classifier and not always translate into an improved performance. Without this step, the risk of overfitting to the training increases, making the classifier less able to categorise a new testing example.

There are different approaches to feature selection such as filter methods or wrapper methods.

In the first method, a *ranking* will be attributed to the features<sup>5</sup>. The least relevant ones will be excluded and the classifier will be trained later [86].

The second method is characterised by the fact that the selection phase includes a classification algorithm, and features will be excluded or selected according to the quality of the trained classifier.

In our implementation, the wrapper method was chosen, and the least relevant features were eliminated recursively.

This choice was based on the fact that the features are ultimately intended to train a classifier. Thus by incorporating a classifier into the selection phase, it was possible to “judge” the relevance of the features in conditions similar to those used during the training phase, making the process logical and efficient.

In computer terms, the feature selection was split into two phases:

- ① Determination of the ideal number of features by applying the *scikit-learn* **RFECV** function – combining recursive elimination and cross-validation;
- ② Determination of the final list of features by making use of the *scikit-learn* **RFE** function.

<sup>5</sup>Using the Pearson correlation coefficient to evaluate the impact that the feature under analysis has on the target class of the training example, or the Mutual Information parameter which defines whether two variables convey shared information

In phase ①, the following was defined as an input argument: the type of classifier (estimator) to be used, the number of features to be excluded in each iteration of the recursive process, and the way in which the cross-validation process takes place.

In this case, an SVM with a linear kernel was chosen as the estimator, based on the assumption that we had linearly separable classes.

The number of features removed in each iteration was equal to 1 and the cross-validation strategy was based on estimating the quality of the classifier using a stratified k-fold logic.

Thus, the process was formed by  $2 \times (N + M)$  iterations corresponding to the original number of features.

In each iteration, a classifier was trained, and in the first iteration all the available features were taken into account in the training phase.

Given that the **RFECV** function includes a cross-validation component, the training set is defined by partitioning the original training set.

$K$  sets are created, each one containing a training subset and a testing subset owing to the partition of the original training set.

Given that use was made of an estimate based on stratified cross layers, in each of the  $K$  sets formed the proportion of examples of the “Positive Fatigue” class and “Negative Fatigue” class was approximately equal for the training subset and for the testing subset.

The classifier created in the form of an object, using the `SVC(kernel='linear')` command, after the training phase was associated with a parameter known as `coef_` which attributes a weight to each feature, resulting from the mathematical formalism arising from the *Support Vector* concept that characterises *Support Vector Machines*.

More relevant features in the training phase are associated with a larger coefficient.

After the training phase, the testing subset was used to estimate the classifier quality.

The **Training** → **Testing** → **Estimation of Quality** sequence took place  $K$  times (one for each *fold*, that is, for each set containing the stratified training and testing subsets).

Thus, for each iteration of the **RFE** method we had  $K$  sub-iterations, that is, per set of features  $K$  classifiers were created, and the respective quality was estimated using the average quality of the classifiers created in the  $K$  sub-iterations.

Once the iteration had ended, and before the following iteration began, the feature with the lowest weight in the training phase was removed (with the lowest coefficient in the `coef_` vector).

Taking account of the new set of features, a new classifier was trained, and the above method was repeated in its entirety, the least relevant feature being excluded in each iteration until only one feature remained.

At the end, the **RFECV** function returned the ideal number of features, corresponding to the number of features involved in the training phase of the classifier with the best quality according to the cross-layer estimation.

Once the ideal number of features was known, the **RFE** function was executed defining this value as one of the input arguments, and the above process was repeated but without the cross-validation phase.

This sequential application of **RFECV** and **RFE** made it possible, firstly, to find out the ideal number of features  $Ideal_{nbr}$  and subsequently, knowing this number, to check what the most relevant features actually were.

Once this process was complete, Phase ② was initiated, and the SVM-type classifier was trained with the original training set of 22 elements and the set of features selected by **RFE**.



## Presentation of Results

This chapter will set out the results that were obtained, particularly in terms of the signal processing, which is key for identifying the EMG and ECG indexes with the potential to provide information about fatigue.

In addition to these results, a description is included of the *plugins* for real-time processing of the EMG and ECG signals. These plugins played an important role in implementing the *offline* fatigue monitoring system, described in the last section.

### 4.1 Indexes with Information Potential

Considering that to extract knowledge about the fatigue state from the EMG and ECG signals one would need to identify patterns in the evolution of the respective indexes, both trend-identification methods were applied, these being described in section 3.2.

The empirical method defined an exploratory approach preceding the meta-analysis, which gave rise to the final list of indexes with the potential to provide information about the fatigue state, since these denote characteristic behaviour over the course of the fatigue induction test for the population sample under study.

Taking into account the criteria established in section 3.2.2 for the empirical method, the parameters in Table 4.1 marked with the ♣ symbol were considered as potential fatigue indexes.

The results are set out in Appendix C.

It should be highlighted that although all the parameters derived from the ECG signal are intended for the same purpose, that of analysing heart rate variability, they provide additional information, which explains why they are all analysed in the current phase of the project.

Table 4.1 also shows the typical evolution of these indexes during the fatigue induction phase. It may be observed that all the HRV indexes convey the information that heart rate variability decreased as fatigue set in.

Once the empirical method had been applied, a meta-analysis of the data was conducted (Appendix C). This provided the definitive list of indexes with fatigue information potential which met both conditions specified in section 3.2.3. These indexes are marked in Table 4.1 with the ♠ symbol.

Table 4.1: List of indexes with fatigue information potential

EMG		
Index Name	Evolution	Flags
Median Frequency ( <i>Fourier Analysis</i> )	↓	♣♠
Median Frequency ( <i>Wavelet Analysis</i> )	↓	♣♠
Major Frequency	↓	♠
Major Time	↓	♠
Convex Hull Area	↑	♣
Time Dispersion	↑	♣
ECG		
Index Name	Evolution	Flags
Maximum Duration of RR Intervals	↓	♣♠
Minimum Duration of RR Intervals	↓	♣♠
Average Duration of RR Intervals	↓	♣♠
rmsSD	↓	♠
SDNN	↓	♣♠
Triangular Index	↓	♣♠
SD2	↓	♣♠
Power in LF Band	↓	♣♠
Power in HF Band	↓	♣♠
Median Frequency	↑	♠

When the results of the two methods are compared, it may be seen that almost all the identified fatigue indexes are flagged by both methodologies.

In addition to the fatigue indexes contemplated by the empirical method, *Major Frequency*, *Major Frequency*, *rmsSD* and *HRV Median Frequency* are part of this list.

The most favourable window size and time-step combination for extracting each index was considered to be that which provides the lowest coefficient of variation, that is, the chosen combination was that which maximised the difference between the value of the variance and the value of the combined slope associated with integrating the evolution information of the index for the various elements of the population sample.

For each index, the ideal extraction conditions are listed in Table 4.2.

Given that the maximum, minimum and average duration of RR intervals provide identical information about the way in which the heart rate evolves, the decision was made to include only the average duration of RR intervals in the fatigue monitoring system.

## 4.2. TYPICAL EVOLUTION OF THE GLOBAL INDEX

Table 4.2: Presentation of the ideal window size and time-step combination for extracting each fatigue index

Signal	Domain	Parameter	Window Size	Time-Step
EMG	Frequency	Median Frequency	10 Bursts	1 Burst
EMG	Time-Frequency	Median Frequency	10 Bursts	1 Burst
EMG	Time-Frequency	Major Frequency	10 Bursts	1 Burst
EMG	Time-Frequency	Major Time	25 Bursts	0 Bursts
ECG	Time	Maximum Duration of RR Intervals	30 s	3 s
ECG	Time	Minimum Duration of RR Intervals	30 s	3 s
ECG	Time	Average Duration of RR Intervals	30 s	3 s
ECG	Time	rmsSD	50 s	45 s
ECG	Time	SDNN	30 s	3 s
ECG	Time	Triangular Index	60 s	30 s
ECG	Time	SD2	30 s	3 s
ECG	Frequency	Power in LF Band	30 s	3 s
ECG	Frequency	Power in HF Band	30 s	3 s
ECG	Frequency	Median Frequency	30 s	3 s

For the same reasons, *rmsSD* was excluded, given the similarities with *SDNN*. It was observed that, according to the criteria established for trend identification, the *rmsSD* parameter is closer to the exclusion zone than *SDNN*.

The *Major Time* was excluded due to the extreme conditions that characterize the best analysis. An OTSU Level of 2 means that the scalogram has a small amount of information, so, we should not take definitive conclusions.

## 4.2 Typical Evolution of the Global Index

Considering that the global fatigue index is a weighted average which takes into account the values of the various indexes contained in the list of section 4.1, before the results were analysed, it could be expected that the global index would decrease as fatigue was acquired, given that almost all the indexes evolve in this direction.

This expectation was confirmed, and a graphical example of this result is provided in Figure 4.1, relating to one of the subjects of the population sample, which is representative of the global behaviour observed for the rest of the sample as may be seen in Figure 4.2.

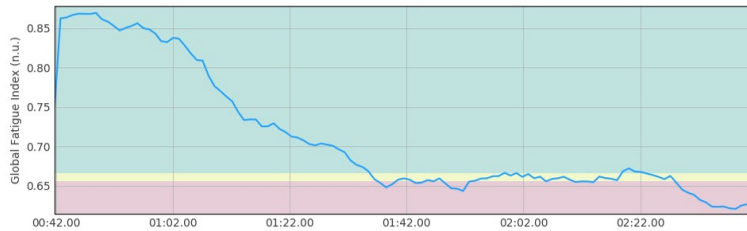


Figure 4.1: Typical evolution of the global fatigue index during the fatigue induction phase

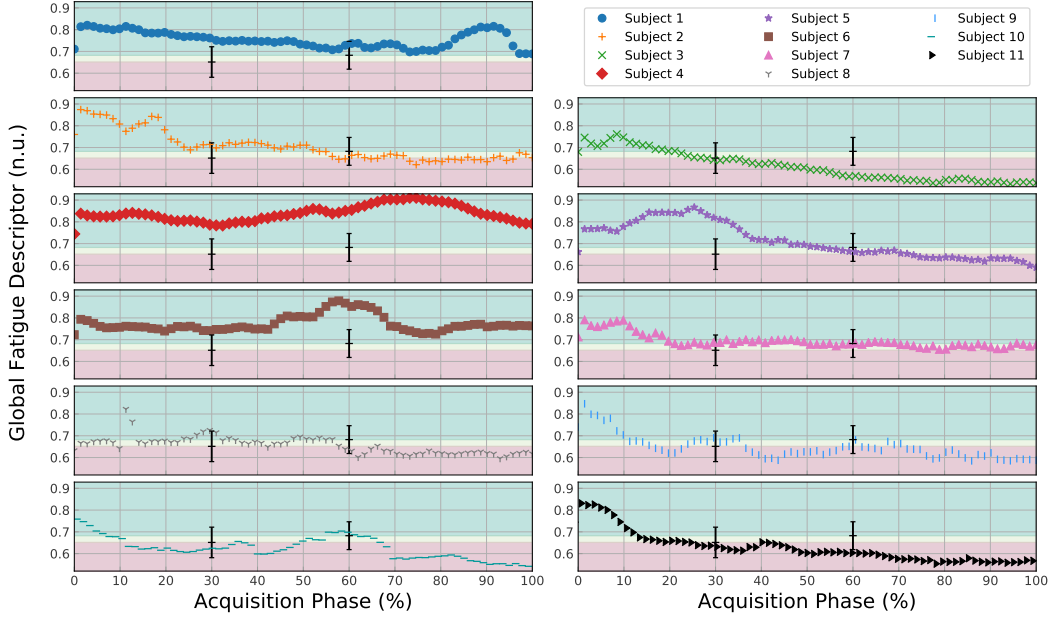


Figure 4.2: Evolution of the global fatigue index during the fatigue induction phase for the 11 subjects (the thresholds between colored zones were determined through the average of thresholds obtained on the calibration protocol of each subject)

### 4.3 Classification Systems - Comparative Study

When implementing a classification system it was considered to be extremely important to have an objective understanding of how said system would behave when interacting with new testing examples.

A classifier should function correctly when the testing examples are very similar to the training examples. However, if there is a testing example with characteristics that are somewhat disparate, the robustness of the system will be challenged.

Thus, what makes a classifier robust is its capacity to establish correspondences even when the similarities are more tenuous.

To estimate the quality of the implemented system, there were different methods to be followed, namely **Cross-Layer Estimation**<sup>1</sup> and **Leave One Out**<sup>2</sup>.

Both methods were applied to the SVM classifier that was created, using the `cross_val_score` function of the *scikit-learn* library, and specifying the methods **LeaveOneOut** and **StratifiedKFold** in the `cv` argument.

The estimated success rates are set out in table 4.3.

<sup>1</sup>In this method, the training set is divided into  $N$  subsets with approximately the same number of examples. Using  $N - 1$  iterations, each of the  $N$  subsets acquires the role of testing set, while the remaining  $N - 1$  subsets are used to train a “partial” classifier. Finally, one obtains an estimate of the error of the original classifier through the partial errors of the  $N - 1$  partial classifiers.

<sup>2</sup>The Leave One Out method is a particular case of cross-layer estimation. It involves creating a number of partial classifiers which is equal to the number of training examples. In each iteration, one training example assumes the role of testing example, while the rest are used to train the “partial” classifier.

Table 4.3: Success rates of the classifier using the Cross-Layer Estimation and Leave One Out methods

Cross-Validation Method	Score <sup>t1</sup>	95 % Confidence Interval
Leave One Out	$0.82 \pm 0.39$	[0.66;0.98]
Stratified K-Fold	$0.82 \pm 0.24$	[0.68;0.96]

<sup>t1</sup> Between 0 and 1

Considering that the **Leave One Out** estimate is often optimistic, attention was focused on the result obtained with the **Stratified K-Fold** method, where the confidence interval is slightly broader.

Recalling the description provided in section 3.4, planning the training phase involved extracting two features from the evolution series of each fatigue index (Section 4.1). Considering the ten parameters with fatigue information potential, each training vector was therefore formed by twenty features.

The results of applying the Recursive Feature Elimination method, which are based on the **RFECV** and **RFE** functions of the *scikit-learn* library as set out in section 3.4, halved the number of features, given the value returned by the **RFECV** function (Figure 4.3). It may be observed that *Feature 2* did not have an impact on the classification, largely because of the smaller scale associated with it. Therefore in order for it to have any significance the scale of the two Features would need to be made the same.

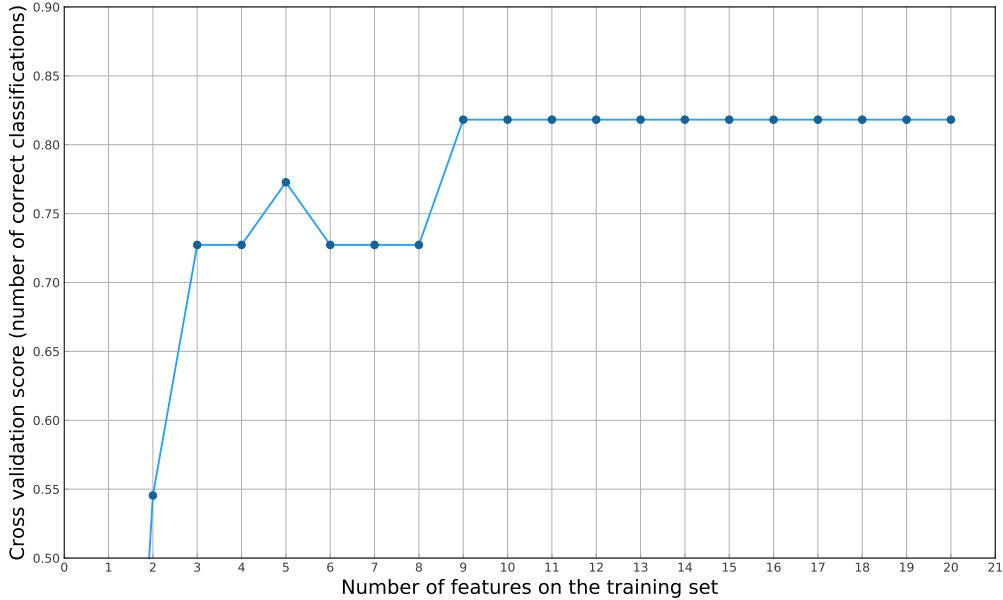


Figure 4.3: Results of applying the **RFECV** function with the scores obtained in each iteration, where the number of features taken into account varied

Thus, in view of the results of the Feature Selection, for the testing examples only *Feature 1* was extracted.

The aim in the implemented system was for the classifier to supply a result over the course of the acquisition. The extracted features which characterise the testing examples were therefore adapted slightly in relation to the features that exist for the training examples, in such a way as to fulfil this aim of ensuring that classification takes place over time. This was important for implementation in an *offline* context and particularly for future real-time versions.

The adaptation of the features (those which remained after the Feature Selection phase described in section 3.4) gave rise to the following formalism:

- **Average value of the normalised series (*Feature 1*)** - substituted by the normalised instantaneous value of the index (the value which represents the processing window)<sup>3</sup>;
- **Relative Variation Rate (*Feature 2*)** - not taken into account in the examples in the final training and consequently in the testing examples.

Prior to the implementation of this logic in programming terms, there was the expectation that the behaviour of the classifier would initially consist in attributing the “**Negative Fatigue**” class and that it would have a degree of certainty in the order of 100%.

This percentage would decrease over the course of the test until the “**Positive Fatigue**” class emerged on top in the final phase of the test. This did indeed occur (Figure 4.4), although this statement carries with it some reservations.

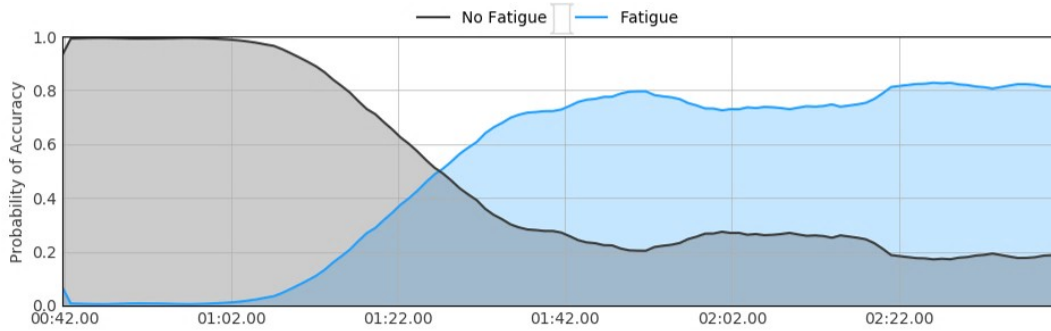


Figure 4.4: Evolution of the classification decision over the course of the acquisition, showing the degree of certainty in the attribution of each class, returned by the **SVC** object

As with the global fatigue index, where the analysed acquisition itself was used as a calibration test, in this case only the acquisitions used in the training examples were available to test the classifier. Therefore it was used a **Leave One Out** strategy to guarantee that the classification results for each subject (Figure 4.5) were not affected by its own training example, which would originate optimistic results.

<sup>3</sup>Considering that not all the fatigue indexes are extracted at the same frequency owing to the different window size, in the *offline* processing, the evolution series of each index are interpolated so that they have the same number of samples (corresponding to the size of the time series with the largest number of samples).

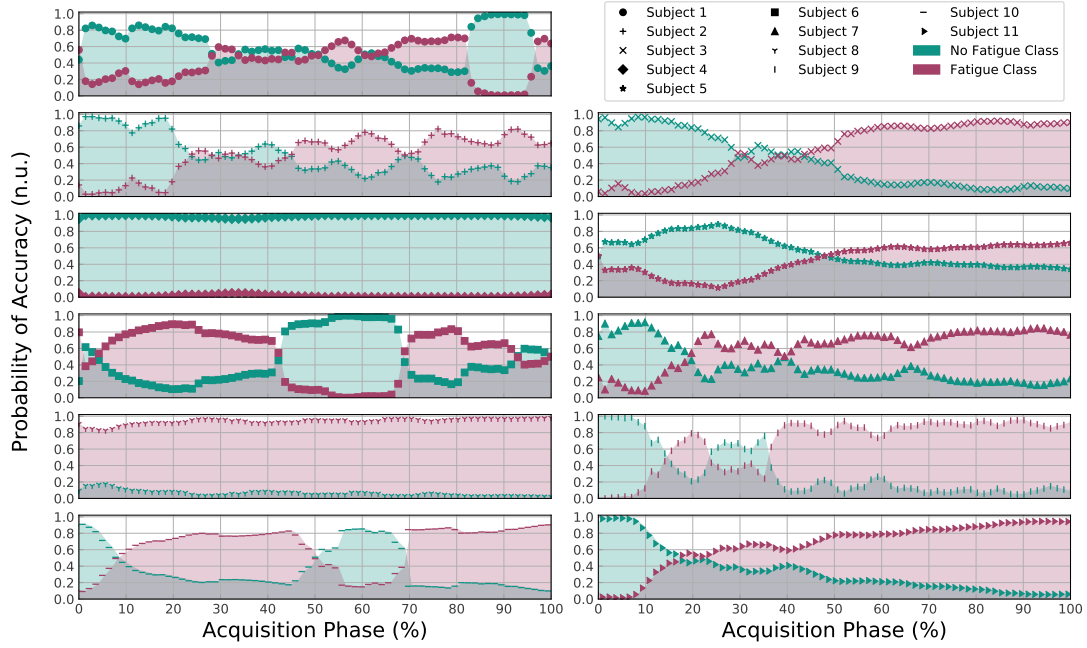


Figure 4.5: Evolution of the classification decision over the course of the acquisition for each one of the 11 subjects

## 4.4 Fatigue Analysis Plugin - Foundations

The implementation of the final monitoring system and future derivations were largely based on the answers to the following questions:

- ① From the list of EMG and ECG indexes (Section 2.3), which provide information about the process of fatigue setting in ?
- ② What are the constraints of a real-time processing system ?

Answering the first question began with the literature review provided in section 2.4.4, while in section 4.1 some of the referenced conclusions were validated, and new indexes of potential interest for evaluating fatigue were identified.

In terms of the second question, one way to answer this would be through experience, given that any computer implementation depends on the context in which it is applied.

In this project, the implemented monitoring system is an *OpenSignals* system, based on programming in *HTML*, *JavaScript* and *Python*. This was the framework within which the first “drafts” of the system were outlined.

*OpenSignals* has three *plugins* for processing ECG and EMG signals *offline*, using a large portion of the indexes intended for analysis during the project. These *plugins* emerged as attractive targets for testing the real-time processing algorithm to be implemented in the future and the sliding-windows system included in the *offline* version of the fatigue monitoring *plugin*.

#### 4.4.1 EMG Plugin

For the EMG signals to be processed, the basic step of identifying the periods of muscular activation must be taken to ensure that the results are not excessively affected by noise.

The EMG signal can be processed *offline* through two *plugins*. The first is focused on detecting periods of muscular activation and parameters such as maximum/minimum amplitude, area and RMS are extracted from each of these (Figure 4.6).

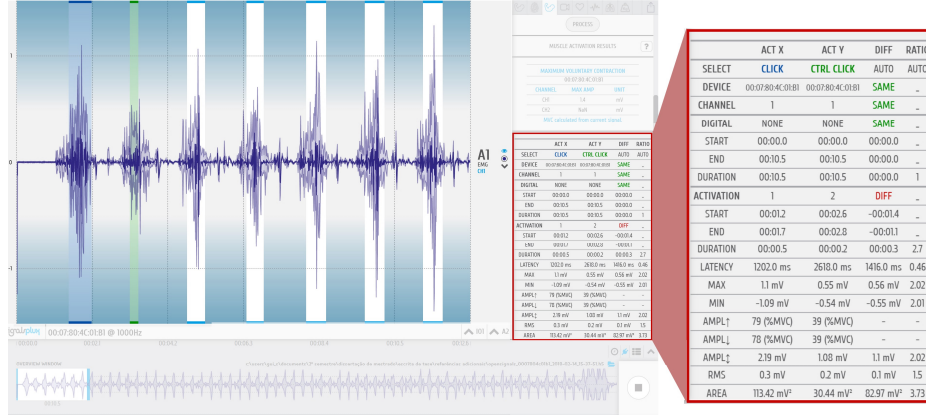
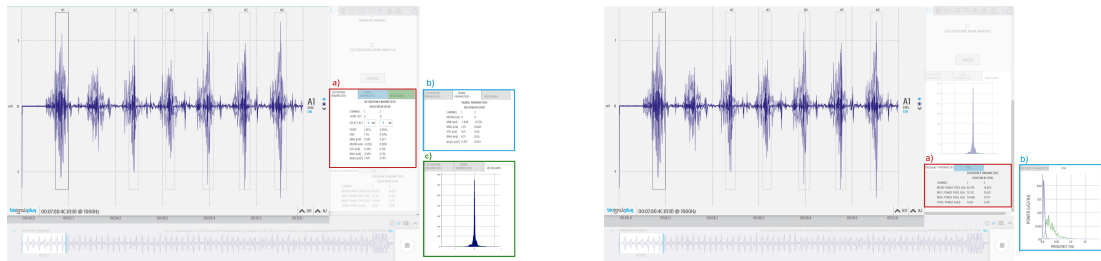


Figure 4.6: Results shown by the first of the two *plugins* for processing the EMG signal (framed by the red rectangle). The first column corresponds to the indexes extracted from the blue period of muscular activation and the second column corresponds to the parameters determined from the green period of muscular activation.

In order to fulfil this purpose, the system functions based on the TKEO algorithm described in section 2.2.1.

In the second *plugin*, in addition to this function of detecting periods of muscular activation, a greater number of indexes is extracted, in particular frequency parameters such as average, maximum and total power. It is also possible to view the histogram of the EMG signal and its power spectrum (Figure 4.7).



a Time Parameters relating to activation period # 1 (a), value of the indexes taking into account the whole signal (b) and histogram (c)

b Frequency Parameters relating to the whole signal (a) and view of the spectral density spectrum (b)

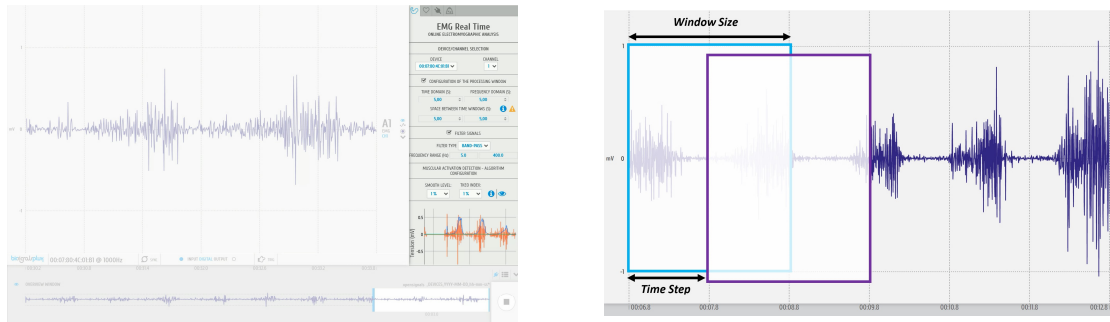
Figure 4.7: Results shown in the second *plugin* for processing the EMG signal, showing the regions in which results are presented in the interface



In view of these functions, the proposed solution for processing the EMG signal in real-time was based on a sliding-windows system used in some studies, where EMG features are extracted [16, 87, 88]. A general view of the interface is provided in Figure 4.8a.

One of the advantages of real-time monitoring is that it allows trends to be analysed, that is, how each index evolves over the course of the acquisition, and in the *plugins* that function *offline* the mainly numerical approach is abandoned for a more graphic analysis.

The user has the option of defining the rate at which the representation is updated and the temporal resolution associated with determining the indexes by specifying the time distance between windows and their duration, respectively (Figure 4.8b).



a General view of the *plugin* interface implemented for the real-time processing solution (incorporated into the *OpenSignals* master interface)

b Configurable parameters in the processing system based on the sliding-windows mechanism

Figure 4.8: Functions of the EMG *plugin* for real-time processing, from the point of view of the user and the programmer

As well as having these configurable options, the user may also decide which type of digital filter to apply to the EMG signal, as well as its cut-off frequency/ies, so that information not directly related to muscular contraction is excluded (Figure 4.9a).

In addition, the interface allows the user to edit the two variables on which the TKEO algorithm depends for detecting periods of muscular activation, these being the smooth level to be applied to the EMG signal<sup>4</sup> and the position of the TKEO threshold<sup>5</sup> (Figure 4.9b).

Following this (optional) configuration phase, the user may initiate the processing by pressing the “Process” button.

There are two categories of extracted index: one of them encompasses the parameters extracted from the time domain (maximum amplitude, minimum amplitude, average amplitude, standard deviation, RMS) and the other, parameters extracted from the frequency domain (total, average and maximum power of the spectrum and median frequency).

Thus, in each processing window, the above nine indexes are extracted. However, not all of them may be displayed at once, given the different units and orders of magnitude.

<sup>4</sup>100% – size of the smooth filter window matches the sampling frequency of the acquisition

<sup>5</sup>100% – the value matches the maximum of the smoothed signal

The decision was made to include only one graphic region in the interface, to display the evolution of the time and frequency indexes.

This region is associated with a set of options allowing the user to select which indexes he or she wishes to observe (Figure 4.9c). If the units are incompatible, the system excludes the problematic index from the representation, giving priority to the user's last action.

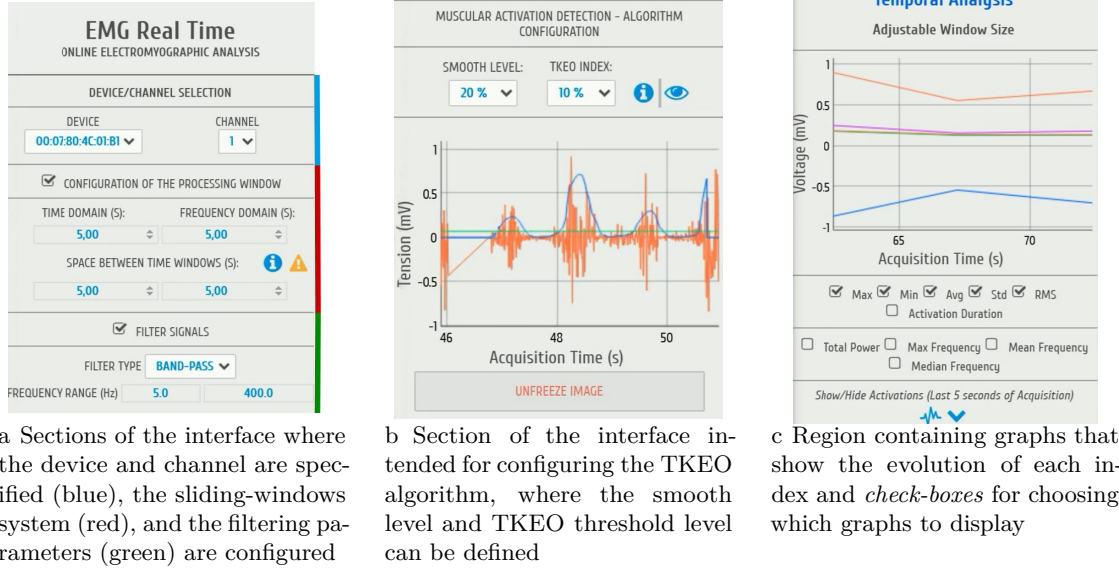


Figure 4.9: Configurable elements in the interface of the *plugin* for monitoring the evolution of EMG parameters in real-time, as well as processing results

Nevertheless, samples continue to be extracted even for the parameters that are not visible. Thus, for each window, the final result of the processing in the *Python* component of the system is nine new samples (1/index).

However, these nine samples (stored individually in the respective array, which contains the past samples of the evolution series of the index) are a summary of the information contained in various sub-windows, given that the aim is to limit the study to the regions of muscular activation and not to the zones of inactivity associated with noise.

In other words, in each window, there are multiple periods of muscular activation that will be detected by the TKEO algorithm, and each of these is established as a sub-window from which the different EMG indexes are individually extracted.

Supposing that a given window contains  $N$  periods of muscular activation (sub-windows), this means that the new sample to be displayed to the user corresponds to an average of the  $N$  samples obtained in the sub-windows.

Taking into account this mechanism, the processing takes place as normal, and the graphs update automatically over the course of the acquisition<sup>6</sup>.

<sup>6</sup>If the reader so wishes, he or she may consult page <https://www.dropbox.com/sh/wb4ucw3dzgq66oc/AAAUFnlvsjLSNDp3rV-r39Z6a?dl=0> to gain a more in-depth understanding of how the program works, by watching a video showing the interface in use.

The efficiency of the EMG monitoring system depends largely on periods of muscular activation being detected correctly, and it is necessary to check whether the quality of detection is preserved when the algorithm is switched from *offline* mode to *online* mode.

In order to perform this check, a test acquisition of around 1 minute and 20 seconds was used. Although this is not enough to generalise the conclusions, it provides an indicator in this respect.

The binarised signal was generated for the *offline* and real-time implementations, and in the second case different combinations of the smooth level and TKEO level configurable parameters were tested.

The Pearson correlation coefficient was then determined between the rectified EMG signal and the binarised signal in *offline* mode, and a value of approximately 0.45 was obtained<sup>7</sup>.

The procedure was repeated for all the binarised graphs generated from the various *Smooth Level* and *TKEO Level* combinations, and the results were displayed in the form of an image (**X dimension** → *TKEO Level*; **Y dimension** → *Smooth Level*; **Colour dimension** → value of the correlation coefficient).

As may be observed in Figure 4.10, the *online* implementation behaves similarly to the *offline* implementation when *TKEO Level* and *Smooth Level* fall within the interval [10, 20] %, demonstrating that the algorithm adapted successfully, and has the additional advantage of allowing the user to configure the parameters used in the TKEO detection algorithm.

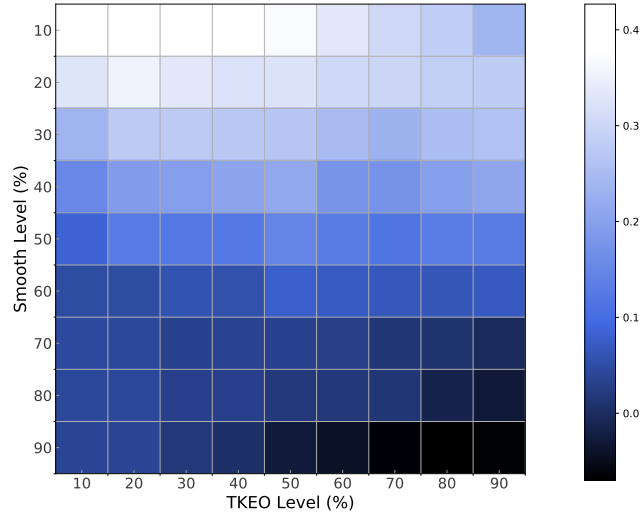


Figure 4.10: Correlation coefficients between the rectified EMG signal and the binarised signal of activations presented in the form of a graph

<sup>7</sup>The correlation coefficient provides an indication of the degree of similarity between the two time series. A high value therefore means that the quality of activation-period detection is considerable, since the binarised graph reflecting the activations conforms to the EMG graph

## 4.4.2 HRV Plugin

In normal conditions, the heart beat varies naturally. The absence of this characteristic could have serious consequences or indicate that the body is in a pathological state.

Understanding the way in which heart rate variability changes in fatigue conditions is one of the main objectives of this project.

Similarly to that described previously, the first steps in this respect involve switching the *offline* HRV processing algorithm in the *OpenSignals plugin* to the real-time analysis.

The logic used was identical to that applied to the EMG *plugin*: a global analysis of the entire ECG signal, in which a sample of each index was extracted, became a graphical analysis of the evolution of the indexes over time, based on a sliding-windows system.

So, for each index there ceased to be just one value and a time series became available.

As mentioned in section 2.2.2, the tachogram corresponds to the time series from which the indexes are extracted, and is a derivation of the ECG in which only its periodic component stands out.

In the *offline plugin*, after determining the instant of occurrence of the R peaks and the respective tachogram, time indexes of a linear nature (maximum, minimum and average duration of RR intervals, SDNN, rmsSD, NN20, pNN20, NN50, pNN50)<sup>8</sup> and a non-linear nature (SD1, SD2 and SD1/SD2) as well as frequency indexes (Power in the ULF, VLF, LF and HF bands) are originally extracted.

The processing results of this *plugin* are presented numerically, with the values of each index having the full tachogram of the acquisition as a basis (Figure 4.11).

In addition, there are some graphical representations, namely the tachogram, Poincaré plot, power spectrum associated with the tachogram and histograms which geometrically reflect how the duration of the RR intervals is distributed.

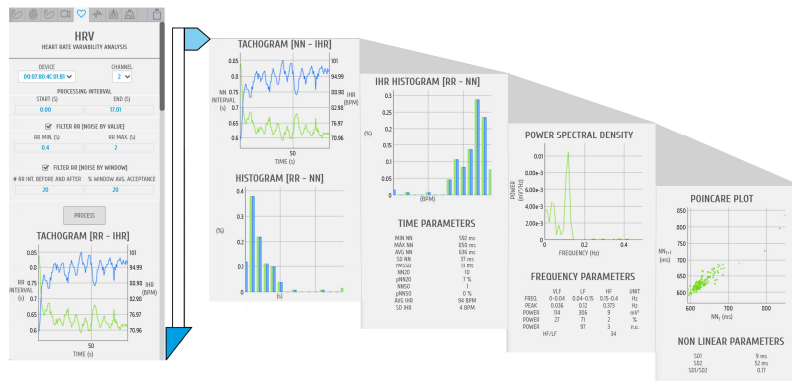


Figure 4.11: Presentation of the processing results of the *plugin* for *offline* heart rate variability analysis

<sup>8</sup>In section 2.3, indexes NN20, NN50, pNN20 and pNN50 were not described, because they were not analysed for fatigue monitoring and therefore do not form part of the final version of the system. NN20 and NN50 establish the number of pairs of RR intervals in which the difference in duration between them is greater than 20 or 50 ms, while pNN20 and pNN50 define the ratio of NN20 and NN50 in relation to the total number of RR intervals.

With regard to the version implemented for real-time processing, in addition to the regions for specifying the device/channel and for configuring the sliding-windows system (referred to above for the real-time EMG *plugin*), there is a section of the interface for defining a tachogram filtering step, that is, the user may specify the minimum and maximum duration required for an RR interval to be included in the processing (manual removal of ectopic beats).

Any RR interval which does not fall within these limits will be removed and will not affect the results.

In terms of displaying the results, the logic of the real-time EMG *plugin* is replicated, and there is a set of *check-boxes* which allow the user to choose which indexes to monitor.

The *Triangular Index* is the only additional parameter in the HRV real-time processing *plugin*, and the parameters NN20, NN50, pNN20 and pNN50 are excluded from the analysis.

In terms of the internal processing operation, the steps and logic are set out in the flowchart of Figure 4.12.

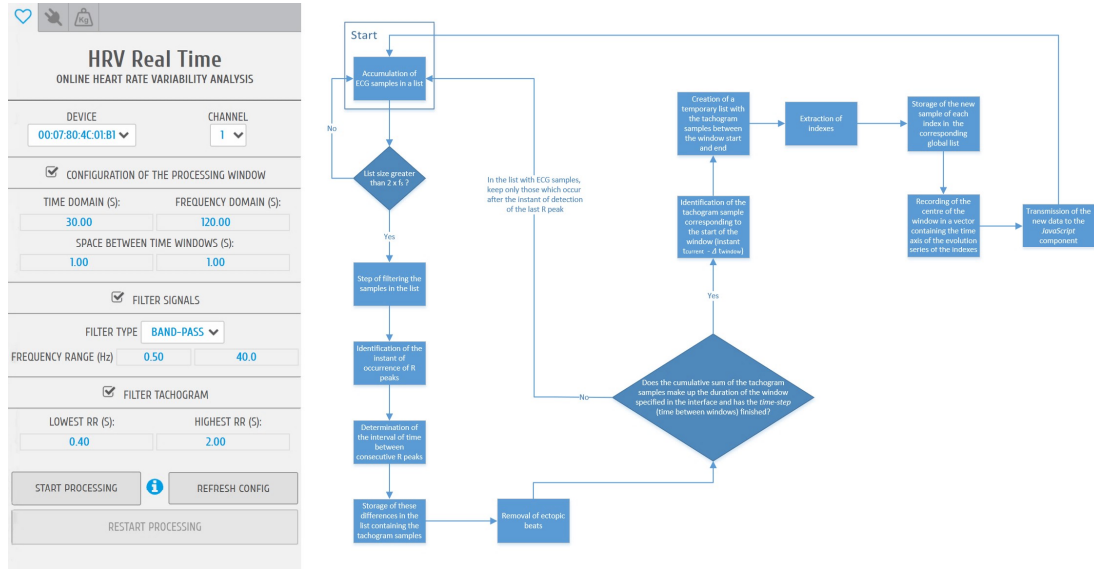


Figure 4.12: Interface of the HRV *plugin* for real-time processing, together with its internal operating logic

The degree of similarity of the tachograms generated by the Pan-Tompkins algorithm in *offline* and real-time contexts was evaluated by correlating the two time series, and a Pearson coefficient of 0.99 was obtained. This indicates that the algorithm was switched correctly (Figure 4.13).

Given that all the processing is dependent on this base structure, the results of the real-time implementation can be partially validated, providing us a bigger confidence about its interpretation during the real-time analysis.

We judged the results by an indirect way, through the evaluation of the efficiency in generating the structure (tachogram) that constitutes the *genesis* of all extracted HRV indexes.

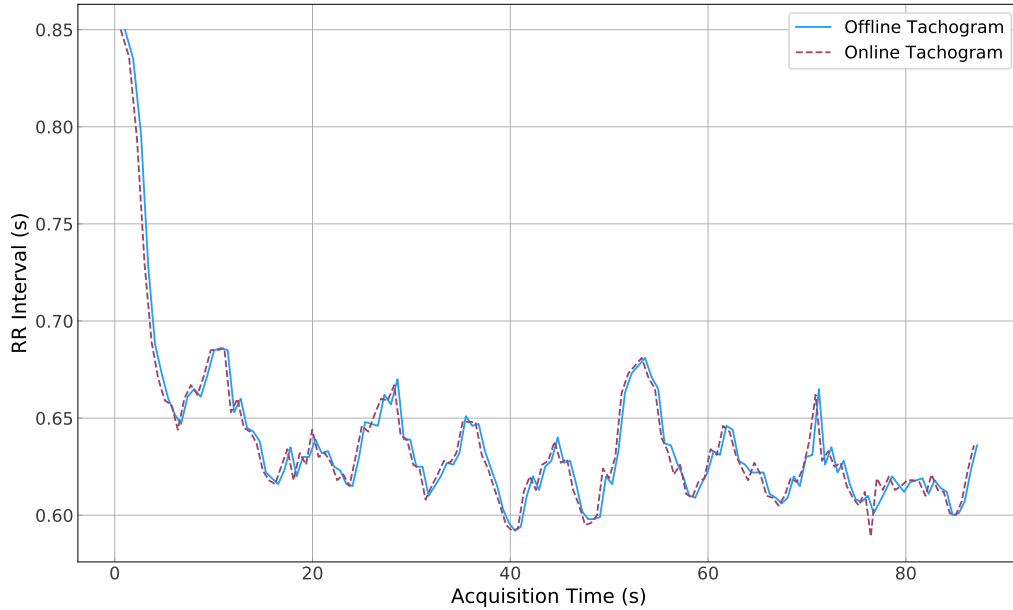


Figure 4.13: Comparison of the tachograms obtained in the *plugin* for *offline* analysis and the *plugin* for real-time analysis, showing almost perfect overlapping

#### 4.4.3 Computational Restrictions

The computational resources of a computer system are limited, giving rise to major constraints when these are not correctly managed or they are over-exploited.

Thus, when implementing these two real-time processing *plugins*, some adjustments to the main projection were necessary to ensure the system worked efficiently and without collapsing.

In the first versions of the *plugin*, a time lag began to emerge between the acquisition and the processed results, that is, the system started operating out of sync with the acquisition.

In order to make the *plugins* work more efficient, the following corrections were made:

- **Reduction in the number of graphical regions in the interface** - this measure was applied by incorporating the *check-boxes* for selecting indexes to observe in the interface;
- **Updating of the content of the Dygraph structure** - as an alternative to creating a new *Dygraph* for each new sample received, the original *Dygraph* is updated using the `updateOptions` method. The user does not notice the effect of this measure, since in both approaches only one *Dygraph* would ever be displayed in the interface. However, if an object was created for each new sample, memory would remain allocated, contributing to the collapse of the system in the long run;

- **Minimisation of the number of data communications between the Python component and JavaScript as well as the volume of data transmitted** - to avoid overloading communication between the two components, instead of the entire time series of index X being transmitted, only the new samples that have not yet been communicated are transmitted. In addition, instead of communication with the *JavaScript* component taking place in each iteration of the *Python* processing (at each packet of 150 samples processed), communication is limited to the iteration in which the indexes are extracted. Only the *Python* processing results for the indexes selected for observation in the interface will be communicated to the *JavaScript* component;
- **Avoid storing information in JavaScript** - all the data will be stored in *Python* and if they are necessary in the *JavaScript* component they will be requested;
- **Minimisation of the Global variables in JavaScript** - considering that information in *JavaScript* is managed by *Garbage Collector*, if a temporary variable is inadvertently declared as a global variable, the data it contains remain allocated to the memory for an indefinite period. In contrast, a local variable defined as **var** is “marked” as disposable, and the *Garbage Collector* eventually excludes it after some runtime. The effects of this unnecessary memory allocation may not be noticed in the short term, but they have implications for the operation of the system in long-lasting acquisitions.
- **Regular cleaning of the Python ↔ JavaScript communications stack** - after some acquisition time, pending communications start to accumulate, generating a gradual lag between the time of acquisition and the processing results being displayed. With this approach, some samples may be lost, but the system is guaranteed to work in sync, a basic requirement for a real-time processing system.

## 4.5 Fatigue Analysis Plugin - Offline

The methods used for processing the information (Chapter 3) and the results of applying them, which are summarised in the preceding sections, are an essential research component for supporting any practical study application.

However, the final solution intended for the user, where all the methods were integrated, remains to be presented.

The implemented system was incorporated into *OpenSignals* as an *offline plugin* for processing EMG and ECG signals, in order to monitor the fatigue state.

The interface was constructed in such a way as to be attractive and functional, incorporating a large part of the functions of the *plugins* described in sections 4.4.1 and 4.4.2. However, a brief description of the interface is required to explain the differences in user interaction (Figure 4.14).



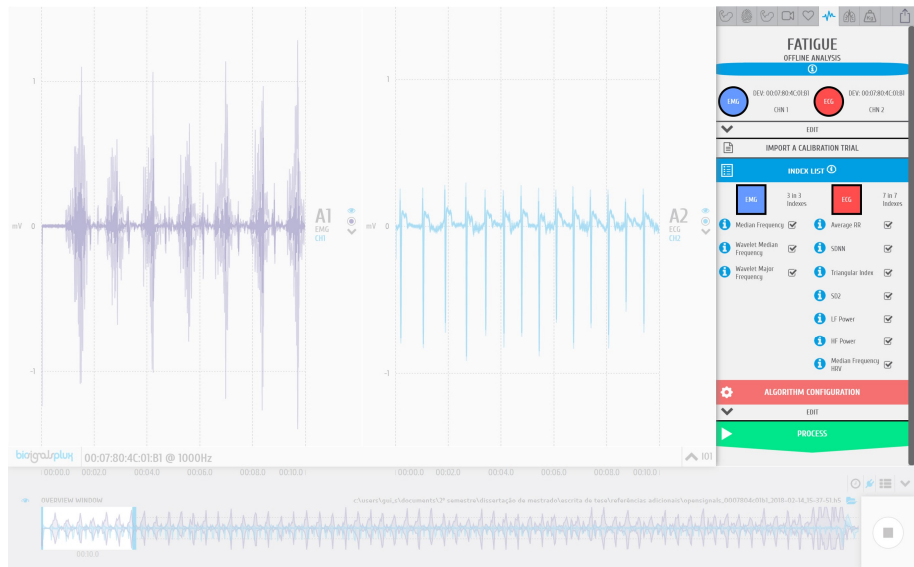


Figure 4.14: View of the interface of the *plugin* for monitoring the fatigue state (highlighted in the right-hand side of the image)

Once the file containing the acquisition has been imported, the system will automatically assign an EMG and ECG origin channel. However, considering the file may contain more channels, if the assigned channel does not meet the user's requirements, he or she may manually configure the channel from which the various fatigue indexes will be extracted, using the tab shown in Figure 4.15.

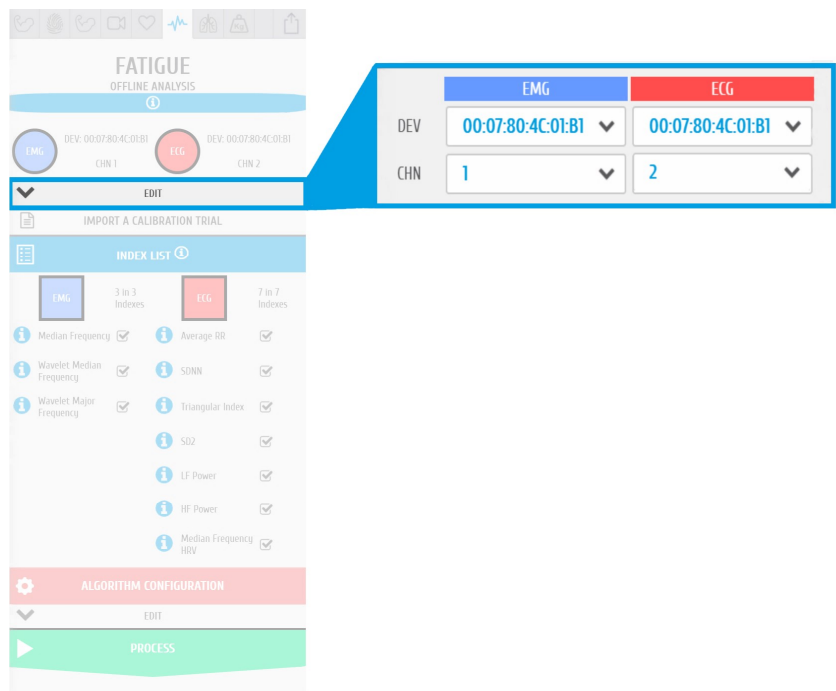


Figure 4.15: Focused view of the tab in the interface for specifying the device and channel associated with each type of signal



The file used for calibration purposes must then be specified.

In the section intended for this purpose, it is possible to import a previously generated calibration file, or, alternatively, to import an acquisition containing EMG and ECG data during the calibration test described in section B.2 (Figure 4.16).

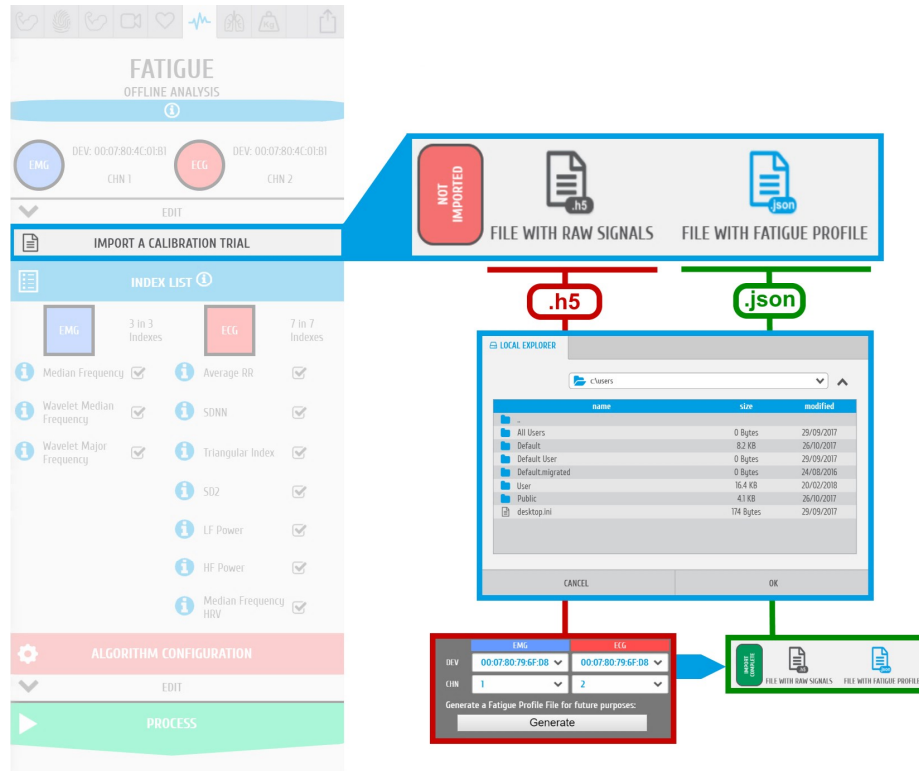


Figure 4.16: File importation options for calibrating the system, and the sequence of steps

The user may then specify the fatigue indexes to be analysed in more detail, namely, the ones whose evolution over the course of the acquisition he or she wishes to view.

Considering that all the indexes will be needed for the classification segment, if at least one of them is not selected, the classification system does not produce results and an alert message appears about this restriction (Figure 4.17).

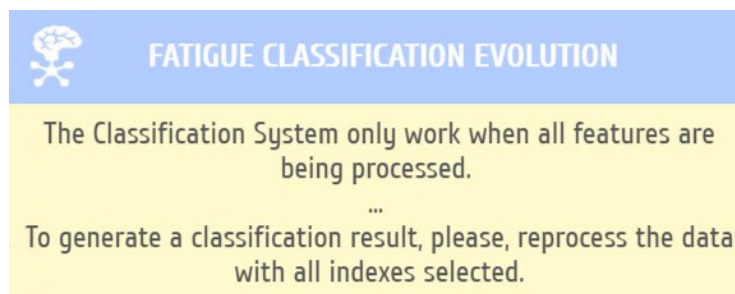


Figure 4.17: Alert message stating that classification of the fatigue state is not possible, given that some indexes have not been extracted

The last section with which the user may interact before the processing phase includes options for configuring the algorithm for detecting periods of muscular activation. The digital filters to be applied to the signals can also be programmed, and the size of the processing window and the time-step for extracting the fatigue indexes can be specified (Figure 4.18).

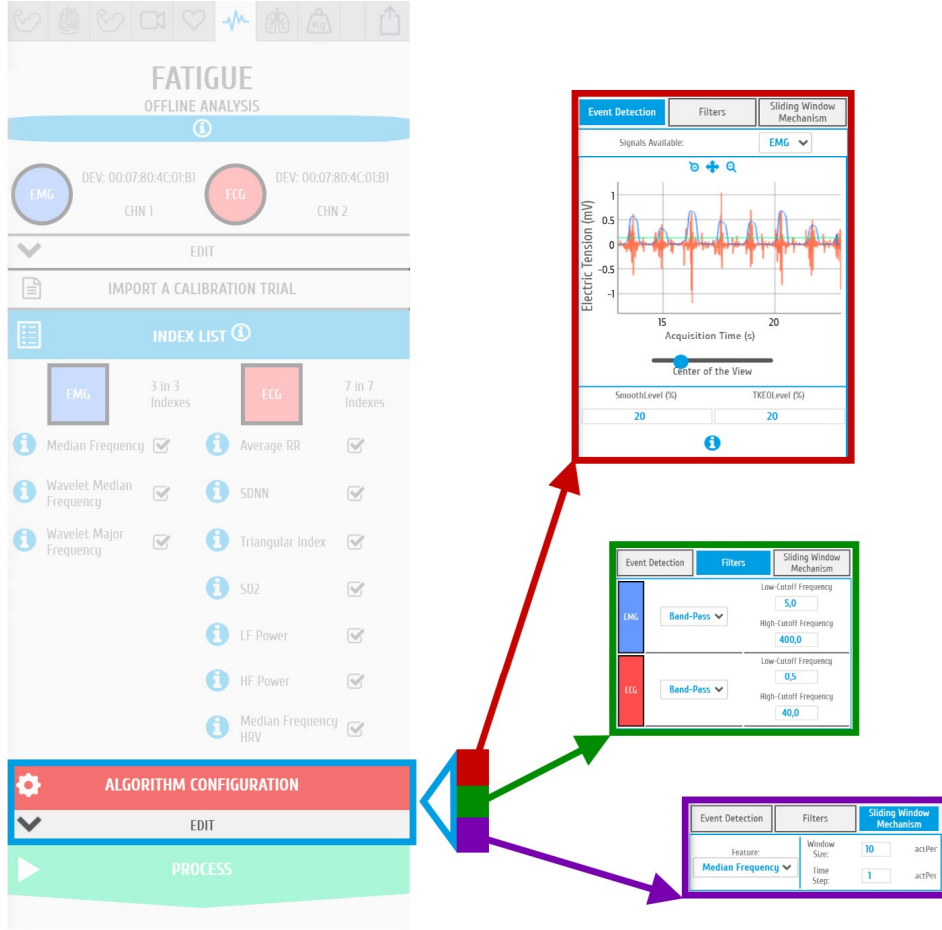


Figure 4.18: Section for configuring algorithms and methods used in the processing phase, showing the tab for specifying the TKEO parameters (in red), the tab for defining the digital filters (in green), and the zone for editing the size of the processing window and the time-step (in purple)

It should be noted that all of the above configurations are optional, and the user may initiate the processing immediately after importing the acquisition, thus keeping the pre-defined values.

Processing takes a few seconds, largely because it relies on the Wavelet Transform and corresponding image processing.

The processing time is proportional to the number of samples contained in the acquired signals. The window size and time-step chosen for extracting each EMG and ECG fatigue index, also have an important impact at this level, considering, for example, that with smaller window sizes more iterations are needed for generating the evolution time series.

Four results are subsequently produced (Figure 4.19):

- **Events detected** - periods of muscular activation in the EMG signal and R peaks in the ECG signal;
- **Evolution of Fatigue Indexes** - the user may select which indexes he or she wishes to observe, using the interactive zone;
- **Evolution of the Global Fatigue Index** - fatigue levels are shown through the colour system;
- **Evolution of the Automatic Classification** - description of the class attributed by the classifier over the course of the acquisition.

To assist the user, there is a function which generates a PDF report summarising the processing results. An example of this is available in Appendix D.

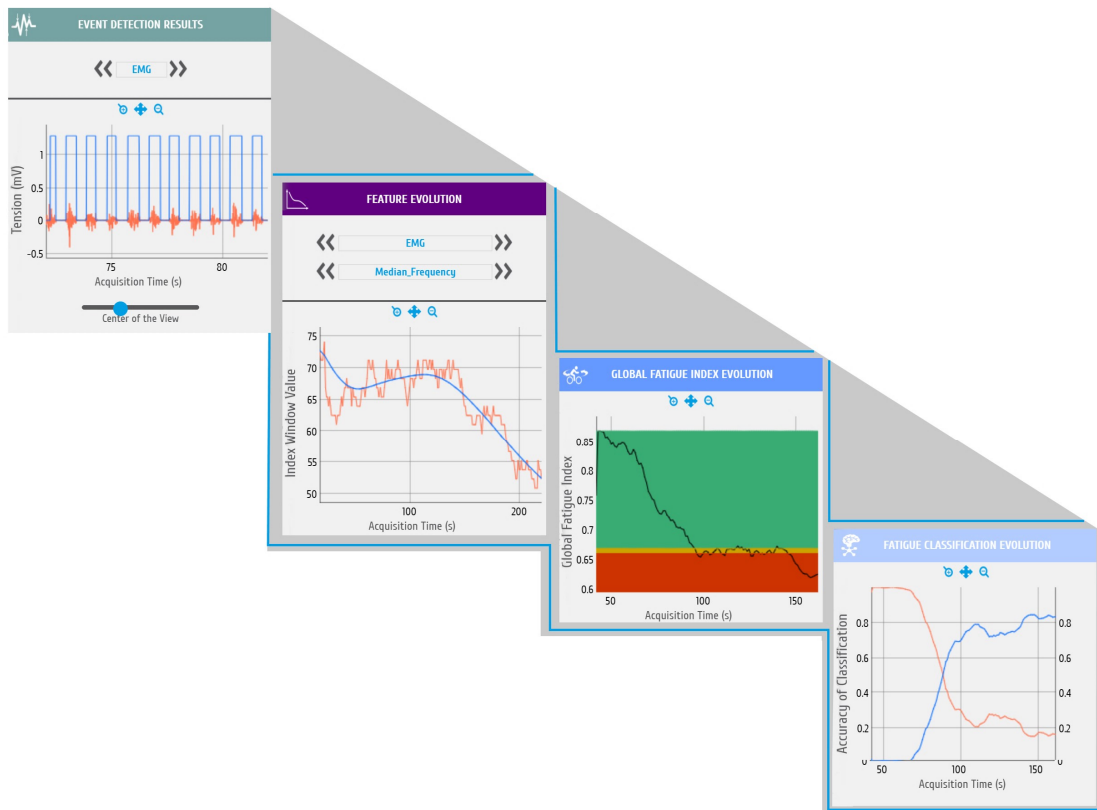


Figure 4.19: View of the various processing results arising from the analysis of the EMG and ECG fatigue indexes



## Discussion of Results and Expectations for the Future

### 5.1 Discussion of Results

One relevant aspect is the discussion on the identification of trends. It may be observed that a large number of the fatigue indexes included in the project are already referenced in other works, suggesting that the method was applied correctly.

On the one hand, the evolution of the indexes derived from the ECG signal suggest, in our analysis, that heart rate variability decreases as fatigue emerges, an idea which is corroborated by various studies [19, 21, 55]. However, there is not a consensus on the evolution of heart rate variability in these conditions [89] owing to the fact that it is a phenomenon which is influenced by different mechanisms and variables, such as age or gender.

In terms of the EMG fatigue indexes (extracted from the frequency domain), the literature reveals more of a consensus. From the start, it could be expected that the spectrum would be compressed in the direction of the low frequencies [16–18], and this was verified in the experiments (Section 4.1).

For trend identification, the linear regression model was chosen as a basis for the method, owing to its simplicity and the fact that it produces a binary quantification of the evolution of time series through a negative or positive slope.

However, there are some constraints when it comes to indexes that may not evolve linearly, and therefore existing the risk that the criteria established in section 3.2.3 could result in fatigue indexes being wrongly excluded or included.

Despite this issue, the results appear to be robust: through the two methods that were applied, two very similar lists of fatigue indexes were generated.

Two ECG indexes (Power in the LF and HF Bands) were extracted in very extreme conditions from time windows of 30 seconds, given that this was the size with the lowest coefficient of variation according to the meta-analysis. This means that the frequency resolution is relatively low and consequently the determination of the power in such narrow bands (LF -[0.04;0.15] Hz and HF - [0.15;0.40] Hz) may not be very precise. The results for these indexes must therefore be interpreted with caution.

With regard to the criteria established for including or excluding EMG/ECG indexes in the list of fatigue indexes, this is the most subjective aspect of the method. However, the choice of criteria is logical considering the specific characteristics of the acquisitions used.

In terms of the trained classification system, it should once again be highlighted that it is experimental in nature, considering that the training set does not contain many examples (twenty-two), and more acquisitions would need to be carried out to increase the training set and thus the quality of the classifier.

Moreover, some fatigue indexes may be perceived as redundant, specifically the indexes for analysing heart rate variability, since all of them are intended for the same purpose (to study heart rate variability) and show the same evolution. There is a great deal of room for improvement in this respect, and it is expected that excluding some indexes will not have too much of an impact on how the classifier works and how the global index evolves.

There is one extremely restrictive aspect: the need for a calibration test to ensure that reliable results can be obtained from the classifier, from determining the global index and from establishing the severity of the fatigue.

This problem is not necessarily associated with the fact that a calibration test is needed. Essentially it lies in the difficulty of conducting one. The current calibration test (protocol of “Day 2”) will involve the subject becoming exhausted and therefore needing a few hours of rest between the calibration test and the testing protocol.

With regard to the fatigue severity levels, extracted from the calibration test, these have not yet been confirmed as valid, given that there are no new acquisitions for the subjects in the sample. In all of the tests performed to date, the test itself was used as a calibration test, giving rise to the desired behaviour with the volunteer gradually nearing the red zone and reaching it in the final phase of the test when he became exhausted.

However, there must be some reservations, since this approach will not be the one applied when the system is used as normal. Thus, in future validation phases the behaviour may move slightly away from that observed, and therefore corrections may need to be made to the way in which the thresholds are defined.

Lastly, it should be noted that the system was designed for indoor cycling on a cycle ergometer, intended for studying the muscles of the lower limb. The number of factors affecting the recording of signals, such as movement artefacts in the ECG signal and the position of the electrodes, was therefore minimised considerably.

The absence of tests in other conditions makes it impossible to assert that the system works in other kinds of conditions. However, we believe that with the right adaptations, the range of monitorable activities may be changed and extended, given the solid basis we have.

It may be concluded that a number of points still need to be considered and corrected, but that the fatigue monitoring potential identified at the start of the project has been demonstrated to exist, and the steps that were followed constituted an initial approach towards transforming this potential into a practical and functional solution.

## 5.2 Future Expectations

One of the objectives mentioned in section 1.2 is to switch the *offline* processing system to real-time mode. This is the next step in the project, considering that the entire *offline* system was programmed using methods that could easily be transposed to *online* processing.

The chosen size for the time windows in *offline* mode may need to be adapted, considering that larger windows are generally needed for frequency indexes to ensure adequate resolution. This means that some of the indexes may not be completely feasible in a real-time application.

In the time domain, literature recommends the use of time windows of at least 20 minutes for the extraction of the triangular index, to ensure a robust statistical approach [41].

Furthermore, the current system only extracts information from EMG and ECG signals, but there are studies with promising results that are based on other types of signal such as MMG and NIRS. In the future, it is expected that fatigue monitoring will be extended to mechanical events or chemical patterns generated as a result of muscular contraction.

One of the studies consulted [90] is particularly interesting considering it applies to cyclic activity in the lower limbs, where a non-linear index is extracted, and it establishes a promising link with fatigue acquisition.

A computer system should be easy to use, and the less that is required of the user the more attractive it is.

The calibration test is an obstacle to this logic, and the aim in the future is for it to no longer be necessary.

One possible approach would be to define reference values for each fatigue index (used to normalise the inputs for computing the global index and the classification system) by calculating an average for the population sample. This would require new acquisitions and a greater number of volunteers.





## Bibliography

- [1] Eurostat. *Mortality and life expectancy statistics*. 2018. URL: [http://ec.europa.eu/eurostat/statistics-explained/index.php/Mortality\\_and\\_life\\_expectancy\\_statistics](http://ec.europa.eu/eurostat/statistics-explained/index.php/Mortality_and_life_expectancy_statistics) (visited on Feb. 3, 2018).
- [2] M. Roser. *Life Expectancy*. 2018. URL: <https://ourworldindata.org/life-expectancy> (visited on Feb. 3, 2018).
- [3] J. Pietzsch. *The Nobel Prize in Physics 1901 - Speed Read: An Illuminating Accident*. 2014. URL: [https://www.nobelprize.org/nobel\\_prizes/physics/laureates/1901/speedread.html](https://www.nobelprize.org/nobel_prizes/physics/laureates/1901/speedread.html) (visited on July 24, 2017).
- [4] F. Firestone. *Flaw detecting device and measuring instrument*. 1942. URL: <https://www.google.com/patents/US2280226>.
- [5] J. Pietzsch. *The Nobel Prize in Physiology or Medicine 1979 - Perspectives: With a Little Help from My Friends*. 2014. URL: [https://www.nobelprize.org/nobel\\_prizes/medicine/laureates/1979/perspectives.html](https://www.nobelprize.org/nobel_prizes/medicine/laureates/1979/perspectives.html) (visited on July 24, 2017).
- [6] J. Pietzsch. *The Nobel Prize in Physiology or Medicine 2003 - Perspectives*. 2014. URL: [http://www.nobelprize.org/nobel\\_prizes/medicine/laureates/2003/perspectives.html](http://www.nobelprize.org/nobel_prizes/medicine/laureates/2003/perspectives.html) (visited on July 24, 2017).
- [7] M. Kazamel and P. P. Warren. “History of electromyography and nerve conduction studies: A tribute to the founding fathers.” In: *Journal of Clinical Neuroscience* 43 (2017), pp. 54–60. URL: <http://linkinghub.elsevier.com/retrieve/pii/S096758681730262X>.
- [8] M. Rivera-Ruiz, C. Cajavilca, and J. Varon. “Einthoven’s string galvanometer: the first electrocardiograph.” In: *Texas Heart Institute Journal* 35.2 (2008), pp. 174–178. URL: <http://www.pubmedcentral.nih.gov/articlerender.fcgi?artid=2435435&tool=pmcentrez&rendertype=abstract>.
- [9] J. Hayward, G. Chansin, and H. Zervos. *Wearable Technology 2017-2027: Markets, Players, Forecasts*. Tech. rep. IDTechEx, 2017.

- [10] Cisco. *Cisco Visual Networking Index: Global Mobile Data Traffic Forecast Update, 2016–2021*. 2017. URL: <https://www.cisco.com/c/en/us/solutions/collateral/service-provider/visual-networking-index-vni/mobile-white-paper-c11-520862.pdf> (visited on Mar. 21, 2018).
- [11] Business Insider. *The Apple Watch is winning in the battle of fitness trackers*. 2016. URL: <http://www.businessinsider.com/smartwatches-are-siphoning-demand-from-fitness-trackers-2016-4-22> (visited on Feb. 3, 2018).
- [12] Consumer Technology Association. *Digital America - State of the U.S. Consumer Technology Industry*. Tech. rep. 2016, p. 130. URL: [https://www.cta.tech/CTA/media/News/2016\\_DigitalAmerica.pdf](https://www.cta.tech/CTA/media/News/2016_DigitalAmerica.pdf).
- [13] P. Lamkin. *Wearable Tech Market to Double by 2021*. 2017. URL: <https://www.forbes.com/sites/paullamkin/2017/06/22/wearable-tech-market-to-double-by-2021/#362967fcd8f3> (visited on Feb. 3, 2018).
- [14] A. Bernardino. *O músculo no limite da fadiga*. 2017. URL: [https://www.publico.pt/2017/11/09/desporto/noticia/musculos-no-limite-da-fadiga-1791877?page=/&pos=5&b=stories\\_b](https://www.publico.pt/2017/11/09/desporto/noticia/musculos-no-limite-da-fadiga-1791877?page=/&pos=5&b=stories_b) (visited on Feb. 4, 2018).
- [15] S. L. Rozzi, S. M. Lephart, and F. H. Fu. “Effects of Muscular Fatigue on Knee Joint Laxity and Neuromuscular Characteristics of Male and Female Athletes.” In: *Journal of athletic training* 34.2 (1999), pp. 106–114. URL: <https://www.ncbi.nlm.nih.gov/pmc/articles/PMC1322898/>.
- [16] M. Cifrek, V. Medved, S. Tonković, and S. Ostojić. “Surface EMG based muscle fatigue evaluation in biomechanics.” In: *Clinical Biomechanics* 24.4 (2009), pp. 327–340. URL: <https://linkinghub.elsevier.com/retrieve/pii/S0268003309000254>.
- [17] C. J. De Luca. “Myoelectrical manifestations of localized muscular fatigue in humans.” In: *Critical Reviews in Biomedical Engineering* 11.4 (1984), pp. 251–279. URL: [http://www.delsys.com/Attachments\\_pdf/nmrc/files/2010/04/026.pdf](http://www.delsys.com/Attachments_pdf/nmrc/files/2010/04/026.pdf).
- [18] R. B. Graham, M. P. Wachowiak, and B. J. Gurd. “The Assessment of Muscular Effort, Fatigue, and Physiological Adaptation Using EMG and Wavelet Analysis.” In: *PLoS ONE* 10.8 (2015), pp. 1–13. URL: <http://journals.plos.org/plosone/article?id=10.1371/journal.pone.0135069>.
- [19] L. Schmitt, J. Regnard, A. L. Parmentier, F. Mauny, L. Mourot, N. Coulmy, and G. P. Millet. “Typology of Fatigue by Heart Rate Variability Analysis in Elite Nordic-skiers.” In: *International Journal of Sports Medicine* 36.12 (2015), pp. 999–1007. URL: <https://www.thieme-connect.de/DOI/DOI?10.1055/s-0035-1548885>.

- 
- [20] J. Murgoitio Larrauri, J. L. G. Temiño, and M. J. G. Larrea. “Heart Rate Variability - Knowing More about HRV Analysis and Fatigue in Transport Studies.” In: *Proceedings of the International Congress on Cardiovascular Technologies* (2013), pp. 107–114. URL: <http://www.scitepress.org/DigitalLibrary/Link.aspx?doi=10.5220/0004666501070114>.
  - [21] L. Schmitt, J. Regnard, D. Auguin, and G. P. Millet. “Monitoring Training and Fatigue Status with Heart Rate Variability: Case Study in a Swimming Olympic Champion.” In: *Journal of Fitness Research* 5.3 (2016), pp. 38–45. URL: <http://research.usc.edu.au/vital/access/manager/Repository/usc:21212?lightbox=true&letter=Y>.
  - [22] L. Faller, G. Neto, V. Button, and P. Nohama. “Muscle fatigue assessment by mechanomyography during application of NMES protocol.” In: *Revista Brasileira de Fisioterapia* 13.5 (2009), pp. 422–429. URL: [http://www.scielo.br/scielo.php?script=sci\\_arttext&pid=S1413-35552009000500009&lng=pt&nrm=iso&tlng=en](http://www.scielo.br/scielo.php?script=sci_arttext&pid=S1413-35552009000500009&lng=pt&nrm=iso&tlng=en).
  - [23] K. T. Ebersole, K. M. O’Connor, and A. P. Wier. “Mechanomyographic and electromyographic responses to repeated concentric muscle actions of the quadriceps femoris.” In: *Journal of Electromyography and Kinesiology* 16.2 (2006), pp. 149–157. URL: <https://www.sciencedirect.com/science/article/pii/S1050641105000787?via%3Dihub>.
  - [24] J. Shi, Y. P. Zheng, X. Chen, and Q. H. Huang. “Assessment of muscle fatigue using sonomyography: Muscle thickness change detected from ultrasound images.” In: *Medical Engineering and Physics* 29.4 (2007), pp. 472–479. URL: [http://www.medengphys.com/article/S1350-4533\(06\)00146-9/fulltext](http://www.medengphys.com/article/S1350-4533(06)00146-9/fulltext).
  - [25] S. K. Stackhouse, D. S. Reisman, and S. A. Binder-Macleod. “Challenging the Role of pH in Skeletal Muscle Fatigue.” In: *Physical therapy* 81.12 (2001), pp. 1897–1903. URL: <https://academic.oup.com/ptj/article/81/12/1897/2857605>.
  - [26] J. Taelman, J. Vanderhaegen, M. Robijns, G. Naulaers, A. Spaepen, and S. Van Huffel. “Estimation of Muscle Fatigue using Surface Electromyography and Near-infrared Spectroscopy.” In: *Advances in Experimental Medicine and Biology* 701 (2011), pp. 353–359. URL: [https://link.springer.com/chapter/10.1007%2F978-1-4419-7756-4\\_48](https://link.springer.com/chapter/10.1007%2F978-1-4419-7756-4_48).
  - [27] BSX Insight. *Next Generation Endurance Testing*. URL: <https://www.bsxinsight.com/technology> (visited on Jan. 18, 2017).
  - [28] BSX Insight. *What is BSXinsight and how does it work?* 2016. URL: <https://support.bsxinsight.com/hc/en-us/articles/204394525-What-is-BSXinsight-and-how-does-it-work-> (visited on July 24, 2017).
  - [29] E. N. Marieb. *Human Anatomy & Physiology*. 5th. San Francisco, 2001. ISBN: 9780805349894.

- [30] R. Merletti. “Standards for Reporting EMG Data.” In: *Journal of Electromyography and Kinesiology* 33 (2017), pp. I–II. URL: <http://linkinghub.elsevier.com/retrieve/pii/S1050641117300998>.
- [31] A. Atkielski. *Schematic diagram of normal sinus rhythm for a human heart as seen on ECG*. 2007. URL: <https://commons.wikimedia.org/wiki/File:SinusRhythmLabels.svg> (visited on Mar. 21, 2017).
- [32] Mayo Clinic. *Bundle branch block*. URL: <https://www.mayoclinic.org/diseases-conditions/bundle-branch-block/multimedia/bundle-branch-block/img-20008362> (visited on Feb. 10, 2018).
- [33] G. R. Naik and K. A. Reddy. “A New Model for ECG Signal Filtering and Feature Extraction.” In: *2016 2nd IEEE International Conference on Computer and Communications (ICCC)*. 2016, pp. 765–768. URL: <http://ieeexplore.ieee.org/document/7924806/>.
- [34] P. Kligfield, L. S. Gettes, J. J. Bailey, R. Childers, B. J. Deal, E. W. Hancock, G. van Herpen, J. A. Kors, P. Macfarlane, D. M. Mirvis, O. Pahlm, P. Rautaharju, and G. S. Wagner. “Recommendations for the Standardization and Interpretation of the Electrocardiogram: Part I: The Electrocardiogram and Its Technology.” In: *Journal of the American College of Cardiology* 49.10 (2007), pp. 1109–1127. URL: <http://www.sciencedirect.com/science/article/pii/S073510970700232X>.
- [35] P. Bonato, T. D’Alessio, and M. Knaflitz. “A Statistical Method for the Measurement of Muscle Activation Intervals from Surface Myoelectric Signal During Gait.” In: *IEEE Transactions on Biomedical Engineering* 45.3 (1998), pp. 287–299. URL: <http://ieeexplore.ieee.org/document/661154/>.
- [36] P. W. Hodges and B. H. Bui. “A comparison of computer-based methods for the determination of onset of muscle contraction using electromyography.” In: *Electroencephalography and Clinical Neurophysiology/Electromyography and Motor Control* 101.6 (1996), pp. 511–519. URL: <http://linkinghub.elsevier.com/retrieve/pii/S0921884X96951905>.
- [37] A. Pimentel, R. Gomes, B. H. Olstad, and H. Gamboa. “A New Tool for the Automatic Detection of Muscular Voluntary Contractions in the Analysis of Electromyographic Signals.” In: *Interacting with Computers* 27.5 (2015), pp. 492–499. URL: <https://academic.oup.com/iwc/article-abstract/27/5/492/710400?redirectedFrom=fulltext>.
- [38] J. Pan and W. J. Tompkins. “A Real-Time QRS Detection Algorithm.” In: *IEEE Transactions on Biomedical Engineering* BME-32.3 (1985), pp. 230–236. URL: <http://ieeexplore.ieee.org/document/4122029/>.
- [39] P. Konrad. *The ABC of EMG: A Practical Introduction to Kinesiological Electromyography*. Version 1.0. Noraxon USA, Inc, 2005. ISBN: 0977162214. URL: <http://bme2.aut.ac.ir/~towhidkhah/MotorControl/Notes/EMG.pdf>.

- [40] U. R. Acharya, K. P. Joseph, N. Kannathal, C. M. Lim, and J. S. Suri. “Heart rate variability: A review.” In: *Medical and Biological Engineering and Computing* 44.12 (2006), pp. 1031–1051. URL: <https://link.springer.com/article/10.1007%2Fs11517-006-0119-0>.
- [41] Task Force of The European Society of Cardiology and the North American Society of Pacing and Electrophysiology. “Heart Rate Variability - Standards of measurement, physiological interpretation, and clinical use Task.” In: *Circulation* 93.5 (1996), pp. 1043–1065. URL: <http://circ.ahajournals.org/content/93/5/1043>.
- [42] G. Swapna, D. N. Ghista, R. J. Martis, A. P. C. Ang, and S. V. Sree. “Ecg Signal Generation and Heart Rate Variability Signal Extraction: Signal Processing, Features Detection, and Their Correlation With Cardiac Diseases.” In: *Journal of Mechanics in Medicine and Biology* 12.4 (2012), pp. 1–26. URL: <http://www.worldscientific.com/doi/abs/10.1142/S021951941240012X>.
- [43] B. K. Barry and R. M. Enoka. “The neurobiology of muscle fatigue: 15 years later.” In: *Integrative and Comparative Biology* 47.4 (2007), pp. 465–473. URL: <https://academic.oup.com/icb/article/47/4/465/632525>.
- [44] J. Shen, J. Barbera, and C. M. Shapiro. “Distinguishing sleepiness and fatigue: Focus on definition and measurement.” In: *Sleep Medicine Reviews* 10.1 (2006), pp. 63–76. URL: [http://www.smr-v-journal.com/article/S1087-0792\(05\)00044-4/fulltext](http://www.smr-v-journal.com/article/S1087-0792(05)00044-4/fulltext).
- [45] M. J. Zwarts, G. Bleijenberg, and B. G. M. van Engelen. “Clinical neurophysiology of fatigue.” In: *Clinical Neurophysiology* 119.1 (2008), pp. 2–10. URL: [www.clinph-journal.com/article/S1388-2457\(07\)00591-3/fulltext](http://www.clinph-journal.com/article/S1388-2457(07)00591-3/fulltext).
- [46] B. Bigland-Ritchie and J. J. Woods. “Change in muscle contractile properties and neural control during human muscular fatigue.” In: *Muscle & Nerve* 7.9 (1984), pp. 691–699. URL: <https://onlinelibrary.wiley.com/doi/abs/10.1002/mus.880070902>.
- [47] W. C. Bowman. “Neuromuscular block.” In: *British Journal of Pharmacology* 147.S1 (2006), pp. 277–286. URL: <https://bpspubs.onlinelibrary.wiley.com/doi/abs/10.1038/sj.bjp.0706404>.
- [48] J. H. Viitasalo and P. V. Komi. “Signal characteristics of EMG during fatigue.” In: *European Journal of Applied Physiology and Occupational Physiology* 37.2 (1977), pp. 111–121. URL: <https://link.springer.com/article/10.1007/BF00421697>.
- [49] P. Bonato, S. H. Roy, M. Knaflitz, and C. J. De Luca. “Time Frequency Parameters of the Surface Myoelectric Signal for Assessing Muscle Fatigue during Cyclic Dynamic Contractions.” In: *IEEE Transactions on Biomedical Engineering* 48.7 (2001), pp. 745–753. URL: <http://ieeexplore.ieee.org/document/930899/>.

- [50] S. K. Chowdhury and A. D. Nimbarte. “Comparison of Fourier and wavelet analysis for fatigue assessment during repetitive dynamic exertion.” In: *Journal of Electromyography and Kinesiology* 25.2 (2015), pp. 205–213. URL: <https://www.sciencedirect.com/science/article/pii/S1050641114002429?via%3Dihub>.
- [51] N. Otsu. “A Threshold Selection Method from Gray-Level Histograms.” In: *IEEE Transactions on Systems, Man, and Cybernetics* 9.1 (1979), pp. 62–66. URL: <http://ieeexplore.ieee.org/document/4310076/>.
- [52] Z. Roja, V. Kalkis, A. Vain, H. Kalkis, and M. Eglite. “Assessment of skeletal muscle fatigue of road maintenance workers based on heart rate monitoring and myotonometry.” In: *Journal of Occupational Medicine and Toxicology* 1.20 (2006), pp. 1–9. URL: <https://occup-med.biomedcentral.com/articles/10.1186/1745-6673-1-20>.
- [53] M. Patel, S. K. L. Lal, D. Kavanagh, and P. Rossiter. “Applying neural network analysis on heart rate variability data to assess driver fatigue.” In: *Expert Systems with Applications* 38.6 (2011), pp. 7235–7242. URL: <https://www.sciencedirect.com/science/article/pii/S0957417410013916?via%3Dihub>.
- [54] T. Kiryu, T. Abe, Y. Ushiyama, H. Yamada, and M. Okada. “Snapshot Evaluation of Fatigue Using Heart Rate Variability and Superimposed M Waves of Myoelectric.” In: *Engineering in Medicine and Biology Society, 1997. Proceedings of the 19th Annual International Conference of the IEEE*. Vol. 4. 1997, pp. 1428–1431. URL: <http://ieeexplore.ieee.org/document/756973/>.
- [55] L. Schmitt, J. Regnard, and G. P. Millet. “Monitoring Fatigue Status with HRV Measures in Elite Athletes: An Avenue Beyond RMSSD?” In: *Frontiers in Physiology* 6.343 (2015), pp. 1–3. URL: <https://www.frontiersin.org/articles/10.3389/fphys.2015.00343/full>.
- [56] T. Leti and V. A. Bricout. “Interest of analyses of heart rate variability in the prevention of fatigue states in senior runners.” In: *Autonomic Neuroscience: Basic and Clinical* 173.1-2 (2013), pp. 14–21. URL: <https://linkinghub.elsevier.com/retrieve/pii/S1566070212001750>.
- [57] Y. Tran, N. Wijesuriya, M. Tarvainen, P. Karjalainen, and A. Craig. “The Relationship Between Spectral Changes in Heart Rate Variability and Fatigue.” In: *Journal of Psychophysiology* 23.3 (2009), pp. 143–151. URL: <https://econtent.hogrefe.com/doi/abs/10.1027/0269-8803.23.3.143>.
- [58] C. Orizio, M. Gobbo, B. Diemont, F. Esposito, and A. Veicsteinas. “The surface mechanomyogram as a tool to describe the influence of fatigue on biceps brachii motor unit activation strategy. Historical basis and novel evidence.” In: *European Journal of Applied Physiology* 90.3-4 (2003), pp. 326–336. URL: <https://link.springer.com/article/10.1007%2Fs00421-003-0924-1>.



- 
- [59] M. T. Tarata. “Mechanomyography versus Electromyography, in monitoring the muscular fatigue.” In: *Biomedical Engineering OnLine* 2.3 (2003), pp. 1–10. URL: <https://biomedical-engineering-online.biomedcentral.com/articles/10.1186/1475-925X-2-3>.
  - [60] M. Shinohara and K. Sogaard. “Mechanomyography for studying force fluctuations and muscle fatigue.” In: *Exercise and Sport Sciences Reviews* 34.2 (2006), pp. 59–64. URL: <https://insights.ovid.com/crossref?an=00003677-200604000-00004>.
  - [61] Z. F. Yang, D. K. Kumar, and S. P. Arjunan. “Mechanomyogram for Identifying Muscle Activity and Fatigue.” In: *Proceedings of the 31st Annual International Conference of the IEEE Engineering in Medicine and Biology Society: Engineering the Future of Biomedicine, EMBC 2009*. 2009, pp. 408–411. URL: <http://ieeexplore.ieee.org/document/5333666/>.
  - [62] R. Boushel and C. A. Piantadosi. “Near-infrared spectroscopy for monitoring muscle oxygenation.” In: *Acta Physiologica Scandinavica* 168.4 (2000), pp. 615–622. URL: <https://onlinelibrary.wiley.com/doi/abs/10.1046/j.1365-201x.2000.00713.x>.
  - [63] Y. Muramatsu and H. Kobayashi. “Assessment of local muscle fatigue by NIRS.” In: *2013 Seventh International Conference on Sensing Technology (ICST)*. 2013, pp. 623–626. URL: [ieeexplore.ieee.org/document/6727728/](http://ieeexplore.ieee.org/document/6727728/).
  - [64] M. A. Hearst, S. T. Dumais, E. Osman, J. Platt, and B. Scholkopf. “Support vector machines.” In: *IEEE Intelligent Systems and their Applications* 13.4 (1998), pp. 18–28. URL: <http://ieeexplore.ieee.org/document/708428/>.
  - [65] C. Cortes and V. Vapnik. “Support-Vector Networks.” In: *Machine Learning* 20.3 (1995), pp. 273–297. URL: <https://link.springer.com/article/10.1023%2FA%3A1022627411411>.
  - [66] J. Weston and C. Watkins. “Support Vector Machines for Multi-Class Pattern Recognition.” In: *Proceedings of the 7th European Symposium on Artificial Neural Networks (ESANN-99)*. 1999, pp. 219–224. URL: <https://www.elen.ucl.ac.be/Proceedings/esann/esannpdf/es1999-461.pdf>.
  - [67] B. Schölkopf and A. J. Smola. “Support Vector Machines and Kernel Algorithms.” In: *Handbook of Brain Theory and Neural Networks*. 2nd. Cambridge, Massachusetts: MIT Press, 2003, pp. 1119–1125. ISBN: 07384602. URL: <https://pdfs.semanticscholar.org/2862/e7b8fefb209cdb4c47a1643f2af71cd67b00.pdf>.
  - [68] R. J. Shephard. *Aging and Exercise*. 1998. URL: <http://www.sportsci.org/encyc/agingex/agingex.html>.

- [69] T. K. Brar, K. D. Singh, and A. Kumar. “Effect of Different Phases of Menstrual Cycle on Heart Rate Variability (HRV).” In: *Journal of Clinical and Diagnostic Research* 9.10 (2015), pp. CC01–CC04. URL: [http://jcdmr.net/article\\_fulltext.asp?issn=0973-709x&year=2015&volume=9&issue=10&page=CC01&issn=0973-709x&id=6592](http://jcdmr.net/article_fulltext.asp?issn=0973-709x&year=2015&volume=9&issue=10&page=CC01&issn=0973-709x&id=6592).
- [70] Comissão de Ética da Nova Medical School. *Normas para submissão de projetos à Comissão Ética da NMS/FCM*. URL: [http://www.nms.unl.pt/main/alldoc/galeria\\_imagens/CEFCM\\_-\\_Normas\\_para\\_submissãõ\\_de\\_projectos\\_1\\_atualizaãõ\\_email.pdf](http://www.nms.unl.pt/main/alldoc/galeria_imagens/CEFCM_-_Normas_para_submissãõ_de_projectos_1_atualizaãõ_email.pdf) (visited on Mar. 21, 2018).
- [71] A. R. Coggan. *Power Profiling*. 2008. URL: <http://home.trainingpeaks.com/blog/article/power-profiling> (visited on Feb. 14, 2017).
- [72] R. M. Enoka. “Mechanisms of Muscle Fatigue: Central Factors and Task Dependency.” In: *Journal of Electromyography and Kinesiology* 5.3 (1995), pp. 141–149. URL: <https://www.sciencedirect.com/science/article/pii/S105064119500010W?via%3Dihub>.
- [73] R. M. Enoka. “Acute Adjustments.” In: *Neuromechanics of Human Movement*. 4th. Human Kinetics, 2008. Chap. 8, pp. 305–348.
- [74] J. P. Vaz. “Adaptation of motor control to training and disuse : contribution of muscle synergy analysis and movement variability.” Doctoral dissertation. Faculty of Human Kinetics of Lisbon University, 2016. URL: <https://www.repository.utl.pt/handle/10400.5/12145>.
- [75] M Knaflitz and P Bonato. “Time-frequency methods applied to muscle fatigue assessment during dynamic contractions.” In: *Journal of Electromyography and Kinesiology* 9.5 (1999), pp. 337–350. URL: <https://www.sciencedirect.com/science/article/pii/S1050641199000097?via%3Dihub>.
- [76] D. M. Rouffet and C. A. Hautier. “EMG normalization to study muscle activation in cycling.” In: *Journal of Electromyography and Kinesiology* 18.5 (2008), pp. 866–878. URL: <https://www.sciencedirect.com/science/article/pii/S1050641107000612?via%3Dihub>.
- [77] T. W. Schoener. “Field Experiments on Interspecific Competition.” In: *The American Naturalist* 122.2 (1983), pp. 240–285. URL: <https://www.jstor.org/stable/2461233>.
- [78] J Connell. “On the Prevalence and Relative Importance of Interspecific Competition: Evidence from Field Experiments.” In: *American Naturalist* 122.5 (1983), pp. 661–696. URL: <https://www.jstor.org/stable/2460847>.
- [79] B. J. Becker and M.-J. Wu. “The Synthesis of Regression Slopes in Meta-Analysis.” In: *Statistical Science* 22.3 (2007), pp. 414–429. URL: <http://projecteuclid.org/euclid.ss/1199285041>.



- 
- [80] M. Borenstein, L. V. Hedges, J. P. T. Higgins, and H. R. Rothstein. “Reporting the Results of a Meta-Analysis.” In: *Introduction to Meta-Analysis*. John Wiley & Sons, Ltd, 2009, pp. 365–370. URL: <https://onlinelibrary.wiley.com/doi/abs/10.1002/9780470743386.ch41>.
  - [81] M. Borenstein, L. V. Hedges, J. P. Higgins, and H. R. Rothstein. “A basic introduction to fixed-effect and random-effects models for meta-analysis.” In: *Research Synthesis Methods* 1.2 (2010), pp. 97–111. URL: <https://onlinelibrary.wiley.com/doi/abs/10.1002/jrsm.12>.
  - [82] G. F. Reed, F. Lynn, and B. D. Meade. “Use of Coefficient of Variation in Assessing Variability of Quantitative Assays.” In: *Clinical and Diagnostic Laboratory Immunology* 9.6 (2002), pp. 1235–1239. URL: <http://cvi.asm.org/content/9/6/1235.long>.
  - [83] L. Tian. “Inferences on the common coefficient of variation.” In: *Statistics in Medicine* 24.14 (2005), pp. 2213–2220. URL: <https://onlinelibrary.wiley.com/doi/abs/10.1002/sim.2088>.
  - [84] T. W. Beck. “Mechanomyographic and Electromyographic Amplitude and Frequency Responses During Fatiguing Isokinetic Muscle Actions of the Biceps Brachii.” Doctoral dissertation. University of Nebraska, 2004.
  - [85] T. Camata, L. Altimari, H. Bortolotti, J. Dantas, E. Fontes, B. Smirmaul, A. Okano, M. Chacon-Mikahil, and A. Moraes. “Electromyographic Activity and Rate of Muscle Fatigue of the Quadriceps Femoris During Cycling Exercise in the Severe Domain.” In: *Journal of Strength and Conditioning Research* 25.9 (2011), pp. 2537–2543. URL: <https://insights.ovid.com/pubmed?pmid=21804424>.
  - [86] G. Chandrashekar and F. Sahin. “A survey on feature selection methods.” In: *Computers and Electrical Engineering* 40.1 (2014), pp. 16–28. URL: <https://www.sciencedirect.com/science/article/pii/S0045790613003066>.
  - [87] J Kilby and K Prasad. “Analysis of Surface Electromyography Signals Using Discrete Fourier Transform Sliding Window Technique.” In: *International Journal of Computer Theory and Engineering* 5.2 (2013), pp. 321–325. URL: <http://www.ijcte.org/papers/702-P054.pdf>.
  - [88] S Thongpanja, A Phinyomark, P Phukpattaranont, and C Limsakul. “Mean and Median Frequency of EMG Signal to Determine Muscle Force Based on Time-dependent Power Spectrum Mean and Median Frequency of EMG Signal to Determine Muscle Force based on Time- dependent Power Spectrum.” In: *Elektronika Ir Elektrotechnika* 19.3 (2013), pp. 51–56. URL: <http://www.eejournal.ktu.lt/index.php/elt/article/view/3697>.
  - [89] A. E. Aubert, B Seps, and F Beckers. “Heart Rate Variability in Athletes.” In: *Sports Medicine* 33.12 (2003), pp. 889–919. URL: <https://link.springer.com/article/10.2165%2F00007256-200333120-00003>.

- [90] I. Shin, S. Ahn, E. Choi, J. Ryu, S. Park, J. Son, and Y. Kim. “Fatigue Analysis of the Quadriceps Femoris Muscle based on Mechanomyography.” In: *International Journal of Precision Engineering and Manufacturing* 17.4 (2016), pp. 473–478. URL: <https://link.springer.com/article/10.1007%2Fs12541-016-0059-z>.
- [91] M. M. Massin, K. Maeyns, N. Withofs, F. Ravet, and P. Gerard. “Circadian rhythm of heart rate and heart rate variability.” In: *Archives of Disease in Childhood* 83.2 (2000), pp. 179–182. URL: <http://adc.bmj.com/content/83/2/179>.
- [92] S. C. Malpas and G. L. Purdie. “Circadian variation of heart rate variability.” In: *Cardiovascular Research* 24.3 (1990), pp. 210–213. URL: <https://academic.oup.com/cardiovasces/article-abstract/24/3/210/290503>.
- [93] V. K. Yeragani, S. Krishnan, H. J. Engels, and R. Gretebeck. “Effects of Caffeine on Linear and Nonlinear Measures of Heart Rate Variability Before and After Exercise.” In: *Depression and Anxiety* 21.3 (2005), pp. 130–134. URL: <https://onlinelibrary.wiley.com/doi/abs/10.1002/da.20061>.
- [94] D. C. Costa, G. L. De Santi, J. C. Crescêncio, L. P. Seabra, E. E. V. Carvalho, V. Papa, F. Marques, L. Gallo Junior, and A. Schmidt. “Use of the Wasserman equation in optimization of the duration of the power ramp in a cardiopulmonary exercise test: A study of Brazilian men.” In: *Brazilian Journal of Medical and Biological Research* 48.12 (2015), pp. 1136–1144. URL: [http://www.scielo.br/scielo.php?script=sci\\_arttext&pid=S0100-879X2015001201136&lng=en&tlng=en](http://www.scielo.br/scielo.php?script=sci_arttext&pid=S0100-879X2015001201136&lng=en&tlng=en).
- [95] K. Wasserman. *Principles of Exercise Testing and Interpretation: Including Pathophysiology and Clinical Applications*. Lippincott Williams & Wilkins, 2005. ISBN: 0781748763.
- [96] S. M. Dyrstad, S. A. Anderssen, E. Edvardsen, and B. H. Hansen. “Cardiorespiratory fitness in groups with different physical activity levels.” In: *Scandinavian Journal of Medicine & Science in Sports* 26.3 (2016), pp. 291–298. URL: <https://onlinelibrary.wiley.com/doi/abs/10.1111/sms.12425>.
- [97] S. Seiler and E. Tønnessen. “Intervals , Thresholds , and Long Slow Distance : the Role of Intensity and Duration in Endurance Training.” In: *Sportscience* 13.8 (2009), pp. 32–53. URL: <http://sportsci.org/2009/ss.htm>.
- [98] J. P. Porcari, C. X. Bryant, and F. Comana. *Exercise Physiology*. Ed. by F. A. D. Company. Quincy McDonald, 2015. ISBN: 0803625553.
- [99] S. E. Gaskill, B. C. Ruby, A. J. Walker, O. A. Sanchez, R. C. Serfass, and A. S. Leon. “Validity and reliability of combining three methods to determine ventilatory threshold.” In: *Medicine and Science in Sports and Exercise* 33.11 (2001), pp. 1841–1848. URL: <https://insights.ovid.com/crossref?an=00005768-200111000-00007>.

- 
- [100] A. E. Wolpern, D. J. Burgos, J. M. Janot, and L. C. Dalleck. “Is a threshold-based model a superior method to the relative percent concept for establishing individual exercise intensity? a randomized controlled trial.” In: *BMC Sports Science, Medicine and Rehabilitation* 7.16 (2015), pp. 1–9. URL: <http://bmc sportsscimedrehabil.biomedcentral.com/articles/10.1186/s13102-015-0011-z>.
- [101] S. E. Slawson, N. Chakravorti, P. P. Conway, J. Cossor, and A. A. West. “The Effect of Knee Angle on Force Production, in Swimming Starts, using the OSB11 Block.” In: *Procedia Engineering* 34 (2012), pp. 801–806. URL: <https://www.sciencedirect.com/science/article/pii/S187770581201750X?via%3Dihub>.
- [102] S. Shenoy, P. Mishra, and J. S. Sandhu. “Peak Torque and IEMG Activity of Quadriceps Femoris Muscle at Three Different Knee Angles in a Collegiate Population.” In: *Journal of Exercise Science and Fitness* 9.1 (2011), pp. 40–45. URL: <https://www.sciencedirect.com/science/article/pii/S1728869X11600051>.
- [103] V. Marginson and R. Eston. “The relationship between torque and joint angle during knee extension in boys and men.” In: *Journal of Sports Sciences* 19.11 (2001), pp. 875–880. URL: <http://www.tandfonline.com/doi/abs/10.1080/026404101753113822>.
- [104] J. L. Dantas, T. V. Camata, M. A.O. C. Brunetto, A. C. Moraes, T. Abrão, and L. R. Altimari. “Fourier and Wavelet spectral analysis of EMG signals in isometric and dynamic maximal effort exercise.” In: *2010 Annual International Conference of the IEEE Engineering in Medicine and Biology Society, EMBC’10*. 2010, pp. 5979–5982. URL: <http://ieeexplore.ieee.org/document/5627579/>.
- [105] S. P. Arjunan, D. K. Kumar, and G. Naik. “Computation and Evaluation of Features of Surface Electromyogram to Identify the Force of Muscle Contraction and Muscle Fatigue.” In: *BioMed Research International* 2014 (2014), pp. 1–6. URL: <https://www.hindawi.com/journals/bmri/2014/197960/>.
- [106] G. D. Clifford. “Signal Processing Methods for Heart Rate Variability.” Doctoral dissertation. Oxford, 2002. URL: <https://pdfs.semanticscholar.org/45b9/d608447dadfb5a80e0a142d5ee6479c28d67.pdf>.



## List of Features (Figures)

In this appendix we introduce some images that complement graphically the description made in section 2.3 about the EMG and ECG indexes

A large number of these graphical equivalences have been reused in the generation of the report that the fatigue monitoring plugin produce, considering that can facilitate the understanding, by the user, of the way in which the different indices are extracted.

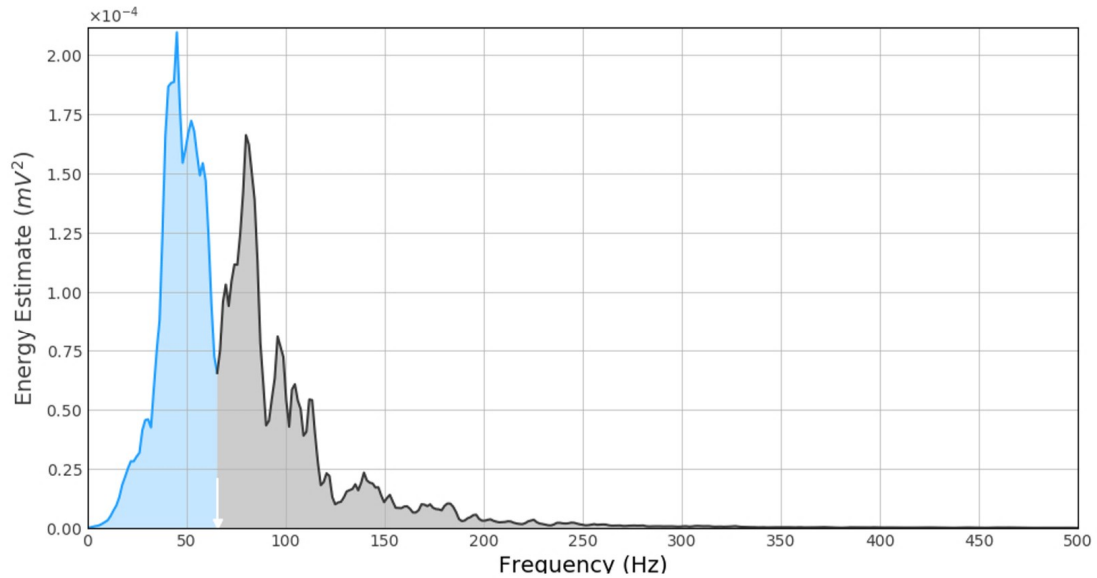


Figure A.1: Illustration of the median frequency concept, observing the division of the spectrum into two regions of equal power

## APPENDIX A. LIST OF FEATURES (FIGURES)

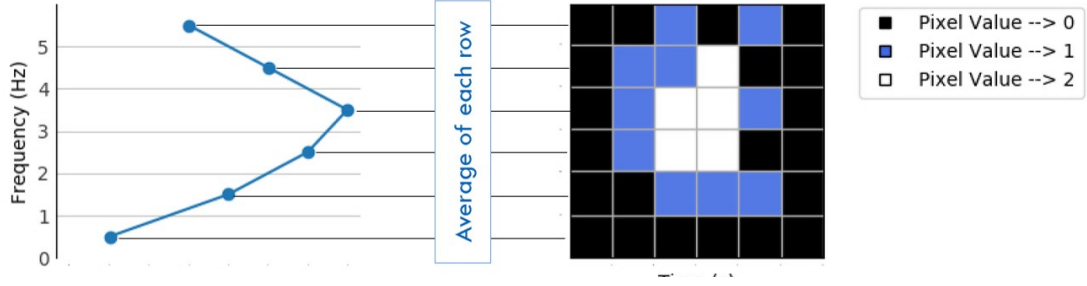


Figure A.2: Description of the proposed logic for determination of the median frequency in the scalogram

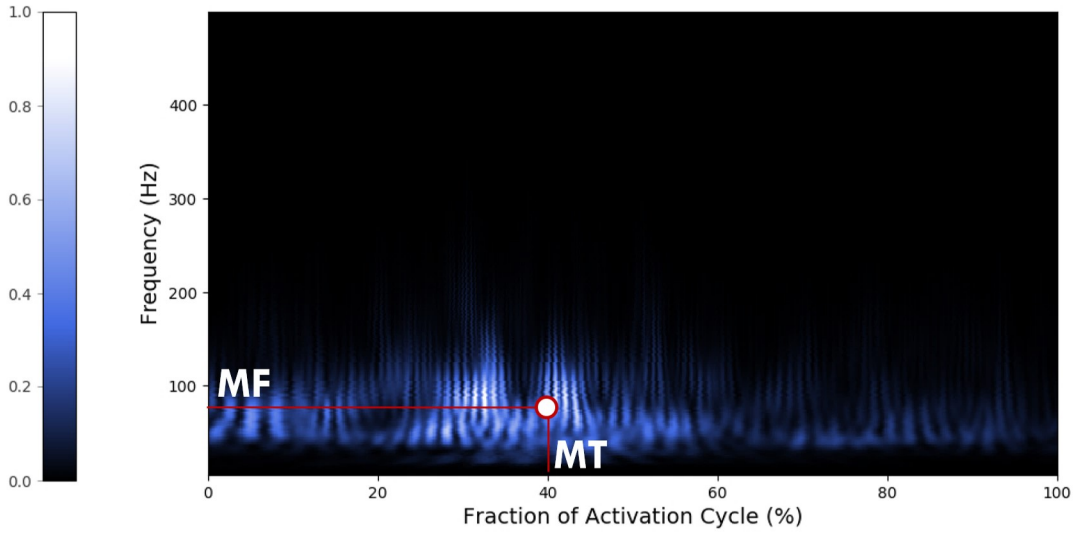


Figure A.3: Identification of the position of the centroid by graphically highlighting the correspondence with the parameters *Major Frequency* (MF) and *Major Time* (MT)

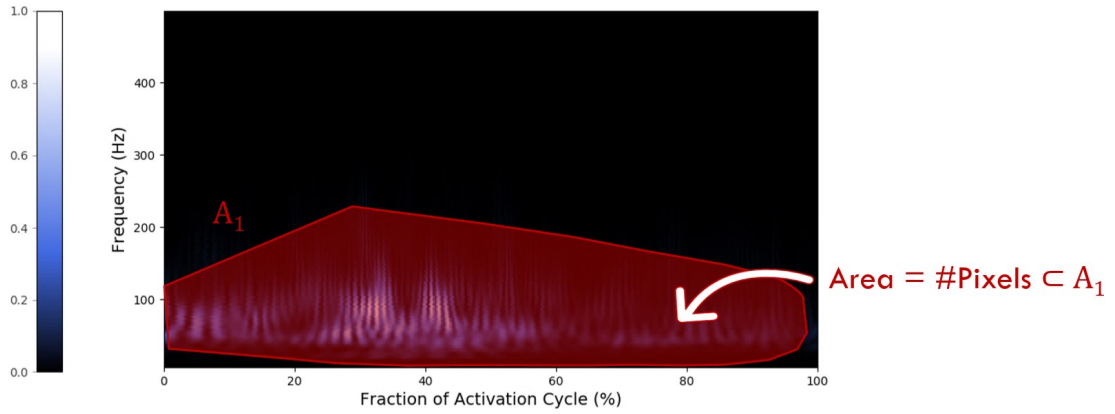


Figure A.4: Illustration of the convex area concept

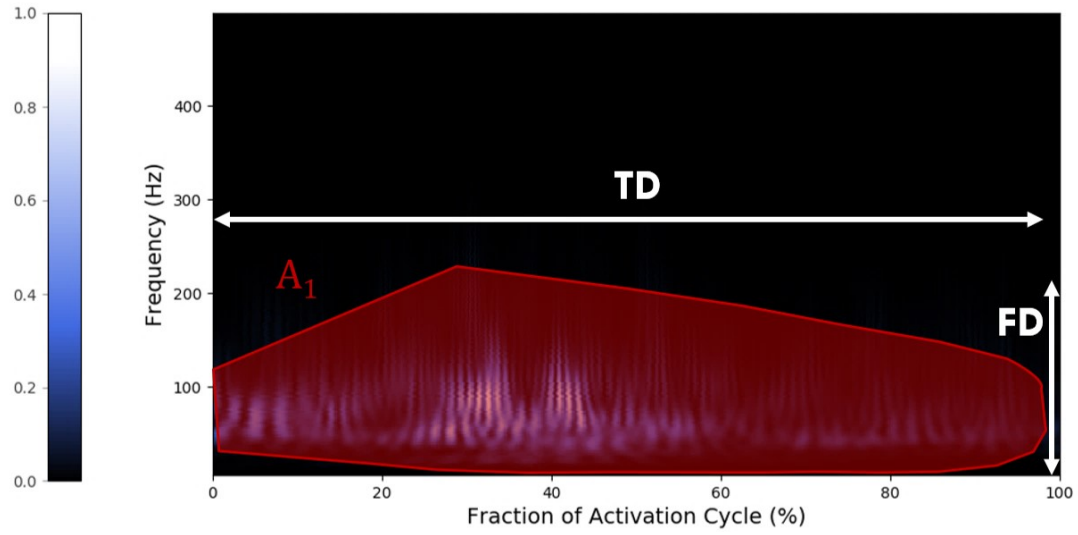


Figure A.5: Presentation of the temporal and frequency dispersion, parameters derived from the determination of the convex area

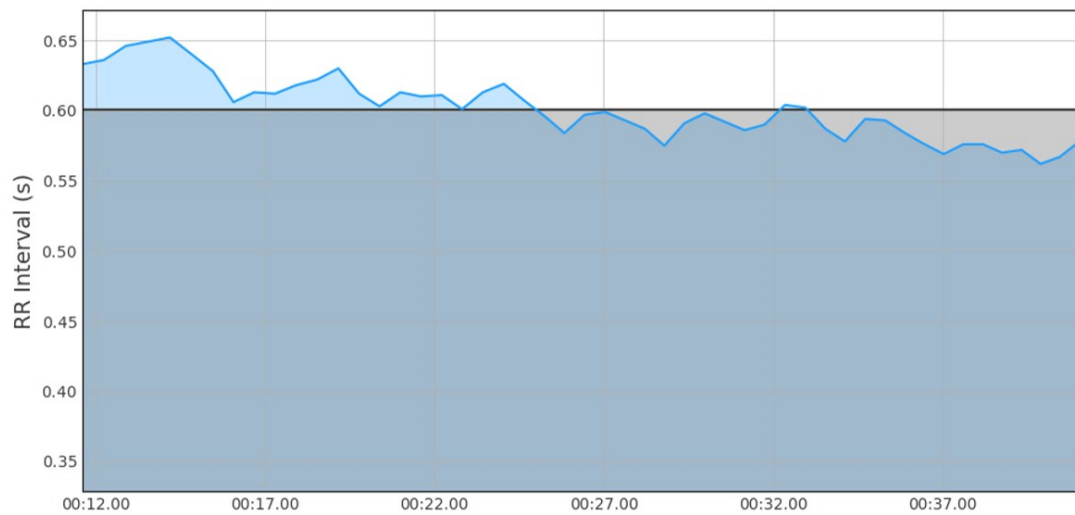


Figure A.6: Graphical identification of the average value of the duration of the RR intervals for the processing window under analysis

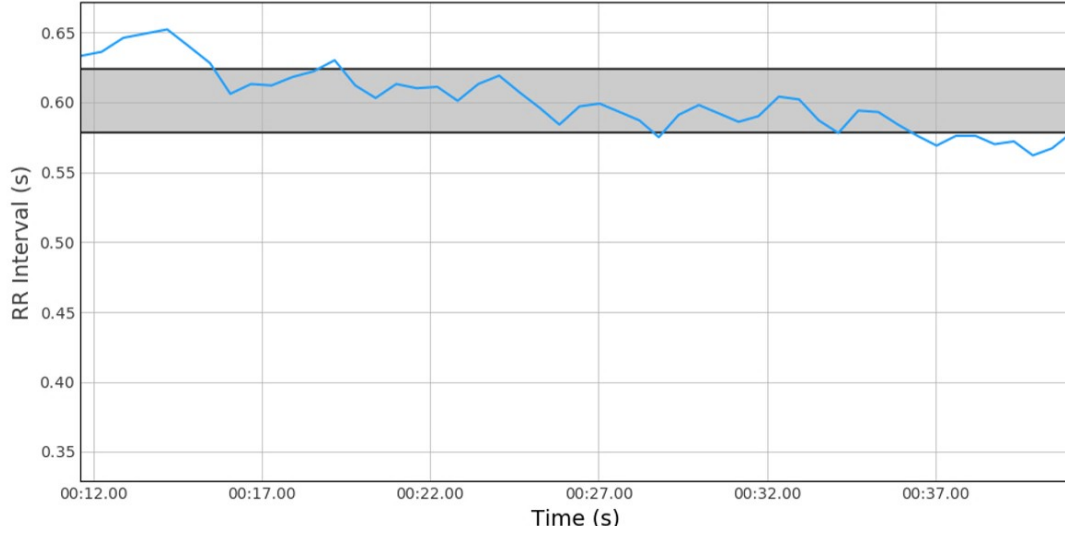


Figure A.7: Representation of the statistical dispersion of the results around the mean value, corresponding in quantitative terms to the standard deviation

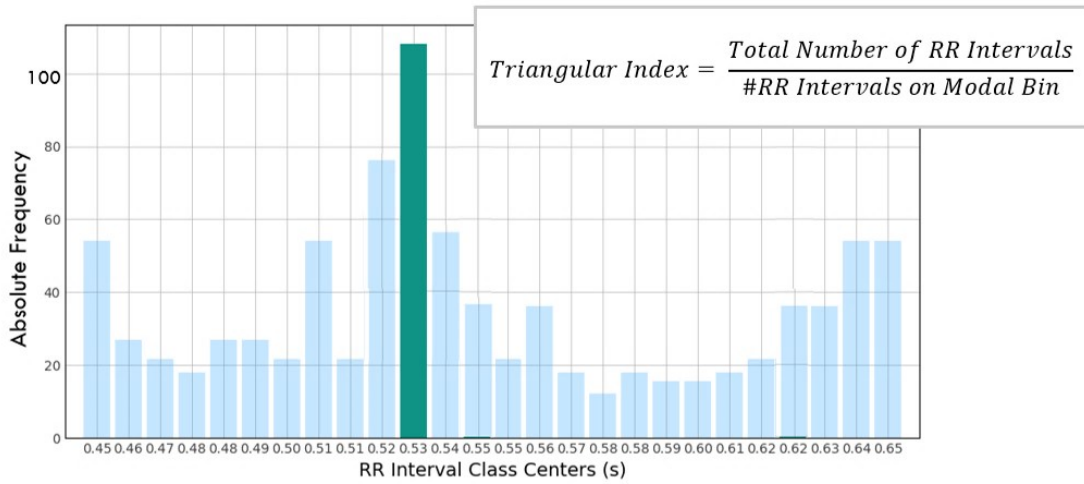


Figure A.8: Detachment of modal *bin* of the histogram associated with the duration of RR intervals, an essential element for the determination of triangular index value



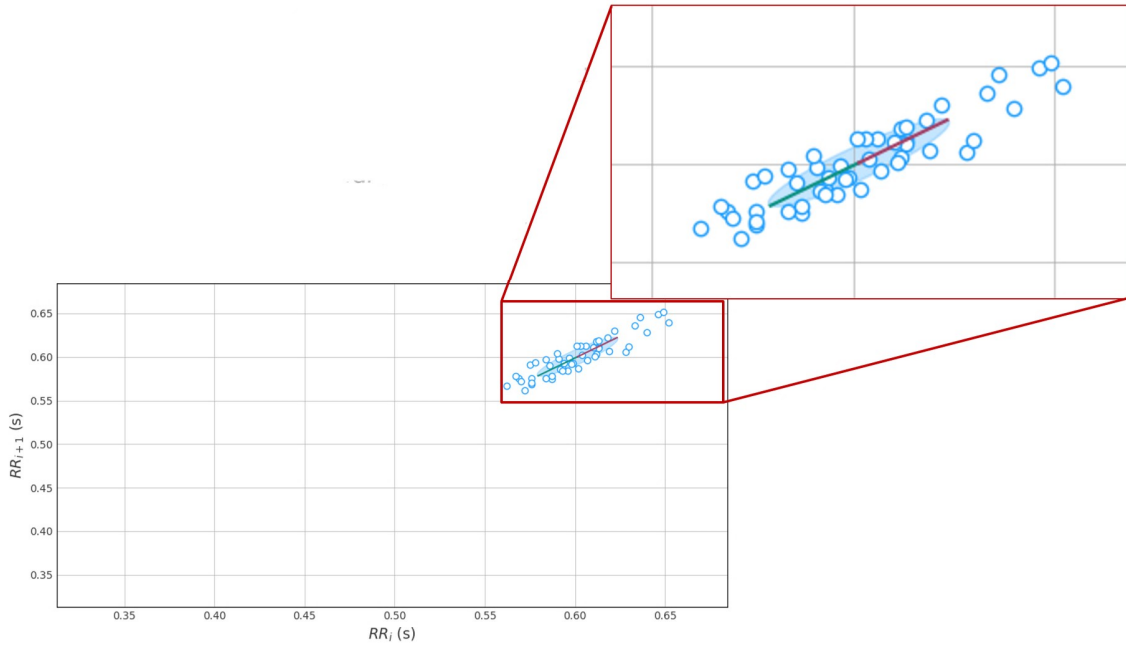


Figure A.9: Presentation of the *Poincaré* plot and one of the semi-axes of the ellipse with dimension  $2 \times SD2$ . The other semi-axis (not presented) has size equal to  $2 \times SD1$

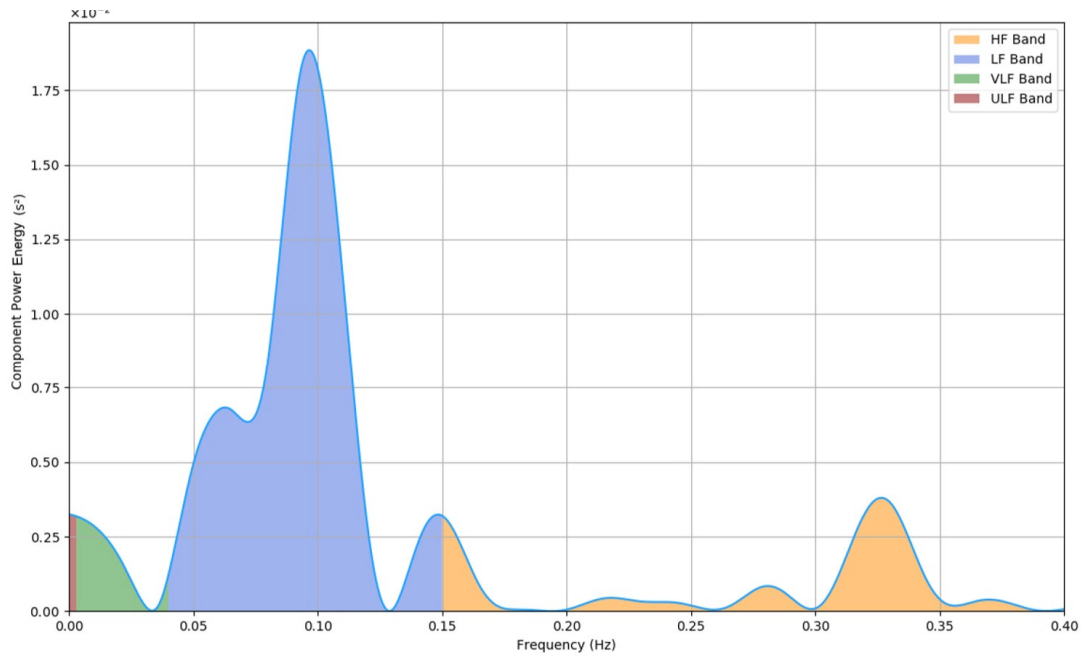


Figure A.10: Power bands typically used for analysing cardiac variability through the tachogram power spectrum





## Experimental Protocol

### B.1 Protocol of Day 1

#### Pre-Acquisition

- ① Present the objective/purpose of the project for which data will be acquired;
- ② Ask the volunteer to read and sign the Consent Sheet;
- ③ Create a directory for storing files with the volunteer identifier: `<first_name>_<last_name>_<date_of_birth>`;
- ④ Conduct the questionnaire, recording:
  - A Name and telephone number/email address;
  - B Age;
  - C Weight;
  - D Height;
  - E Time of signal acquisition;

This parameter is important owing to circadian rhythms. Studies show that there are well-defined fluctuations during a daily 24-hour cycle, as a result of the variations in activity between the sympathetic and parasympathetic components of the autonomic nervous system.

There may therefore be ideal periods for evaluating heart rate variability and records must be prepared during the same daily period so that these factors may be excluded from the analysis of results [91, 92].

The acquisition will take place in the morning, and will be preceded by 3 hours of fasting.

This restriction means that the acquisition window will probably be from 11:00 am to 12:00 am, for volunteers who have breakfast between 8:00 am and 9:00 am.

This time frame will suit the volunteers, since they will not have to make significant changes to their daily routines, and they can still eat their meals at the normal times without having to skip them.

The fast is a means of minimising variables between tests. It prevents the procedure from becoming distorted, specifically by the increase in heart rate variability during digestion or the stimulating effect of xanthines or their derivatives (constituents of coffee, tea, etc.) [93].

⑤ **Describe/exemplify the protocol procedure.**

**Acquisition**

- ① **Do a 3-minute warm-up on the ergometer at low power (60 RPM at a power of 25 W);**
- ② **Fit the mask (connected to the gas analyser) to the volunteer's face;**
- ③ **Determine the power increment ( $\Delta P$ ) to be applied to the volunteer during the test;**

The procedure of “Day 1” is intended to induce a state of exhaustion in the volunteer, so that  $VO_{2max}$  and  $VT1$  can be determined.

To achieve this objective the protocol is based on incremental effort, where the power that the volunteer has to exert increases gradually.

However, there is a critical parameter in this procedure: the power increment step must be such that a state of exhaustion is reached in a period of between 8 and 12 minutes.

Specifying a static power increment for the entire sample runs the risk that some volunteers will become exhausted before 8 minutes or after 12 minutes.

Thus, in order to ensure that the test time is the same and that fatigue sets in at a pace appropriate to the specific physiological characteristics of the volunteer, the Wasserman Formula is used. This makes it possible to determine the most suitable increment step for the volunteer, using his anthropometric characteristics such as weight, age and height [94, 95].

$$\dot{V}O_2^{no\ load}(mL/min) = 150 + 6 \times mass(kg) \quad (B.1)$$

$$\dot{V}O_2^{peak}(mL/min) = (height(cm) - age(years)) \times 20 \quad (B.2)$$

$$\Delta P(W/min) = \frac{\dot{V}O_2^{no\ load}(mL/min) - \dot{V}O_2^{peak}(mL/min)}{100} \quad (B.3)$$

- ④ **Set the initial power of the ergometer to a value equal to  $\Delta P$  from Step ③;**

The first minute of the test must be carried out at a power identical to  $\Delta P$  instead of starting at a state with no load.

- ⑤ **Start exercise on the ergometer maintaining a rhythm in the interval of  $80 \pm 5$  RPM;**

The volunteer must maintain a stable rhythm at each power level (in the order of 80 RPM) to ensure that his effort does not shift towards the cardiorespiratory component and get away from the muscular component (which is the subject of the study). This change could happen if the rhythm is adapted.

The power exerted depends on the rhythm and the load. If the rhythm were changed the ergometric system would adjust the load to provide the same programmed power.

Despite the fact that the volunteer would be exposed to an identical power, as a result of the load being adjusted to fit the variation in the rhythm, the conditions/specific characteristics of the test would not be the same, so this variability must be avoided.

- ⑥ **Increase the power by  $\Delta P$  every minute;**

The increment value is that determined in Step ③.

- ⑦ **End the test when the volunteer is unable to maintain a rhythm of  $80 \pm 5$  RPM for more than 20 seconds continuously (when he reaches a state of exhaustion);**

In this phase, the volunteer starts to lose the ability to react physiologically, even when exposed to a greater load, and he maintains the level of oxygen supply. This means that he has reached the exhaustion threshold and therefore the *plateau* characteristic of  $VO_{2max}$  begins to form.

The margin surrounding  $80 \pm 5$  RPM is a result of the fact that it is impossible to maintain RPM at an exact value. There must be a little flexibility, but not too much, for the reasons explained in Step ③. This is made possible by the value  $\pm 5$  RPM.

- ⑧ **Record the power values at which the  $VT1$  and  $VO_{2max}$  were reached;**

These values are good indicators of the performance/capacity of the volunteer in cardiorespiratory terms [96]. They serve as a reference for establishing the levels **Moderate Effort**, **Substantial Effort** and **Rigorous Effort** to be used in the Protocol of “Day 2”.

- ⑨ **Outline the Cyclist’s Power Profile based on the values determined in Step ⑧ (Figure B.1);**

**Moderate Effort:** 75% of the Power recorded in  $VT1$

**Substantial Effort:**  $\Delta$  25% of the Power recorded between  $VT1$  and  $VO_{2max}$

**Rigorous Effort**  $\Delta$  75% of the Power recorded between  $VT1$  and  $VO_{2max}$

These values have been chosen to ensure that the effort falls within the central region of the typical training zones of the ternary model.

The volunteer’s power profile depends on the power corresponding to  $VT1$  and  $VO_{2max}$ .

The power recorded in  $VO_{2max}$ , meanwhile, corresponds to the power to which the volunteer is subjected when a *plateau* starts to form in the  $VO_2$  curve as a function of power, as described above (inability to respond to the increase in load) (Figure B.2).

With regard to  $VT1$ , the procedure is not so linear, and it is necessary to monitor  $VE$  (ventilation) and  $V_{CO_2}$  in addition to  $VO_2$ .

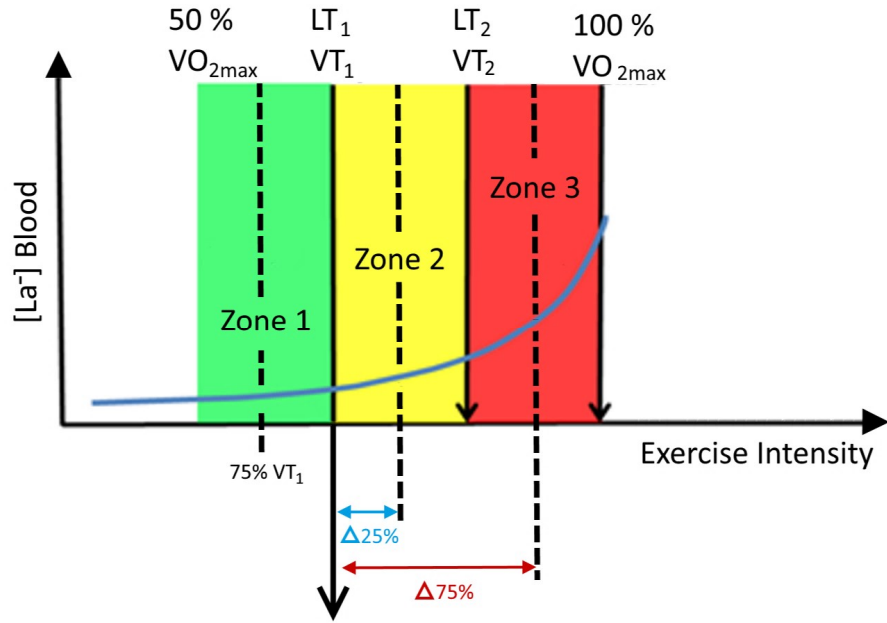


Figure B.1: Ternary Model defining the training zones.  $[La^-]_{Blood}$  is the concentration of lactates in the blood,  $LT$  stands for *Lactic Threshold*,  $VT$  stands for *Ventilatory Threshold*, and  $VO_{2max}$  defines the maximum oxygen consumption [97]

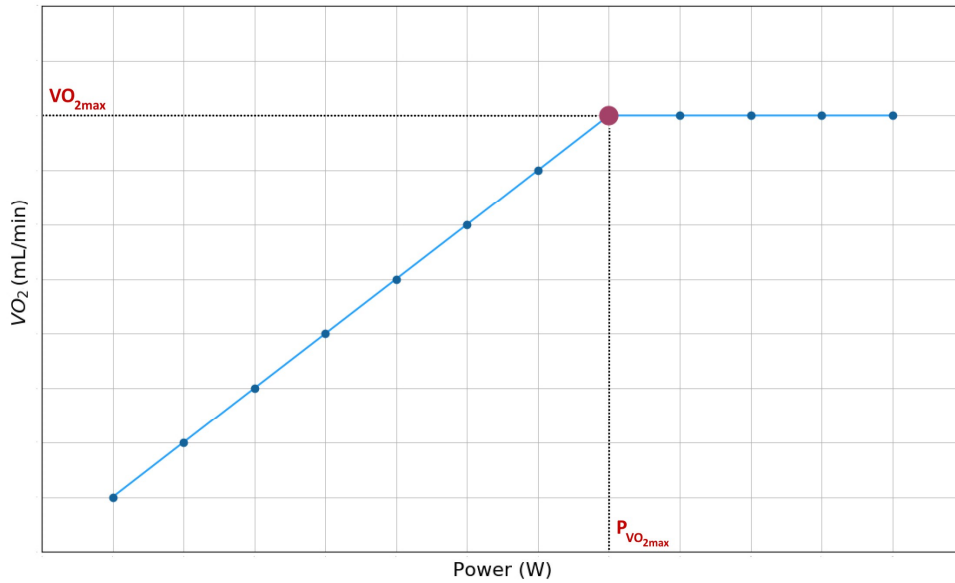


Figure B.2: Graphical illustration of the value of  $VO_{2max}$  in the graph showing the evolution of oxygen consumption as a function of the power setting on the ergometer (exercise difficulty)

These three parameters produce two derived curves corresponding to the equivalent ventilations ( $VE/VO_2(P)$  and  $VE/V_{CO_2}(P)$ ).

The power defined by  $VT1$  will correspond to the value at the point of the curve  $VE/VO_2(P)$  where a growing segment (positive slope) starts and is unaccompanied by an identical trend in the curve  $VE/V_{CO_2}(P)$  indicating that the  $VT1$  threshold (Ventilatory Threshold 1) has been exceeded, that is, ventilation increases, but it is not accompanied by an increase at the same rate in oxygen consumption [98–100] (Figure B.3).

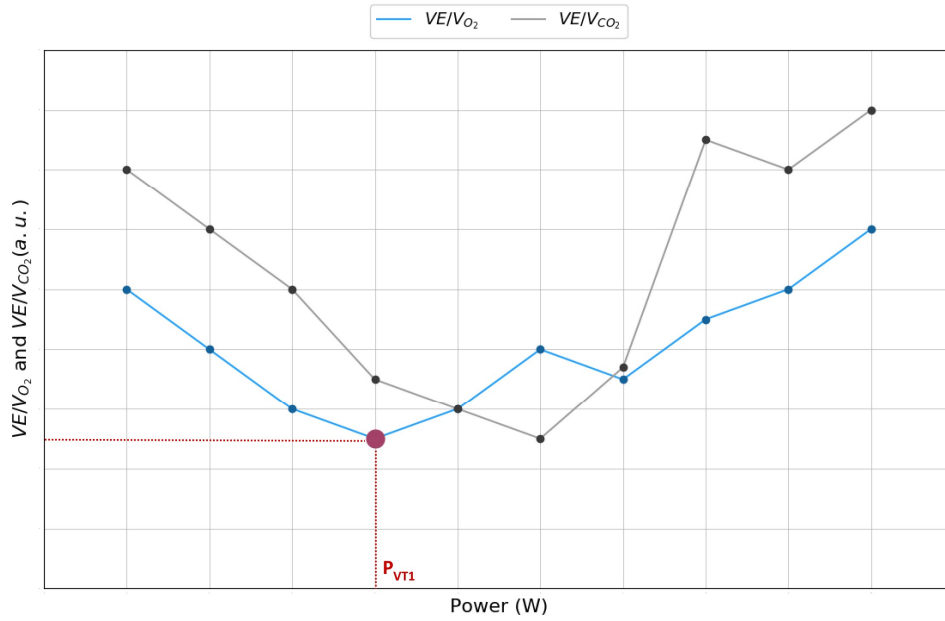


Figure B.3: Graphical illustration of the value of  $VT1$  in the graph showing the evolution of the equivalent ventilations of  $O_2$  and  $CO_2$

⑩ **Copy the Power Profile data to the volunteer's form.**

The volunteer's form will be a *Word* form (with read-only sections which cannot be edited and editable sections for entering data).

## B.2 Protocol of Day 2

### Pre-Acquisition

- ① Locate the directory associated with the volunteer that was created on “Day 1”, to store the new files later on (`<first_name>_<last_name>_<date_of_birth>`);
- ② Exemplify/describe the protocol procedure;
- ③ Apply EMG sensors (longitudinally to the direction of the muscle fibres) in order to collect local information related to the activity of the *Rectus Femoris*, *Vastus Lateralis* and *Vastus Medialis* muscles of the *quadriceps femoris*, while the more global information will be extracted from the ECG signal;

**Acquisition**

- ① **Position the volunteer on the ergometer, adjusting the height of the saddle to a comfortable level;**

- ② **Maintain a rest position for 5 minutes;**

This procedure ensures that when the exercise/acquisition begins the volunteer starts from a rest state, in which heart rate is stable.

The sitting position on the ergometer is not an arbitrary detail: this support ensures that fatigue does not set in in the muscles under analysis as a result of maintaining the posture, which could occur if the rest period was conducted in a standing position, the maintenance of which would require the contraction of muscle groups relevant to the exercise phase.

- ③ **Start acquisitions, establishing a sampling frequency for the system (*biosignalsplux*) of 1000 Hz;**

The sampling frequency of 1000 Hz will be necessary to record the high-frequency muscular components in the order of 500 Hz, considering that for these components and the EMG signal itself to be represented correctly, the principle of the Nyquist Theorem must be taken into account ( $f_{sampling} > 2 \times f_{max}$ ).

The EMG signal will be the limiting factor, requiring the greatest sampling frequency, and the remaining signals will be oversampled. This does not affect the feasibility of the analysis (all the signals will be collected at the same sampling frequency).

- ④ **Block the ergometer pedal with a connected force cell (in a position that allows an angle of around 80° to form when the knee is flexed);**

The pedal providing the main support must be positioned in such a way that it allows the volunteer to exert maximum contraction (most favourable conditions). This is achieved when the angle between the thigh and the leg is around 80° [101–103].

The angle formed by the flexing of the knee will be measured with a goniometer.

- ⑤ **Ask the volunteer to exert maximum pressure on the pedal in three series of maximum voluntary contraction (MVC) lasting for 5 seconds and 1 minute apart;**

In this period, a record is taken of the exerted force and the EMG signal with the aim of determining the median frequency in a static context. This may be a useful parameter when validating the evolution of this index in a dynamic context, considering it is more reliable/sensitive in these conditions of stationarity, which are required in the Fourier Analysis [104, 105].

- ⑥ **Unblock the pedal;**

- ⑦ **Set the ergometer power according to the volunteer's profile, as determined in the procedure of "Day 1", in relation to the Rigorous Effort class;**



- ⑧ **Start ergometric exercise maintaining a rhythm in the interval of  $60 \pm 5$  RPM, giving regular encouragement to the volunteer;**

The rhythm must remain constant, in this case in the order of  $60 \pm 5$  RPM, so as to prolong the test.

In addition, a longer test ensures it is possible to carry out a well-founded analysis of heart rate variability that has statistical significance (time windows with a minimum duration of 5 minutes).

In any of the signals, the analysis will be facilitated since the experimental conditions remain unchanged throughout the test [106].

In some circumstances, the size of the time window could be reduced to around 2 minutes [41].

- ⑨ **Stop the exercise when the volunteer is unable to maintain the rhythm ( $60 \pm 5$  RPM) for 20 seconds;**

- ⑩ **Repeat Steps ④ and ⑤;**

Record the median frequency in a static context.

- ⑪ **Save the generated files in the directory created during the “Pre-Acquisition” Procedure of “Day 1”;**

- ⑫ **Remove sensors and clean the region where they were applied.**





## Processing Results for Tendency Evaluation

This appendix aims at the extensive presentation of the processing results obtained during the identification of trends in the various EMG and ECG indices by the empirical method and through the meta-analysis.

Using a color system, the differences / similarities in the evolution of a certain index under conditions of fatigue (Fatigue +) and recovery (Fatigue -) are highlighted.

In addition, cells that contain the most relevant results are flagged.

Table C.1: EMG processing results generated during the iterative application of the empirical method with different window sizes and time-steps for identifying which is the best combination to extract the feature and to evaluate the respective tendency. The values presented are the *scores* determined by a voting mechanism. At the last row is shown the average score, that is extremely important for identifying when a tendency exists.

			Time Domain		Frequency Domain				Time-Frequency Domain															
			RMS		Median Frequency 🍀		Total Power		Major Frequency		Major Time		Mean Power		Area 🍀		Volume		Time Dispersion 🍀		Frequency Dispersion		Median Frequency 🍀	
Window Size (# Bursts)	Overlap Fraction	Otsu-Level	Fatigue +	Fatigue -	Fatigue +	Fatigue -	Fatigue +	Fatigue -	Fatigue +	Fatigue -	Fatigue +	Fatigue -	Fatigue +	Fatigue -	Fatigue +	Fatigue -	Fatigue +	Fatigue -	Fatigue +	Fatigue -	Fatigue +	Fatigue -	Fatigue +	Fatigue -
1	0	None	1.00	0.86	-0.71	-0.14	1.00	0.86	-0.71	-0.43	-0.43	-0.43	1.00	0.86	0.00	0.00	1.00	0.86	0.00	0.00	0.00	0.00	-0.71	-0.14
1	0	0	-	-	-	-	-	-	-0.57	0.23	0.14	-0.23	1.00	0.69	0.93	0.77	1.00	0.85	0.93	0.77	0.64	0.46	-0.57	0.23
1	0	1	-	-	-	-	-	-	-0.57	0.54	0.14	-0.23	1.00	0.69	1.00	0.62	1.00	0.77	1.00	0.62	0.86	0.77	-0.71	0.54
1	0	2	-	-	-	-	-	-	-0.71	0.46	0.00	-0.31	0.71	0.62	1.00	0.62	0.86	0.62	1.00	0.46	0.86	0.46	-0.86	0.77
5	0	None	1.00	0.86	-0.71	0.00	1.00	0.86	-0.71	0.00	-0.43	-0.29	1.00	0.86	0.00	0.00	1.00	0.86	0.00	0.00	0.00	0.00	-0.71	-0.14
5	0	0	-	-	-	-	-	-	-0.57	0.57	0.29	0.00	1.00	0.71	1.00	0.71	1.00	0.86	1.00	0.71	0.71	0.71	-0.57	0.43
5	0	1	-	-	-	-	-	-	-0.43	0.57	0.14	-0.14	1.00	0.71	1.00	0.71	1.00	0.71	1.00	0.57	0.86	0.71	-0.57	0.71
5	0	2	-	-	-	-	-	-	-0.71	0.71	0.14	-0.43	0.86	0.86	1.00	0.79	1.00	0.79	1.00	0.79	0.71	0.79	-0.57	0.71
5	0.10	None	1.00	0.86	-0.71	0.00	1.00	0.86	-0.71	0.00	-0.43	-0.29	1.00	0.86	0.00	0.00	1.00	0.86	0.00	0.00	0.00	0.00	-0.71	-0.14
5	0.10	0	-	-	-	-	-	-	-0.57	0.57	0.29	0.00	1.00	0.71	1.00	0.71	1.00	0.86	1.00	0.71	0.71	0.71	-0.57	0.43
5	0.10	1	-	-	-	-	-	-	-0.43	0.57	0.14	-0.14	1.00	0.71	1.00	0.71	1.00	0.71	1.00	0.57	0.86	0.71	-0.57	0.71
5	0.10	2	-	-	-	-	-	-	-0.71	0.71	0.14	-0.43	0.86	0.86	1.00	0.79	1.00	0.79	1.00	0.79	0.71	0.79	-0.57	0.71
5	0.25	None	1.00	0.86	-0.71	0.29	1.00	0.86	-0.86	0.14	-0.43	-0.29	1.00	0.86	0.00	0.00	1.00	0.86	0.00	0.00	0.00	0.00	-0.86	-0.14
5	0.25	0	-	-	-	-	-	-	-0.43	0.43	0.00	-0.29	1.00	0.71	1.00	0.71	1.00	0.86	1.00	0.71	0.71	0.71	-0.43	0.43
5	0.25	1	-	-	-	-	-	-	-0.29	0.43	0.29	-0.43	1.00	0.71	1.00	0.43	1.00	0.86	1.00	0.43	0.86	0.71	-0.43	0.71
5	0.25	2	-	-	-	-	-	-	-0.14	0.43	0.00	-0.57	0.86	0.57	1.00	0.71	0.86	0.86	1.00	0.57	0.86	0.86	-0.29	0.43
5	0.50	None	1.00	0.86	-0.86	0.00	1.00	0.86	-0.71	0.14	-0.29	-0.29	1.00	0.86	0.00	0.00	1.00	0.86	0.00	0.00	0.00	0.00	-0.71	0.00
5	0.50	0	-	-	-	-	-	-	-0.57	0.57	0.00	-0.29	1.00	0.86	1.00	0.57	1.00	0.86	1.00	0.71	0.71	0.71	-0.57	0.43
5	0.50	1	-	-	-	-	-	-	-0.57	0.86	0.29	-0.29	1.00	0.86	1.00	0.57	1.00	0.86	1.00	0.57	0.71	0.86	-0.57	0.57
5	0.50	2	-	-	-	-	-	-	-0.57	0.57	-0.14	-0.43	0.86	0.71	1.00	0.86	0.86	0.86	1.00	0.71	0.57	0.86	-0.71	0.86
5	0.75	None	1.00	0.86	-0.71	0.14	1.00	0.86	-0.71	0.00	-0.43	-0.29	1.00	0.86	0.00	0.00	1.00	0.71	0.00	0.00	0.00	0.00	-0.71	0.14
5	0.75	0	-	-	-	-	-	-	-0.29	0.43	0.14	-0.29	1.00	0.86	1.00	0.71	1.00	0.86	1.00	0.71	0.57	0.71	-0.43	0.57
5	0.75	1	-	-	-	-	-	-	-0.29	0.71	0.43	-0.29	1.00	0.71	1.00	0.57	1.00	0.71	1.00	0.57	1.00	0.86	-0.43	0.57
5	0.75	2	-	-	-	-	-	-	-0.43	0.57	0.14	-0.29	0.86	0.57	0.86	0.86	0.86	0.86	1.00	0.86	0.71	0.86	-0.29	0.57
5	0.90	None	1.00	0.86	-0.71	0.00	1.00	0.86	-0.71	0.00	-0.29	-0.14	1.00	0.86	0.00	0.00	1.00	0.86	0.00	0.00	0.00	0.00	-0.71	0.00
5	0.90	0	-	-	-	-	-	-	-0.57	0.57	0.00	-0.29	1.00	0.86	1.00	0.71	1.00	0.86	1.00	0.57	0.57	0.71	-0.57	0.57
5	0.90	1	-	-	-	-	-	-	-0.43	0.57	0.29	-0.29	1.00	0.86	1.00	0.57	1.00	0.71	1.00	0.57	0.86	0.86	-0.43	0.57
5	0.90	2	-	-	-	-	-	-	-0.43	0.57	0.29	-0.57	0.86	0.71	1.00	0.86	0.86	0.86	1.00	0.86	0.71	0.86	-0.43	0.57
10	0	None	1.00	0.86	-0.86	0.29	1.00	0.86	-0.71	0.43	-0.29	-0.14	1.00	0.86	0.00	0.00	1.00	0.86	0.00	0.00	0.00	0.00	-0.57	0.43
10	0	0	-	-	-	-	-	-	-0.29	0.71	0.14	-0.29	1.00	0.86	1.00	0.57	1.00	0.86	1.00	0.57	0.86	0.71	-0.29	0.71
10	0	1	-	-	-	-	-	-	-0.29	0.86	0.14	-0.43	1.00	0.71	1.00	0.43	1.00	0.86	1.00	0.14	0.86	0.86	-0.29	0.71
10	0	2	-	-	-	-	-	-	-0.29	0.86	0.00	-0.43	0.86	0.86	0.86	0.86	0.71	0.71	0.86	0.86	0.43	0.71	-0.29	0.86
10	0.10	None	1.00	0.86	-0.86	0.43	1.00	0.86	-0.86	0.29	-0.29	-0.43	1.00	0.86	0.00	0.00	1.00	0.57	0.00	0.00	0.00	0.00	-1.00	0.57
10	0.10	0	-	-	-	-	-	-	-0.43	0.71	0.29	-0.29	1.00	0.86	0.86	0.57	1.00	0.86	0.86	0.57	0.86	0.71	-0.43	0.57
10	0.10	1	-	-	-	-	-	-	-0.57	0.57	0.43	-0.29	1.00	0.57	1.00	0.71	1.00	0.71	1.00	0.29	0.86	0.86	-0.57	0.43
10	0.10	2	-	-	-	-	-	-	-0.14	0.57	0.14	-0.29	0.86	0.71	1.00	0.43	0.86	0.71	1.00	0.43	0.71	0.86	-0.14	0.57
10	0.25	None	1.00	0.86	-0.86	0.14	1.00	0.86	-0.86	0.14	-0.43	-0.29	1.00	0.86	0.00	0.00	1.00	0.86	0.00	0.00	0.00	0.00	-1.00	0.29
10	0.25	0	-	-	-	-	-	-	-0.57	0.71	0.00	-0.29	1.00	0.71	1.00	0.43	1.00	0.86	1.00	0.43	0.71	0.71	-0.71	0.71
10	0.25	1	-	-	-	-	-																	

Table C.2: ECG processing results (Time-Domain features) generated during the iterative application of the empirical method with different window sizes and time-steps for identifying which is the best combination to extract the feature and to evaluate the respective tendency. The values presented are the *scores* determined by a voting mechanism. At the last row is shown the average score, that is extremely important for identifying when a tendency exists.

Window Size (s)	Overlap Fraction	Time Domain																	
		Maximum RR ♣		Minimum RR ♣		Average RR ♣		SDNN ♣		rmsSD		Triangular Index ♣		SD1		SD2 ♣		SD1 / SD2	
		Fatigue +	Fatigue -	Fatigue +	Fatigue -	Fatigue +	Fatigue -	Fatigue +	Fatigue -	Fatigue +	Fatigue -	Fatigue +	Fatigue -	Fatigue +	Fatigue -	Fatigue +	Fatigue -	Fatigue +	Fatigue -
30	0	-1.00	1.00	-0.82	1.00	-0.82	1.00	-0.82	0.27	-0.27	0.45	-1.00	-0.27	-0.27	0.45	-0.64	0.27	0.82	0.64
30	0.10	-0.82	1.00	-0.82	1.00	-0.82	1.00	-0.64	0.27	-0.27	0.45	-1.00	-0.09	-0.27	0.45	-0.64	0.09	0.82	0.64
30	0.25	-1.00	1.00	-0.82	1.00	-1.00	1.00	-0.64	0.09	-0.27	0.45	-1.00	-0.09	-0.27	0.45	-0.64	0.09	0.82	0.64
30	0.50	-0.82	1.00	-0.82	1.00	-0.82	1.00	-0.64	0.27	-0.27	0.45	-1.00	-0.27	-0.27	0.45	-0.64	0.27	0.82	0.64
30	0.75	-0.82	1.00	-0.82	1.00	-0.82	1.00	-0.64	0.27	-0.27	0.45	-1.00	-0.27	-0.27	0.45	-0.64	0.27	0.82	0.64
30	0.90	-0.82	1.00	-0.82	1.00	-0.82	1.00	-0.64	0.27	-0.27	0.45	-1.00	-0.27	-0.27	0.45	-0.64	0.27	0.82	0.64
40	0	-1.00	1.00	-1.00	1.00	-0.82	1.00	-0.64	-0.45	-0.27	0.45	-1.00	-0.45	-0.27	0.45	-0.64	-0.45	0.82	0.82
40	0.10	-1.00	1.00	-1.00	1.00	-1.00	1.00	-0.82	-0.09	-0.27	0.45	-1.00	-0.45	-0.27	0.45	-0.82	-0.09	0.82	0.64
40	0.25	-0.82	1.00	-0.82	1.00	-0.82	1.00	-0.64	-0.27	-0.27	0.45	-1.00	-0.45	-0.27	0.45	-0.64	-0.27	0.82	0.64
40	0.50	-1.00	1.00	-1.00	1.00	-0.82	1.00	-0.64	-0.27	-0.27	0.45	-1.00	-0.45	-0.27	0.45	-0.64	-0.45	0.82	0.82
40	0.75	-0.82	1.00	-0.82	1.00	-0.82	1.00	-0.64	-0.27	-0.27	0.45	-1.00	-0.45	-0.27	0.45	-0.64	-0.45	0.82	0.64
40	0.90	-0.82	1.00	-0.82	1.00	-0.82	1.00	-0.64	-0.27	-0.27	0.45	-1.00	-0.27	-0.27	0.45	-0.64	-0.45	0.82	0.64
50	0	-0.82	1.00	-0.82	1.00	-0.82	1.00	-0.82	-0.09	-0.27	0.45	-1.00	-0.45	-0.27	0.45	-0.82	-0.09	0.82	1.00
50	0.10	-1.00	1.00	-1.00	1.00	-1.00	1.00	-0.82	-0.45	-0.27	0.45	-1.00	-0.45	-0.27	0.45	-0.82	-0.64	0.82	0.82
50	0.25	-1.00	1.00	-0.82	1.00	-0.82	1.00	-0.64	-0.45	-0.27	0.45	-1.00	-0.45	-0.27	0.45	-0.64	-0.45	0.82	0.82
50	0.50	-0.82	1.00	-0.82	1.00	-0.82	1.00	-0.64	-0.45	-0.27	0.45	-1.00	-0.45	-0.27	0.45	-0.64	-0.82	0.82	0.64
50	0.75	-0.82	1.00	-0.82	1.00	-0.82	1.00	-0.64	-0.82	-0.27	0.45	-0.82	-0.27	-0.27	0.45	-0.64	-0.82	0.82	0.82
50	0.90	-0.82	1.00	-0.82	1.00	-0.82	1.00	-0.64	-0.82	-0.27	0.45	-0.82	-0.27	-0.27	0.45	-0.64	-0.82	0.82	0.64
60	0	-1.00	1.00	-1.00	1.00	-0.82	1.00	-0.64	-0.64	-0.27	0.45	-1.00	-0.27	-0.09	0.45	-0.64	-0.64	0.82	0.82
60	0.10	-1.00	1.00	-1.00	1.00	-1.00	1.00	-0.82	-0.64	-0.27	0.45	-1.00	-0.27	-0.09	0.45	-0.82	-0.64	0.82	1.00
60	0.25	-1.00	1.00	-1.00	1.00	-0.82	1.00	-0.64	-0.45	-0.27	0.45	-1.00	-0.27	-0.09	0.45	-0.64	-0.45	0.82	0.91
60	0.50	-1.00	1.00	-0.82	1.00	-0.82	1.00	-0.64	-0.82	-0.27	0.45	-0.82	-0.27	-0.27	0.45	-0.64	-0.82	0.82	0.82
60	0.75	-0.82	1.00	-0.82	1.00	-0.82	1.00	-0.64	-0.82	-0.27	0.45	-0.82	-0.27	-0.27	0.45	-0.64	-0.82	0.82	0.82
60	0.90	-0.82	1.00	-0.82	1.00	-0.82	1.00	-0.64	-0.82	-0.27	0.45	-0.82	-0.27	-0.27	0.45	-0.64	-0.82	0.82	0.82
70	0	-1.00	1.00	-1.00	1.00	-1.00	1.00	-1.00	0.09	-0.27	0.45	-0.82	-0.45	-0.27	0.45	-1.00	0.09	0.82	0.36
70	0.10	-1.00	1.00	-1.00	1.00	-1.00	1.00	-0.64	-0.09	-0.27	0.45	-0.82	-0.09	-0.27	0.45	-0.64	-0.09	0.82	0.45
70	0.25	-1.00	1.00	-0.82	1.00	-0.82	1.00	-1.00	-0.64	-0.27	0.45	-0.82	-0.45	-0.09	0.45	-1.00	-0.64	0.82	0.82
70	0.50	-1.00	1.00	-0.82	1.00	-0.82	1.00	-0.64	-0.64	-0.09	0.45	-0.64	-0.45	-0.09	0.45	-0.64	-0.64	0.82	0.82
70	0.75	-0.82	1.00	-0.82	1.00	-0.82	1.00	-0.64	-0.82	-0.27	0.45	-0.82	-0.27	-0.27	0.45	-0.64	-0.82	0.82	0.64
70	0.90	-0.82	1.00	-0.82	1.00	-0.82	1.00	-0.64	-0.82	-0.27	0.45	-0.82	-0.27	-0.27	0.45	-0.64	-0.82	0.82	0.82
80	0	-1.00	1.00	-0.82	1.00	-0.82	1.00	-0.82	-0.40	-0.09	0.40	-1.00	-0.20	-0.09	0.40	-0.82	-0.40	1.00	0.60
80	0.10	-1.00	1.00	-0.82	1.00	-0.82	1.00	-1.00	0.09	-0.27	0.45	-1.00	-0.27	-0.27	0.45	-1.00	0.09	1.00	0.45
80	0.25	-1.00	1.00	-1.00	1.00	-1.00	1.00	-0.82	0.09	0.09	0.45	-0.82	-0.45	0.09	0.45	-0.82	0.09	1.00	0.36
80	0.50	-1.00	1.00	-1.00	1.00	-0.82	1.00	-1.00	-0.45	-0.27	0.45	-0.82	-0.27	-0.27	0.45	-1.00	-0.45	0.82	0.45
80	0.75	-1.00	1.00	-1.00	1.00	-0.82	1.00	-0.82	-0.82	-0.27	0.45	-0.82	-0.27	-0.27	0.45	-0.82	-0.82	0.82	0.82
80	0.90	-0.82	1.00	-0.82	1.00	-0.82	1.00	-0.64	-0.82	-0.09	0.45	-0.82	-0.27	-0.09	0.45	-0.64	-0.82	0.82	0.82
90	0	-1.00	1.00	-1.00	1.00	-1.00	1.00	-0.60	-0.80	0.20	0.40	-0.80	-0.20	0.20	0.40	-0.60	-0.80	0.90	1.00
90	0.10	-1.00	1.00	-0.82	1.00	-0.82	1.00	-0.82	-0.80	-0.09	0.40	-0.82	-0.20	-0.09	0.40	-0.82	-0.80	0.82	0.90
90	0.25	-1.00	1.00	-1.00	1.00	-0.82	1.00	-1.00	0.00	-0.27	0.40	-0.82	-0.40	-0.27	0.40	-1.00	-0.20	0.82	0.60
90	0.50	-1.00	1.00	-1.00	1.00	-0.82	1.00	-1.00	-0.82	-0.09	0.45	-0.82	-0.27	-0.09	0.45	-1.00	-0.82	0.82	1.00
90	0.75	-1.00	1.00	-0.82	1.00	-0.82	1.00	-0.82	-0.82	-0.27	0.45	-0.82	-0.27	-0.27	0.45	-0.82	-0.82	0.82	1.00
90	0.90	-1.00	1.00	-0.82	1.00	-0.82	1.00	-0.82	-0.82	-0.27	0.45	-0.82	-0.27	-0.27	0.45	-0.82	-0.82	0.82	0.82
100	0	-	-	-	-	-	-	-	-	-	-	-	-	-	-	-	-	-	-
100	0.10	-1.00	0.86	-1.00	1.00	-1.00	1.00	-0.80	-1.00	0.20	0.14	-0.60	-0.43	0.20	0.14	-0.80	-1.00	0.90	0.71
100	0.25	-1.00	0.90	-0.80	1.00	-0.80	1.00	-1.00	-0.80	0.00	0.40	-0.60	-0.40	0.00	0.40	-1.00	-0.80	0.80	0.90
100	0.50	-1.00	0.91	-0.82	1.00	-0.82	1.00	-1.00	0.09	-0.27	0.45	-0.64	-0.45	-0.09	0.45	-1.00	0.09	0.82	0.64
100	0.75	-1.00	0.91	-0.82	1.00	-0.82	1.00	-0.82	-0.82	-0.27	0.45	-0.64	-0.45	-0.27	0.45	-0.82	-0.82	0.82	0.82
100	0.90	-1.00	0.91	-0.82	1.00	-0.82	1.00	-0.82	-0.82	-0.27	0.45	-0.64	-0.27	-0.27	0.45	-0.82	-0.82	0.82	1.00
110	0	-	-	-	-	-	-	-	-	-	-	-	-	-	-	-	-	-	-
110	0.10	-	-	-	-	-	-	-	-	-	-	-	-	-	-	-	-	-	-
110	0.25	-1.00	1.00	-1.00	1.00	-1.00	1.00	-1.00	-1.00	0.20	0.50	-0.60	0.00	0.20	0.50	-1.00	-1.00	1.00	1.00
110	0.50	-1.00	0.90	-1.00	1.00	-1.00	1.00	-1.00	-0.40	0.09	0.40	-0.64	-0.40	0.09	0.40	-1.00	-0.40	1.00	0.90
110	0.75	-1.00	0.82	-1.00	1.00	-0.82	1.00	-0.82	-0.64	-0.27	0.45	-0.64	-0.27	-0.27	0.45	-0.82	-0.45	0.82	0.91
110	0.90	-1.00	0.82	-0.82	1.00	-0.82	1.00	-0.82	-0.82	-0.27	0.45	-0.64	-0.45	-0.27	0.45	-0.82	-0.82	0.82	1.00
120	0	-	-	-	-	-	-	-	-	-	-	-	-	-	-	-	-	-	-
120	0.10	-	-	-	-	-	-	-	-	-	-	-	-	-	-	-	-	-	-
120	0.25	-	-	-	-	-	-	-	-	-	-	-	-	-	-	-	-	-	-
120	0.50	-1.00	0.80	-1.00	1.00	-0.80	1.00	-1.00	-0.60	0.00	0.40	-0.40	-0.40	0.00	0.40	-1.00	-0.60	1.00	1.00
120	0.75	-1.00	0.73	-1.00	1.00	-0.82	1.00	-0.82	-0.64	-0.09	0.45	-0.45	-0.45	-0.09	0.45	-0.82	-0.64	0.82	1.00
120	0.90	-1.00	0.73	-1.00	1.00	-0.82	1.00	-0.82	-0.64	-0.27	0.45	-0.64	-0.45	-0.27	0.45	-0.82	-0.64	0.82	1.00
Average Scores		-0.95	0.97	-0.89	1.0	-0.85	1.0	-0.77	-0.46	-0.2	0.44	-0.84	-0.33	-0.19	0.44	-0.77	-0.48	0.84	0.77

♣ - Parameter with informative potential about fatigue, considering the empirical method criterion for identifying tendencies (Section 3.2.2)

**Green Score** - Positive *scores* defining an increasing tendency for the population sample in study

**Red Score** - Negative *scores* defining a decreasing tendency for the population sample in study

In simple terms, a parameter is defined as a fatigue index (i) if the average score changes signal (summarized by color) between the trial where fatigue is induced (**Fatigue +**) and the trial where fatigue decreases (**Fatigue -**) or (ii) if the average score module in **Fatigue +** is bigger than 0.50 and in **Fatigue -** is less than 0.50.

Table C.3: ECG processing results (Frequency-Domain features) generated during the iterative application of the empirical method with different window sizes and time-steps for identifying which is the best combination to extract the feature and to evaluate the respective tendency. The values presented are the *scores* determined by a voting mechanism. At the last row is shown the average score, that is extremely important for identifying when a tendency exists.

		Frequency Domain													
		Total Power		ULF Power		VLF Power		LF Power ♣		HF Power ♣		LF/HF Power Ratio		Median Frequency	
Window Size (s)	Overlap Fraction	Fatigue +	Fatigue -	Fatigue +	Fatigue -	Fatigue +	Fatigue -	Fatigue +	Fatigue -	Fatigue +	Fatigue -	Fatigue +	Fatigue -	Fatigue +	Fatigue -
30	0	-0.45	-0.27	-	-	-0.82	-0.82	-0.45	0.45	-0.64	0.45	0.27	0.09	1.00	-1.00
30	0.10	-0.45	-0.27	-	-	-0.45	-0.64	-0.45	0.45	-0.45	0.64	0.09	-0.09	0.82	-1.00
30	0.25	-0.45	-0.09	-	-	-0.45	-0.64	-0.45	0.45	-0.64	0.64	0.27	0.45	1.00	-1.00
30	0.50	-0.45	-0.09	-	-	-0.45	-0.82	-0.45	0.45	-0.64	0.64	0.27	0.09	1.00	-1.00
30	0.75	-0.45	-0.09	-	-	-0.45	-0.82	-0.45	0.82	-0.64	0.64	0.45	0.09	0.82	-1.00
30	0.90	-0.45	-0.27	-	-	-0.45	-0.82	-0.45	0.82	-0.64	0.64	0.09	0.09	0.82	-1.00
40	0	-0.64	-0.45	-0.82	-1.00	-0.64	-0.82	-0.45	-0.45	-0.64	0.45	-0.09	-0.64	1.00	-1.00
40	0.10	-0.82	-0.27	-0.82	-1.00	-0.82	-0.64	-0.45	0.09	-0.64	0.09	0.27	-0.27	1.00	-1.00
40	0.25	-0.45	-0.27	-0.82	-1.00	-0.64	-0.82	-0.45	-0.09	-0.64	0.27	0.27	-0.09	0.82	-1.00
40	0.50	-0.64	-0.45	-0.82	-1.00	-0.64	-1.00	-0.45	-0.09	-0.64	0.27	0.09	0.09	1.00	-1.00
40	0.75	-0.45	-0.45	-0.64	-1.00	-0.45	-1.00	-0.45	-0.09	-0.64	0.27	0.45	0.09	0.82	-1.00
40	0.90	-0.45	-0.45	-0.64	-1.00	-0.45	-1.00	-0.45	-0.09	-0.64	0.45	0.09	0.09	0.82	-1.00
50	0	-0.82	-0.45	-1.00	-0.82	-0.82	-0.64	-0.45	-0.27	-0.82	0.27	0.27	-0.64	0.82	-1.00
50	0.10	-0.82	-0.82	-0.82	-1.00	-0.82	-1.00	-0.45	-0.45	-0.82	0.09	0.09	-0.09	1.00	-1.00
50	0.25	-0.45	-0.64	-0.82	-1.00	-0.45	-1.00	-0.45	-0.09	-0.45	0.64	0.27	-0.45	1.00	-1.00
50	0.50	-0.64	-0.82	-0.82	-1.00	-0.64	-1.00	-0.45	0.09	-0.82	0.64	-0.09	0.09	0.82	-1.00
50	0.75	-0.45	-0.82	-0.64	-1.00	-0.64	-1.00	-0.45	-0.27	-0.64	0.45	0.27	0.09	0.82	-1.00
50	0.90	-0.45	-0.82	-0.82	-1.00	-0.64	-1.00	-0.45	-0.27	-0.64	0.64	0.09	-0.09	1.00	-1.00
60	0	-0.82	-0.64	-1.00	-0.82	-0.82	-1.00	-0.45	-0.45	-0.64	0.09	0.09	-0.09	1.00	-1.00
60	0.10	-0.82	-0.64	-1.00	-0.82	-0.82	-0.82	-0.45	-0.27	-0.64	0.45	0.27	-0.27	1.00	-1.00
60	0.25	-0.82	-0.64	-1.00	-0.64	-1.00	-0.64	-0.45	-0.45	-0.64	0.45	-0.09	-0.64	1.00	-1.00
60	0.50	-0.45	-0.82	-1.00	-1.00	-0.64	-1.00	-0.45	-0.45	-0.45	0.27	0.27	-0.09	1.00	-1.00
60	0.75	-0.45	-0.82	-1.00	-1.00	-0.64	-1.00	-0.45	-0.27	-0.64	0.27	0.27	-0.27	1.00	-1.00
60	0.90	-0.45	-0.82	-0.82	-1.00	-0.64	-1.00	-0.45	-0.45	-0.45	0.27	0.27	-0.09	0.82	-1.00
70	0	-1.00	-0.09	-1.00	0.09	-1.00	0.09	-0.64	-0.27	-1.00	0.64	-0.09	-0.45	1.00	-1.00
70	0.10	-0.64	-0.09	-1.00	-0.09	-0.64	-0.09	-0.45	-0.27	-0.82	0.45	-0.09	-0.27	1.00	-1.00
70	0.25	-1.00	-0.64	-1.00	-0.64	-1.00	-0.82	-0.64	-0.45	-1.00	0.09	-0.09	0.09	1.00	-1.00
70	0.50	-0.82	-0.82	-1.00	-1.00	-1.00	-1.00	-0.45	-0.45	-0.64	0.27	-0.27	-0.09	1.00	-1.00
70	0.75	-0.45	-0.82	-1.00	-1.00	-0.82	-1.00	-0.45	-0.64	-0.45	0.27	0.09	-0.09	0.82	-1.00
70	0.90	-0.45	-0.82	-0.82	-1.00	-0.82	-1.00	-0.45	-0.45	-0.45	0.27	0.45	-0.09	0.82	-1.00
80	0	-0.82	-0.60	-1.00	-0.60	-0.82	-0.60	-0.45	-0.20	-0.82	0.60	0.09	-0.40	0.82	-1.00
80	0.10	-1.00	-0.09	-1.00	-0.45	-1.00	0.09	-0.82	-0.45	-1.00	0.27	0.27	-0.45	1.00	-1.00
80	0.25	-0.82	0.09	-1.00	-0.09	-0.82	0.09	-0.45	-0.45	-0.64	0.09	-0.09	-0.45	1.00	-1.00
80	0.50	-0.82	-0.64	-1.00	-0.64	-1.00	-0.64	-0.45	-0.27	-0.64	0.45	0.09	-0.45	1.00	-1.00
80	0.75	-0.64	-0.82	-1.00	-1.00	-0.82	-1.00	-0.45	-0.64	-0.45	0.27	0.27	-0.45	1.00	-1.00
80	0.90	-0.64	-1.00	-1.00	-1.00	-0.82	-1.00	-0.45	-0.45	-0.64	-0.09	0.45	-0.09	0.82	-1.00
90	0	-0.60	-0.80	-1.00	-0.80	-1.00	-1.00	-0.60	-0.40	-0.60	0.00	-0.20	0.00	1.00	-1.00
90	0.10	-0.82	-0.80	-1.00	-0.80	-1.00	-0.80	-0.45	-0.40	-0.82	0.40	0.09	0.20	0.82	-1.00
90	0.25	-1.00	-0.40	-1.00	-0.40	-1.00	-0.20	-0.64	-0.60	-1.00	0.40	-0.27	-0.40	1.00	-1.00
90	0.50	-0.82	-0.82	-1.00	-0.82	-1.00	-1.00	-0.45	-0.45	-0.82	-0.09	-0.27	-0.09	1.00	-1.00
90	0.75	-0.64	-0.82	-1.00	-1.00	-0.82	-1.00	-0.45	-0.45	-0.45	-0.09	-0.09	-0.27	1.00	-1.00
90	0.90	-0.82	-0.82	-1.00	-1.00	-0.82	-1.00	-0.45	-0.64	-0.82	-0.09	0.09	-0.09	0.82	-1.00
100	0	-	-	-	-	-	-	-	-	-	-	-	-	-	-
100	0.10	-1.00	-1.00	-1.00	-1.00	-1.00	-1.00	-0.60	-1.00	-0.80	-0.43	0.00	-0.14	1.00	-1.00
100	0.25	-0.80	-0.80	-1.00	-0.80	-1.00	-0.80	-0.60	-0.40	-0.80	0.20	0.00	-0.20	0.80	-1.00
100	0.50	-1.00	-0.27	-1.00	-0.27	-1.00	-0.27	-0.64	-0.27	-0.82	0.09	0.09	-0.45	0.82	-1.00
100	0.75	-0.82	-0.82	-1.00	-0.82	-0.82	-0.82	-0.64	-0.45	-0.82	0.09	0.09	-0.45	0.82	-1.00
100	0.90	-0.82	-0.82	-1.00	-1.00	-0.82	-1.00	-0.45	-0.64	-0.64	0.09	0.09	-0.09	1.00	-1.00
110	0	-	-	-	-	-	-	-	-	-	-	-	-	-	-
110	0.10	-	-	-	-	-	-	-	-	-	-	-	-	-	-
110	0.25	-1.00	-1.00	-1.00	-1.00	-1.00	-1.00	-0.60	-1.00	-0.60	0.00	0.00	-0.50	1.00	-1.00
110	0.50	-1.00	-0.60	-1.00	-0.60	-1.00	-0.40	-0.45	-0.40	-0.64	-0.20	-0.09	0.00	1.00	-1.00
110	0.75	-0.82	-0.64	-1.00	-0.64	-0.82	-0.45	-0.45	-0.45	-0.64	-0.09	-0.09	-0.09	1.00	-1.00
110	0.90	-0.82	-1.00	-1.00	-1.00	-0.82	-1.00	-0.45	-0.64	-0.64	0.09	0.09	-0.45	1.00	-1.00
120	0	-	-	-	-	-	-	-	-	-	-	-	-	-	-
120	0.10	-	-	-	-	-	-	-	-	-	-	-	-	-	-
120	0.25	-	-	-	-	-	-	-	-	-	-	-	-	-	-
120	0.50	-1.00	-0.80	-1.00	-0.80	-1.00	-0.80	-0.40	-0.60	-0.60	0.00	0.00	0.00	1.00	-1.00
120	0.75	-0.82	-0.82	-1.00	-0.82	-0.82	-0.82	-0.45	-0.64	-0.64	-0.09	-0.27	-0.09	1.00	-1.00
120	0.90	-0.82	-0.82	-1.00	-0.82	-0.82	-0.82	-0.45	-0.64	-0.64	0.09	0.09	-0.27	1.00	-1.00
Average Scores		-0.71	-0.6	-0.94	-0.81	-0.78	-0.78	-0.50	-0.3	-0.67	0.26	0.09	-0.17	0.94	-1.0

♣ - Parameter with informative potential about fatigue, considering the empirical method criterion for identifying tendencies (Section 3.2.2)

Green Score - Positive *scores* defining an increasing tendency for the population sample in study

Red Score - Negative *scores* defining a decreasing tendency for the population sample in study

In simple terms, a parameter is defined as a fatigue index (i) if the average score changes signal (summarized by color) between the trial where fatigue is induced (**Fatigue +**) and the trial where fatigue decreases (**Fatigue -**) or (ii) if the average score module in **Fatigue +** is bigger than 0.50 and in **Fatigue -** is less than 0.50.



Table C.4: EMG processing results generated during the iterative application of the meta-analysis with different window sizes and time-steps for identifying which is the best combination to extract the feature and to evaluate the respective tendency. The values presented correspond to the combined slope, determined from the slopes of the regression line that best fits the evolution of each parameter for the different subjects inside the sample. The uncertainty is given by the half-length of the 95 % confidence interval.






Table C.5: ECG processing results (Time-Domain features) generated during the iterative application of the meta-analysis with different window sizes and time-steps for identifying which is the best combination to extract the feature and to evaluate the respective tendency. The values presented correspond to the combined slope, determined from the slopes of the regression line that best fits the evolution of each parameter for the different subjects inside the sample. The uncertainty is given by the half-length of the 95 % confidence interval.

		Time Domain																	
		Maximum RR $\blacktriangle$		Minimum RR $\blacktriangle$		Average RR $\blacktriangle$		SDNN $\blacktriangle$		rmsSD $\blacktriangle$		Triangular Index $\blacktriangle$		SD1		SD2 $\blacktriangle$		SD1 / SD2	
Window Size (s)	Overlap Fraction	Fatigue +	Fatigue -	Fatigue +	Fatigue -	Fatigue +	Fatigue -	Fatigue +	Fatigue -	Fatigue +	Fatigue -	Fatigue +	Fatigue -	Fatigue +	Fatigue -	Fatigue +	Fatigue -	Fatigue +	Fatigue -
30	0	$-1.99 \times 10^{-1} \pm 1.97 \times 10^{-2}$	$8.88 \times 10^{-1} \pm 8.24 \times 10^{-2}$	$-1.74 \times 10^{-1} \pm 1.23 \times 10^{-2}$	$9.30 \times 10^{-1} \pm 6.29 \times 10^{-2}$	$-1.86 \times 10^{-1} \pm 1.35 \times 10^{-2}$	$8.50 \times 10^{-1} \pm 5.34 \times 10^{-2}$	$-8.53 \times 10^{-3} \pm 2.81 \times 10^{-3}$	$-1.16 \times 10^{-3} \pm 1.98 \times 10^{-2}$	$1.27 \times 10^{-3} \pm 9.56 \times 10^{-4}$	$3.85 \times 10^{-3} \pm 3.55 \times 10^{-3}$	$-1.18 \times 10^{-2} \pm 3.18 \times 10^{-3}$	$-8.89 \times 10^{-3} \pm 1.75 \times 10^{-2}$	$1.11 \times 10^{-3} \pm 6.87 \times 10^{-4}$	$2.39 \times 10^{-3} \pm 2.40 \times 10^{-3}$	$-1.41 \times 10^{-2} \pm 4.14 \times 10^{-3}$	$-6.00 \times 10^{-3} \pm 2.86 \times 10^{-2}$	$1.94 \times 10^{-3} \pm 3.81 \times 10^{-4}$	$1.26 \times 10^{-3} \pm 5.18 \times 10^{-4}$
30	0.10	$-1.95 \times 10^{-1} \pm 1.87 \times 10^{-2}$	$7.12 \times 10^{-1} \pm 5.84 \times 10^{-2}$	$-1.75 \times 10^{-1} \pm 1.12 \times 10^{-2}$	$8.34 \times 10^{-1} \pm 6.17 \times 10^{-2}$	$-1.85 \times 10^{-1} \pm 1.29 \times 10^{-2}$	$8.07 \times 10^{-1} \pm 4.22 \times 10^{-2}$	$-8.04 \times 10^{-3} \pm 2.56 \times 10^{-3}$	$1.88 \times 10^{-2} \pm 1.24 \times 10^{-2}$	$1.44 \times 10^{-3} \pm 8.29 \times 10^{-4}$	$1.01 \times 10^{-2} \pm 2.87 \times 10^{-3}$	$-1.07 \times 10^{-2} \pm 2.75 \times 10^{-3}$	$-8.96 \times 10^{-3} \pm 1.51 \times 10^{-2}$	$1.20 \times 10^{-3} \pm 5.97 \times 10^{-4}$	$6.98 \times 10^{-3} \pm 1.99 \times 10^{-3}$	$-1.33 \times 10^{-2} \pm 3.79 \times 10^{-3}$	$1.85 \times 10^{-2} \pm 2.01 \times 10^{-2}$	$1.66 \times 10^{-3} \pm 3.13 \times 10^{-4}$	$1.29 \times 10^{-3} \pm 3.97 \times 10^{-4}$
30	0.25	$-1.96 \times 10^{-1} \pm 1.63 \times 10^{-2}$	$8.72 \times 10^{-1} \pm 6.22 \times 10^{-2}$	$-1.72 \times 10^{-1} \pm 1.08 \times 10^{-2}$	$8.78 \times 10^{-1} \pm 5.19 \times 10^{-2}$	$-1.83 \times 10^{-1} \pm 1.13 \times 10^{-2}$	$8.16 \times 10^{-1} \pm 4.18 \times 10^{-2}$	$-8.36 \times 10^{-3} \pm 2.35 \times 10^{-3}$	$-2.23 \times 10^{-3} \pm 1.33 \times 10^{-2}$	$1.24 \times 10^{-3} \pm 7.81 \times 10^{-4}$	$4.23 \times 10^{-3} \pm 2.79 \times 10^{-3}$	$-1.21 \times 10^{-2} \pm 3.03 \times 10^{-3}$	$-7.24 \times 10^{-3} \pm 1.50 \times 10^{-2}$	$9.91 \times 10^{-4} \pm 5.58 \times 10^{-4}$	$2.91 \times 10^{-3} \pm 1.94 \times 10^{-3}$	$-1.39 \times 10^{-2} \pm 3.47 \times 10^{-3}$	$-5.98 \times 10^{-3} \pm 1.92 \times 10^{-2}$	$1.92 \times 10^{-3} \pm 3.26 \times 10^{-4}$	$1.06 \times 10^{-3} \pm 3.68 \times 10^{-4}$
30	0.50	$-1.90 \times 10^{-1} \pm 1.27 \times 10^{-2}$	$8.28 \times 10^{-1} \pm 5.45 \times 10^{-2}$	$-1.72 \times 10^{-1} \pm 8.07 \times 10^{-3}$	$8.65 \times 10^{-1} \pm 4.55 \times 10^{-2}$	$-1.80 \times 10^{-1} \pm 8.68 \times 10^{-3}$	$8.52 \times 10^{-1} \pm 3.50 \times 10^{-2}$	$-7.26 \times 10^{-3} \pm 1.80 \times 10^{-3}$	$8.91 \times 10^{-5} \pm 1.31 \times 10^{-2}$	$1.03 \times 10^{-3} \pm 6.46 \times 10^{-4}$	$4.05 \times 10^{-3} \pm 2.33 \times 10^{-3}$	$-9.91 \times 10^{-3} \pm 2.21 \times 10^{-3}$	$-8.37 \times 10^{-3} \pm 1.30 \times 10^{-2}$	$8.33 \times 10^{-4} \pm 4.59 \times 10^{-4}$	$2.82 \times 10^{-3} \pm 1.62 \times 10^{-3}$	$-1.24 \times 10^{-2} \pm 2.65 \times 10^{-3}$	$-4.59 \times 10^{-3} \pm 1.90 \times 10^{-2}$	$1.83 \times 10^{-3} \pm 2.76 \times 10^{-4}$	$1.40 \times 10^{-3} \pm 3.71 \times 10^{-4}$
30	0.75	$-1.86 \times 10^{-1} \pm 8.54 \times 10^{-3}$	$8.41 \times 10^{-1} \pm 3.72 \times 10^{-2}$	$-1.72 \times 10^{-1} \pm 5.66 \times 10^{-3}$	$8.20 \times 10^{-1} \pm 2.98 \times 10^{-2}$	$-1.78 \times 10^{-1} \pm 5.96 \times 10^{-3}$	$8.31 \times 10^{-1} \pm 2.31 \times 10^{-2}$	$-6.67 \times 10^{-3} \pm 1.20 \times 10^{-3}$	$5.36 \times 10^{-3} \pm 8.80 \times 10^{-3}$	$1.29 \times 10^{-3} \pm 4.49 \times 10^{-4}$	$4.26 \times 10^{-3} \pm 1.63 \times 10^{-3}$	$-9.51 \times 10^{-3} \pm 1.62 \times 10^{-3}$	$-5.35 \times 10^{-3} \pm 9.06 \times 10^{-3}$	$9.90 \times 10^{-4} \pm 3.19 \times 10^{-4}$	$3.07 \times 10^{-3} \pm 1.14 \times 10^{-3}$	$-1.16 \times 10^{-2} \pm 1.77 \times 10^{-3}$	$3.08 \times 10^{-3} \pm 1.28 \times 10^{-2}$	$1.77 \times 10^{-3} \pm 1.79 \times 10^{-4}$	$1.30 \times 10^{-3} \pm 2.57 \times 10^{-4}$
30	0.90	$-1.82 \times 10^{-1} \pm 5.16 \times 10^{-3}$	$8.48 \times 10^{-1} \pm 2.39 \times 10^{-2}$	$-1.71 \times 10^{-1} \pm 3.46 \times 10^{-3}$	$8.16 \times 10^{-1} \pm 1.83 \times 10^{-2}$	$-1.76 \times 10^{-1} \pm 3.64 \times 10^{-3}$	$8.37 \times 10^{-1} \pm 1.43 \times 10^{-2}$	$-6.09 \times 10^{-3} \pm 7.12 \times 10^{-4}$	$6.07 \times 10^{-3} \pm 5.57 \times 10^{-3}$	$1.33 \times 10^{-3} \pm 2.87 \times 10^{-4}$	$4.51 \times 10^{-3} \pm 1.03 \times 10^{-3}$	$-8.68 \times 10^{-3} \pm 9.93 \times 10^{-4}$	$-4.19 \times 10^{-3} \pm 5.80 \times 10^{-3}$	$1.03 \times 10^{-3} \pm 2.04 \times 10^{-4}$	$3.11 \times 10^{-3} \pm 7.14 \times 10^{-4}$	$-1.09 \times 10^{-2} \pm 1.05 \times 10^{-3}$	$4.16 \times 10^{-3} \pm 8.10 \times 10^{-3}$	$1.76 \times 10^{-3} \pm 1.13 \times 10^{-4}$	$1.26 \times 10^{-3} \pm 1.58 \times 10^{-4}$
40	0	$-2.11 \times 10^{-1} \pm 2.45 \times 10^{-2}$	$1.01 \pm 6.32 \times 10^{-2}$	$-1.81 \times 10^{-1} \pm 1.30 \times 10^{-2}$	$1.28 \pm 3.97 \times 10^{-2}$	$-1.88 \times 10^{-1} \pm 1.64 \times 10^{-2}$	$1.07 \pm 3.01 \times 10^{-2}$	$-1.07 \times 10^{-2} \pm 3.38 \times 10^{-3}$	$-4.43 \times 10^{-2} \pm 1.62 \times 10^{-2}$	$1.37 \times 10^{-3} \pm 1.01 \times 10^{-3}$	$3.40 \times 10^{-2} \pm 1.04 \times 10^{-4}$	$-1.43 \times 10^{-2} \pm 3.66 \times 10^{-3}$	$-6.38 \times 10^{-3} \pm 2.71 \times 10^{-2}$	$1.10 \times 10^{-3} \pm 7.22 \times 10^{-4}$	$2.37 \times 10^{-2} \pm 4.64 \times 10^{-4}$	$-1.71 \times 10^{-2} \pm 5.03 \times 10^{-3}$	$-7.97 \times 10^{-2} \pm 2.11 \times 10^{-2}$	$1.71 \times 10^{-3} \pm 3.34 \times 10^{-4}$	$1.43 \times 10^{-3} \pm 3.07 \times 10^{-4}$
40	0.10	$-2.11 \times 10^{-1} \pm 2.32 \times 10^{-2}$	$1.03 \pm 6.36 \times 10^{-2}$	$-1.83 \times 10^{-1} \pm 1.43 \times 10^{-2}$	$1.00 \pm 6.59 \times 10^{-2}$	$-1.87 \times 10^{-1} \pm 1.52 \times 10^{-2}$	$8.19 \times 10^{-1} \pm 5.65 \times 10^{-2}$	$-1.09 \times 10^{-2} \pm 3.54 \times 10^{-3}$	$-3.25 \times 10^{-2} \pm 1.64 \times 10^{-2}$	$1.92 \times 10^{-3} \pm 8.91 \times 10^{-4}$	$2.65 \times 10^{-3} \pm 2.44 \times 10^{-3}$	$-1.43 \times 10^{-2} \pm 3.92 \times 10^{-3}$	$-4.26 \times 10^{-3} \pm 1.52 \times 10^{-2}$	$1.43 \times 10^{-3} \pm 6.29 \times 10^{-4}$	$2.05 \times 10^{-3} \pm 1.76 \times 10^{-3}$	$-1.74 \times 10^{-2} \pm 5.23 \times 10^{-3}$	$-4.82 \times 10^{-2} \pm 2.32 \times 10^{-2}$	$1.59 \times 10^{-3} \pm 3.21 \times 10^{-4}$	$1.24 \times 10^{-3} \pm 2.99 \times 10^{-4}$
40	0.25	$-2.00 \times 10^{-1} \pm 2.01 \times 10^{-2}$	$9.38 \times 10^{-1} \pm 4.31 \times 10^{-2}$	$-1.76 \times 10^{-1} \pm 1.23 \times 10^{-2}$	$9.32 \times 10^{-1} \pm 6.49 \times 10^{-2}$	$-1.83 \times 10^{-1} \pm 1.30 \times 10^{-2}$	$8.49 \times 10^{-1} \pm 4.52 \times 10^{-2}$	$-9.53 \times 10^{-3} \pm 3.16 \times 10^{-3}$	$-1.88 \times 10^{-2} \pm 2.05 \times 10^{-2}$	$2.16 \times 10^{-4} \pm 8.57 \times 10^{-4}$	$1.73 \times 10^{-2} \pm 1.98 \times 10^{-3}$	$-1.25 \times 10^{-2} \pm 3.42 \times 10^{-3}$	$-2.40 \times 10^{-2} \pm 1.62 \times 10^{-2}$	$3.41 \times 10^{-4} \pm 6.15 \times 10^{-4}$	$1.40 \times 10^{-2} \pm 1.29 \times 10^{-3}$	$-1.57 \times 10^{-2} \pm 4.64 \times 10^{-3}$	$-3.16 \times 10^{-2} \pm 2.97 \times 10^{-2}$	$1.44 \times 10^{-3} \pm 2.54 \times 10^{-4}$	$1.28 \times 10^{-3} \pm 3.67 \times 10^{-4}$
40	0.50	$-1.94 \times 10^{-1} \pm 1.53 \times 10^{-2}$	$8.32 \times 10^{-1} \pm 6.69 \times 10^{-2}$	$-1.72 \times 10^{-1} \pm 9.23 \times 10^{-3}$	$9.11 \times 10^{-1} \pm 4.79 \times 10^{-2}$	$-1.79 \times 10^{-1} \pm 1.01 \times 10^{-2}$	$8.13 \times 10^{-1} \pm 3.49 \times 10^{-2}$	$-8.96 \times 10^{-3} \pm 2.46 \times 10^{-3}$	$-1.42 \times 10^{-2} \pm 1.80 \times 10^{-2}$	$1.79 \times 10^{-3} \pm 7.03 \times 10^{-4}$	$8.92 \times 10^{-3} \pm 2.60 \times 10^{-3}$	$-1.12 \times 10^{-2} \pm 2.97 \times 10^{-3}$	$-1.58 \times 10^{-2} \pm 1.88 \times 10^{-2}$	$1.31 \times 10^{-3} \pm 4.98 \times 10^{-4}$	$5.84 \times 10^{-3} \pm 1.82 \times 10^{-3}$	$-1.50 \times 10^{-2} \pm 3.63 \times 10^{-3}$	$-2.61 \times 10^{-2} \pm 2.59 \times 10^{-2}$	$1.59 \times 10^{-3} \pm 2.42 \times 10^{-4}$	$1.22 \times 10^{-3} \pm 2.74 \times 10^{-4}$
40	0.75	$-1.88 \times 10^{-1} \pm 1.04 \times 10^{-2}$	$8.28 \times 10^{-1} \pm 4.60 \times 10^{-2}$	$-1.67 \times 10^{-1} \pm 6.28 \times 10^{-3}$	$8.76 \times 10^{-1} \pm 3.49 \times 10^{-2}$	$-1.76 \times 10^{-1} \pm 6.73 \times 10^{-3}$	$8.40 \times 10^{-1} \pm 2.54 \times 10^{-2}$	$-8.11 \times 10^{-3} \pm 1.60 \times 10^{-3}$	$-8.53 \times 10^{-3} \pm 1.18 \times 10^{-2}$	$1.51 \times 10^{-3} \pm 4.97 \times 10^{-4}$	$6.21 \times 10^{-3} \pm 1.67 \times 10^{-3}$	$-1.09 \times 10^{-2} \pm 2.08 \times 10^{-3}$	$-1.94 \times 10^{-2} \pm 1.17 \times 10^{-2}$	$1.11 \times 10^{-3} \pm 3.52 \times 10^{-4}$	$4.23 \times 10^{-3} \pm 1.16 \times 10^{-3}$	$-1.39 \times 10^{-2} \pm 2.36 \times 10^{-3}$	$-1.79 \times 10^{-2} \pm 1.72 \times 10^{-2}$	$1.38 \times 10^{-3} \pm 1.42 \times 10^{-4}$	$1.27 \times 10^{-3} \pm 2.61 \times 10^{-4}$
40	0.90	$-1.84 \times 10^{-1} \pm 6.17 \times 10^{-3}$	$8.49 \times 10^{-1} \pm 2.93 \times 10^{-2}$	$-1.65 \times 10^{-1} \pm 3.78 \times 10^{-3}$	$8.55 \times 10^{-1} \pm 2.13 \times 10^{-2}$	$-1.75 \times 10^{-1} \pm 4.05 \times 10^{-3}$	$8.38 \times 10^{-1} \pm 1.56 \times 10^{-2}$	$-7.76 \times 10^{-3} \pm 9.65 \times 10^{-4}$	$-8.18 \times 10^{-3} \pm 7.47 \times 10^{-3}$	$1.54 \times 10^{-3} \pm 3.08 \times 10^{-4}$	$6.47 \times 10^{-3} \pm 1.07 \times 10^{-3}$	$-1.11 \times 10^{-2} \pm 1.30 \times 10^{-3}$	$-1.73 \times 10^{-2} \pm 7.55 \times 10^{-3}$	$1.16 \times 10^{-3} \pm 2.19 \times 10^{-4}$	$4.59 \times 10^{-3} \pm 7.45 \times 10^{-4}$	$-1.34 \times 10^{-2} \pm 1.43 \times 10^{-3}$	$-1.70 \times 10^{-2} \pm 1.09 \times 10^{-2}$	$1.39 \times 10^{-3} \pm 9.32 \times 10^{-5}$	$1.24 \times 10^{-3} \pm 1.63 \times 1$



Table C.6: ECG processing results (Frequency-Domain features) generated during the iterative application of the meta-analysis with different window sizes and time-steps for identifying which is the best combination to extract the feature and to evaluate the respective tendency. The values presented correspond to the combined slope, determined from the slopes of the regression line that best fits the evolution of each parameter for the different subjects inside the sample. The uncertainty is given by the half-length of the 95 % confidence interval.

		Frequency Domain													
		Total Power		ULF Power		VLF Power		LF Power 		HF Power 		LF/HF Power Ratio		Median Frequency 	
Window Size (s)	Overlap Fraction	Fatigue +	Fatigue -	Fatigue +	Fatigue -	Fatigue +	Fatigue -	Fatigue +	Fatigue -	Fatigue +	Fatigue -	Fatigue +	Fatigue -	Fatigue +	Fatigue -
30	0	<u><math>-7.16 \times 10^1 \pm 3.22 \times 10^1</math></u>	$-3.49 \times 10^2 \pm 3.67 \times 10^2$	-	-	<u><math>-1.16 \times 10^1 \pm 5.03</math></u>	$-1.04 \times 10^2 \pm 6.21 \times 10^1$	<u><math>-2.84 \pm 1.06</math></u>	<u><math>1.05 \times 10^1 \pm 1.07 \times 10^1</math></u>	<u><math>-1.56 \pm 5.47 \times 10^{-1}</math></u>	<u><math>2.97 \pm 2.98</math></u>	<u><math>-3.34 \times 10^{-3} \pm 2.14 \times 10^{-3}</math></u>	<u><math>-5.41 \times 10^{-3} \pm 8.06 \times 10^{-3}</math></u>	<u><math>3.38 \times 10^{-3} \pm 4.18 \times 10^{-4}</math></u>	<u><math>-5.73 \times 10^{-3} \pm 7.11 \times 10^{-4}</math></u>
30	0.10	<u><math>-6.46 \times 10^1 \pm 2.82 \times 10^1</math></u>	$-8.62 \pm 2.99 \times 10^2$	-	-	<u><math>-9.66 \pm 4.27</math></u>	$-9.36 \times 10^1 \pm 5.85 \times 10^1$	<u><math>-2.58 \pm 1.02</math></u>	<u><math>1.29 \times 10^1 \pm 1.13 \times 10^1</math></u>	<u><math>-1.69 \pm 4.65 \times 10^{-1}</math></u>	<u><math>2.66 \pm 3.53</math></u>	<u><math>-3.90 \times 10^{-3} \pm 2.19 \times 10^{-3}</math></u>	<u><math>-8.83 \times 10^{-3} \pm 6.03 \times 10^{-3}</math></u>	<u><math>3.57 \times 10^{-3} \pm 3.91 \times 10^{-4}</math></u>	<u><math>-5.70 \times 10^{-3} \pm 7.66 \times 10^{-4}</math></u>
30	0.25	<u><math>-6.88 \times 10^1 \pm 2.55 \times 10^1</math></u>	$-2.44 \times 10^2 \pm 2.44 \times 10^2$	-	-	<u><math>-1.02 \times 10^1 \pm 4.06</math></u>	$-6.91 \times 10^1 \pm 4.41 \times 10^1$	<u><math>-2.69 \pm 8.86 \times 10^{-1}</math></u>	<u><math>5.17 \pm 1.15 \times 10^1</math></u>	<u><math>-1.48 \pm 4.16 \times 10^{-1}</math></u>	<u><math>7.34 \times 10^{-1} \pm 1.78</math></u>	<u><math>-2.91 \times 10^{-3} \pm 2.15 \times 10^{-3}</math></u>	<u><math>-6.10 \times 10^{-3} \pm 7.47 \times 10^{-3}</math></u>	<u><math>3.61 \times 10^{-3} \pm 3.50 \times 10^{-4}</math></u>	<u><math>-5.61 \times 10^{-3} \pm 6.15 \times 10^{-4}</math></u>
30	0.50	<u><math>-5.65 \times 10^1 \pm 1.92 \times 10^1</math></u>	$-2.19 \times 10^2 \pm 2.44 \times 10^2$	-	-	<u><math>-9.38 \pm 3.15</math></u>	$-7.80 \times 10^1 \pm 4.33 \times 10^1$	<u><math>-2.33 \pm 6.39 \times 10^{-1}</math></u>	<u><math>1.12 \times 10^1 \pm 8.92</math></u>	<u><math>-1.28 \pm 3.13 \times 10^{-1}</math></u>	<u><math>1.06 \pm 1.94</math></u>	<u><math>-4.11 \times 10^{-3} \pm 1.63 \times 10^{-3}</math></u>	<u><math>-5.96 \times 10^{-3} \pm 6.43 \times 10^{-3}</math></u>	<u><math>3.62 \times 10^{-3} \pm 2.89 \times 10^{-4}</math></u>	<u><math>-5.54 \times 10^{-3} \pm 5.28 \times 10^{-4}</math></u>
30	0.75	<u><math>-4.71 \times 10^1 \pm 1.21 \times 10^1</math></u>	$-1.25 \times 10^2 \pm 1.59 \times 10^2$	-	-	<u><math>-8.67 \pm 2.05</math></u>	$-6.05 \times 10^1 \pm 2.79 \times 10^1$	<u><math>-1.87 \pm 3.76 \times 10^{-1}</math></u>	<u><math>1.33 \times 10^1 \pm 7.11</math></u>	<u><math>-1.10 \pm 1.97 \times 10^{-1}</math></u>	<u><math>1.31 \pm 1.42</math></u>	<u><math>-3.35 \times 10^{-3} \pm 1.24 \times 10^{-3}</math></u>	<u><math>-1.91 \times 10^{-3} \pm 5.35 \times 10^{-3}</math></u>	<u><math>3.60 \times 10^{-3} \pm 2.02 \times 10^{-4}</math></u>	<u><math>-5.48 \times 10^{-3} \pm 3.45 \times 10^{-4}</math></u>
30	0.90	<u><math>-3.92 \times 10^1 \pm 6.80</math></u>	<u><math>-1.13 \times 10^2 \pm 9.90 \times 10^1</math></u>	-	-	<u><math>-7.98 \pm 1.18</math></u>	<u><math>-5.91 \times 10^1 \pm 1.74 \times 10^1</math></u>	<u><math>-1.51 \pm 1.97 \times 10^{-1}</math></u>	<u><math>1.45 \times 10^1 \pm 4.54</math></u>	<u><math>-8.51 \times 10^{-1} \pm 1.04 \times 10^{-1}</math></u>	<u><math>1.59 \pm 1.16</math></u>	<u><math>-3.75 \times 10^{-3} \pm 7.72 \times 10^{-4}</math></u>	<u><math>-4.06 \times 10^{-3} \pm 3.34 \times 10^{-3}</math></u>	<u><math>3.65 \times 10^{-3} \pm 1.25 \times 10^{-4}</math></u>	<u><math>-5.44 \times 10^{-3} \pm 2.18 \times 10^{-4}</math></u>
40	0	<u><math>-1.26 \times 10^2 \pm 5.09 \times 10^1</math></u>	<u><math>-1.76 \times 10^3 \pm 5.24 \times 10^2</math></u>	<u><math>-3.50 \pm 1.28</math></u>	<u><math>-1.31 \times 10^2 \pm 1.72 \times 10^1</math></u>	<u><math>-1.66 \times 10^1 \pm 6.49</math></u>	<u><math>-3.16 \times 10^2 \pm 7.98 \times 10^1</math></u>	<u><math>-4.48 \pm 1.61</math></u>	<u><math>-3.12 \times 10^1 \pm 2.46 \times 10^1</math></u>	<u><math>-2.00 \pm 7.82 \times 10^{-1}</math></u>	<u><math>7.99 \pm 3.74</math></u>	<u><math>-8.50 \times 10^{-4} \pm 3.05 \times 10^{-3}</math></u>	<u><math>-3.59 \times 10^{-3} \pm 6.31 \times 10^{-3}</math></u>	<u><math>3.61 \times 10^{-3} \pm 4.76 \times 10^{-4}</math></u>	<u><math>-6.93 \times 10^{-3} \pm 4.53 \times 10^{-4}</math></u>
40	0.10	<u><math>-1.33 \times 10^2 \pm 5.61 \times 10^1</math></u>	<u><math>-1.40 \times 10^3 \pm 5.19 \times 10^2</math></u>	<u><math>-3.46 \pm 1.58</math></u>	<u><math>-6.60 \times 10^1 \pm 1.89 \times 10^1</math></u>	<u><math>-1.80 \times 10^1 \pm 7.61</math></u>	<u><math>-2.43 \times 10^2 \pm 8.32 \times 10^1</math></u>	<u><math>-4.35 \pm 1.81</math></u>	<u><math>5.73 \pm 2.38 \times 10^1</math></u>	<u><math>-2.13 \pm 7.32 \times 10^{-1}</math></u>	<u><math>-4.72 \pm 3.66</math></u>	<u><math>-3.18 \times 10^{-4} \pm 2.93 \times 10^{-3}</math></u>	<u><math>-5.12 \times 10^{-3} \pm 8.35 \times 10^{-3}</math></u>	<u><math>3.51 \times 10^{-3} \pm 4.64 \times 10^{-4}</math></u>	<u><math>-5.84 \times 10^{-3} \pm 6.32 \times 10^{-4}</math></u>
40	0.25	<u><math>-1.09 \times 10^2 \pm 4.88 \times 10^1</math></u>	<u><math>-1.06 \times 10^3 \pm 6.64 \times 10^2</math></u>	<u><math>-3.52 \pm 1.57</math></u>	<u><math>-5.57 \times 10^1 \pm 2.44 \times 10^1</math></u>	<u><math>-1.56 \times 10^1 \pm 6.68</math></u>	<u><math>-2.05 \times 10^2 \pm 1.03 \times 10^2</math></u>	<u><math>-4.12 \pm 1.37</math></u>	<u><math>-1.33 \times 10^1 \pm 1.97 \times 10^1</math></u>	<u><math>-1.69 \pm 6.50 \times 10^{-1}</math></u>	<u><math>1.92 \pm 3.25</math></u>	<u><math>-1.59 \times 10^{-3} \pm 2.88 \times 10^{-3}</math></u>	<u><math>-1.11 \times 10^{-2} \pm 6.83 \times 10^{-3}</math></u>	<u><math>3.51 \times 10^{-3} \pm 4.55 \times 10^{-4}</math></u>	<u><math>-6.17 \times 10^{-3} \pm 5.75 \times 10^{-4}</math></u>
40	0.50	<u><math>-9.86 \times 10^1 \pm 3.76 \times 10^1</math></u>	<u><math>-1.00 \times 10^3 \pm 5.65 \times 10^2</math></u>	<u><math>-3.17 \pm 1.12</math></u>	<u><math>-5.55 \times 10^1 \pm 2.11 \times 10^1</math></u>	<u><math>-1.53 \times 10^1 \pm 5.44</math></u>	<u><math>-1.77 \times 10^2 \pm 8.89 \times 10^1</math></u>	<u><math>-3.53 \pm 1.12</math></u>	<u><math>-8.01 \pm 1.96 \times 10^1</math></u>	<u><math>-1.42 \pm 4.70 \times 10^{-1}</math></u>	<u><math>1.93 \pm 2.93</math></u>	<u><math>-3.01 \times 10^{-3} \pm 2.21 \times 10^{-3}</math></u>	<u><math>-7.76 \times 10^{-3} \pm 7.38 \times 10^{-3}</math></u>	<u><math>3.68 \times 10^{-3} \pm 3.40 \times 10^{-4}</math></u>	<u><math>-5.91 \times 10^{-3} \pm 4.89 \times 10^{-4}</math></u>
40	0.75	<u><math>-8.43 \times 10^1 \pm 2.32 \times 10^1</math></u>	<u><math>-7.38 \times 10^2 \pm 3.52 \times 10^2</math></u>	<u><math>-2.99 \pm 7.57 \times 10^{-1}</math></u>	<u><math>-4.52 \times 10^1 \pm 1.31 \times 10^1</math></u>	<u><math>-1.36 \times 10^1 \pm 3.42</math></u>	<u><math>-1.49 \times 10^2 \pm 5.48 \times 10^1</math></u>	<u><math>-3.06 \pm 7.09 \times 10^{-1}</math></u>	<u><math>2.80 \pm 1.41 \times 10^1</math></u>	<u><math>-1.18 \pm 2.88 \times 10^{-1}</math></u>	<u><math>6.58 \times 10^{-1} \pm 2.03</math></u>	<u><math>-3.13 \times 10^{-3} \pm 1.70 \times 10^{-3}</math></u>	<u><math>-7.40 \times 10^{-3} \pm 5.58 \times 10^{-3}</math></u>	<u><math>3.79 \times 10^{-3} \pm 2.43 \times 10^{-4}</math></u>	<u><math>-5.73 \times 10^{-3} \pm 3.26 \times 10^{-4}</math></u>
40	0.90	<u><math>-7.51 \times 10^1 \pm 1.33 \times 10^1</math></u>	<u><math>-6.53 \times 10^2 \pm 2.19 \times 10^2</math></u>	<u><math>-2.85 \pm 4.46 \times 10^{-1}</math></u>	<u><math>-4.31 \times 10^1 \pm 8.31</math></u>	<u><math>-1.27 \times 10^1 \pm 1.99</math></u>	<u><math>-1.43 \times 10^2 \pm 3.49 \times 10^1</math></u>	<u><math>-2.77 \pm 4.05 \times 10^{-1}</math></u>	<u><math>8.02 \pm 8.48</math></u>	<u><math>-1.05 \pm 1.60 \times 10^{-1}</math></u>	<u><math>1.38 \pm 1.65</math></u>	<u><math>-4.40 \times 10^{-3} \pm 9.57 \times 10^{-4}</math></u>	<u><math>-7.66 \times 10^{-3} \pm 4.30 \times 10^{-3}</math></u>	<u><math>3.67 \times 10^{-3} \pm 1.48 \times 10^{-4}</math></u>	<u><math>-5.60 \times 10^{-3} \pm 2.01 \times 10^{-4}</math></u>
50	0	<u><math>-1.79 \times 10^2 \pm 9.27 \times 10^1</math></u>	<u><math>-1.60 \times 10^3 \pm 5.89 \times 10^2</math></u>	<u><math>-6.07 \pm 2.99</math></u>	<u><math>-6.91 \times 10^1 \pm 3.19 \times 10^1</math></u>	<u><math>-2.85 \times 10^1 \pm 1.44 \times 10^1</math></u>	<u><math>-3.14 \times 10^2 \pm 1.54 \times 10^2</math></u>	<u><math>-5.44 \pm 2.51</math></u>	<u><math>-3.53 \times 10^1 \pm 2.18 \times 10^1</math></u>	<u><math>-2.49 \pm 1.08</math></u>	<u><math>9.28 \times 10^{-1} \pm 1.03 \times 10^{-1}</math></u>	<u><math>-1.67 \times 10^{-3} \pm 2.07 \times 10^{-3}</math></u>	<u><math>-2.88 \times 10^{-2} \pm 2.54 \times 10^{-3}</math></u>	<u><math>3.45 \times 10^{-3} \pm 5.08 \times 10^{-4}</math></u>	<u><math>-7.17 \times 10^{-3} \pm 4.45 \times 10^{-5}</math></u>
50	0.10	<u><math>-1.75 \times 10^2 \pm 8.33 \times 10^1</math></u>	<u><math>-1.61 \times 10^3 \pm 5.96 \times 10^2</math></u>	<u><math>-5.60 \pm 2.73</math></u>	<u><math>-6.15 \times 10^1 \pm 1.14 \times 10^1</math></u>	<u><math>-2.66 \times 10^1 \pm 1.22 \times 10^1</math></u>	<u><math>-2.55 \times 10^2 \pm 4.05 \times 10^1</math></u>	<u><math>-5.13 \pm 2.25</math></u>	<u><math>-1.53 \times 10^1 \pm 2.58 \times 10^1</math></u>	<u><math>-2.29 \pm 9.74 \times 10^{-1}</math></u>	<u><math>-1.66 \pm 2.19</math></u>	<u><math>-3.40 \times 10^{-3} \pm 2.54 \times 10^{-3}</math></u>	<u><math>-5.52 \times 10^{-4} \pm 7.84 \times 10^{-3}</math></u>	<u><math>3.46 \times 10^{-3} \pm 4.67 \times 10^{-4}</math></u>	<u><math>-6.21 \times 10^{-3} \pm 6.62 \times 10^{-4}</math></u>
50	0.25	<u><math>-1.92 \times 10^2 \pm 8.42 \times 10^1</math></u>	<u><math>-3.37 \times 10^3 \pm 1.24 \times 10^3</math></u>	<u><math>-6.47 \pm 2.82</math></u>	<u><math>-1.78 \times 10^2 \pm 4.12 \times 10^1</math></u>	<u><math>-3.16 \times 10^1 \pm 1.28 \times 10^1</math></u>	<u><math>-6.18 \times 10^2 \pm 2.02 \times 10^2</math></u>	<u><math>-4.60 \pm 2.20</math></u>	<u><math>-1.66 \times 10^1 \pm 1.79 \times 10^1</math></u>	<u><math>-2.28 \pm 8.71 \times 10^{-1}</math></u>	<u><math>-3.44 \pm 5.83</math></u>	<u><math>-1.50 \times 10^{-3} \pm 2.35 \times 10^{-3}</math></u>	<u><math>-1.27 \times 10^{-2} \pm 1.23 \times 10^{-2}</math></u>	<u><math>3.37 \times 10^{-3} \pm 4.62 \times 10^{-4}</math></u>	<u><math>-7.29 \times 10^{-3} \pm 5.32 \times 10^{-4}</math></u>
50	0.50	<u><math>-1.53 \times 10^2 \pm 5.96 \times 10^1</math></u>	<u><math>-3.00 \times 10^3 \pm 9.93 \times 10^2</math></u>	<u><math>-4.92 \pm 1.75</math></u>	<u><math>-1.24 \times 10^2 \pm 4.00 \times 10^1</math></u>	<u><math>-2.50 \times 10^1 \pm 9.01</math></u>	<u><math>-4.82 \times 10^2 \pm 1.89 \times 10^2</math></u>	<u><math>-4.48 \pm 1.57</math></u>	<u><math>-4.95 \times 10^{-1} \pm 1.54 \times 10^1</math></u>	<u><math>-1.87 \pm 6.34 \times 10^{-1}</math></u>	<u><math>6.19 \times 10^{-1} \pm 4.27</math></u>	<u><math>-4.41 \times 10^{-3} \pm 1.66 \times 10^{-3}</math></u>	<u><math>-1.10 \times 10^{-2} \pm 6.92 \times 10^{-3}</math></u>	<u><math>3.45 \times 10^{-3} \pm 3.56 \times 10^{-4}</math></u>	<u><math>-6.11 \times 10^{-3} \pm 5.81 \times 10^{-4}</math></u>
50	0.75	<u><math>-1.41 \times 10^2 \pm 4.13 \times 10^1</math></u>	<u><math>-2.01 \times 10^3 \pm 6.71 \times 10^2</math></u>	<u><math>-5.11 \pm 1.35</math></u>	<u><math>-9.75 \times 10^1 \pm 2.70 \times 10^1</math></u>										

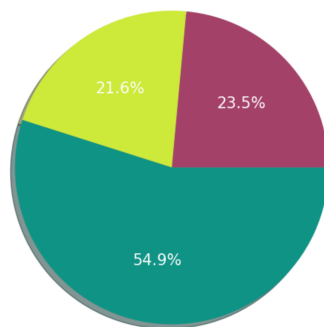
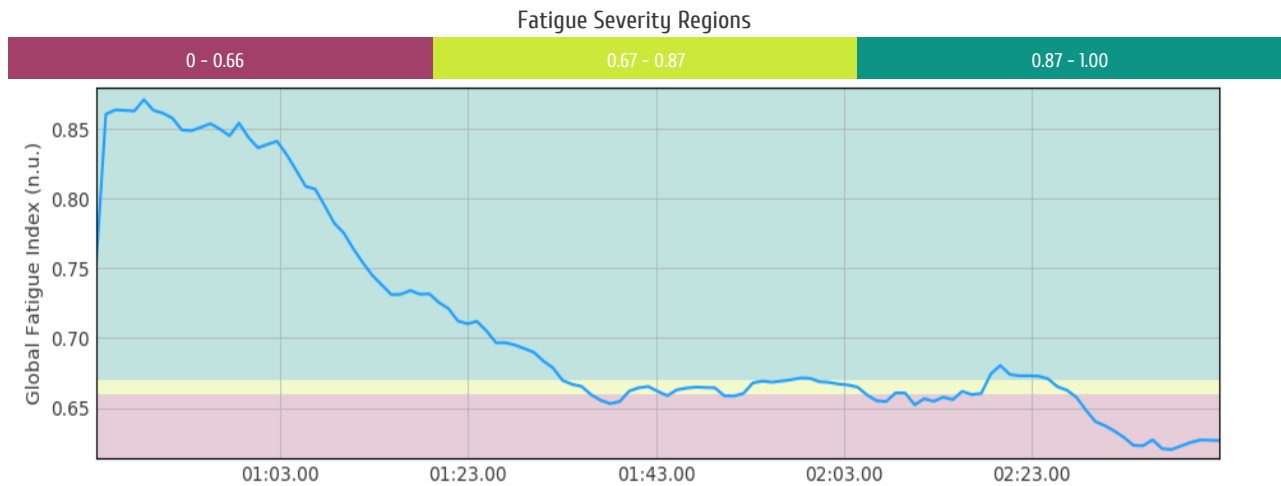




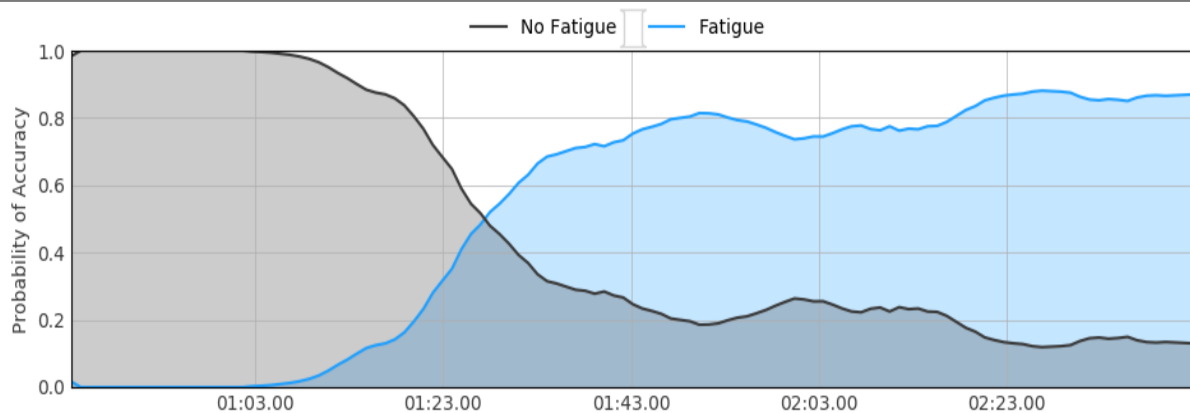
## Report Generated by the *Offline* Fatigue Monitoring Plugin

Following the visual approach to the interpretation of the EMG and ECG indexes, performed in Appendix [A](#), we present a report generated by the fatigue monitoring *plugin*, serving as a structural example of the expected results during a test where fatigue is induced.

## Evolution of the Global Fatigue Index



## Evolution of the Classification Results



## Electromyographic Component

unit  
Millivolt

session time  
04:04.0

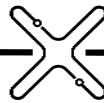
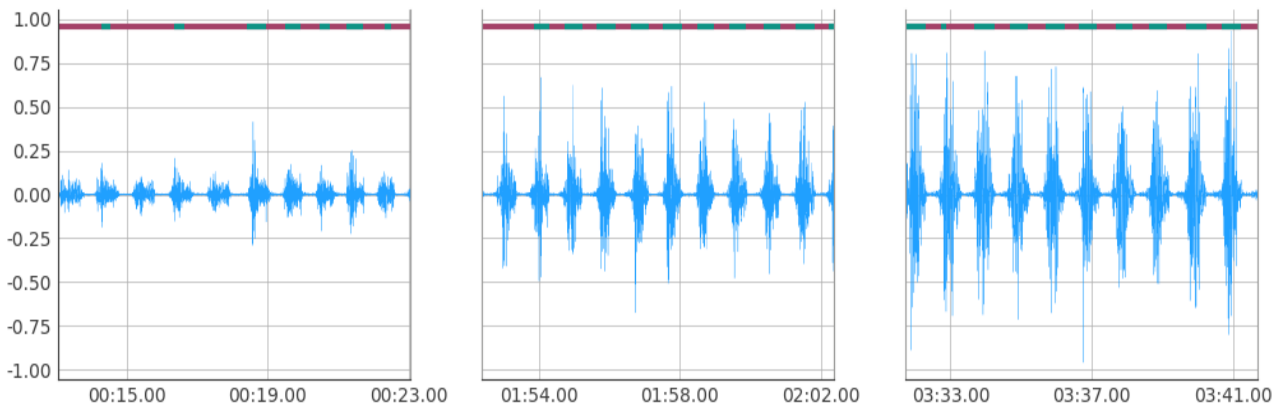
selection start  
00:13.1

selection end  
03:41.7

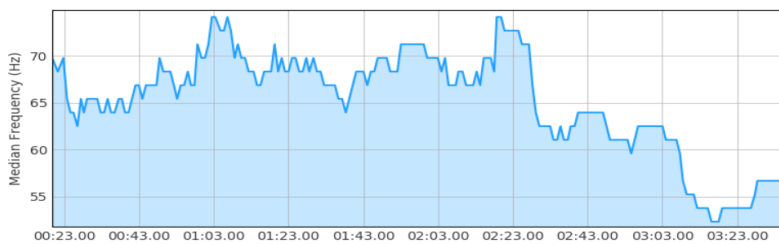
total processed time  
03:28.6

00:07:80:79:6F:D8

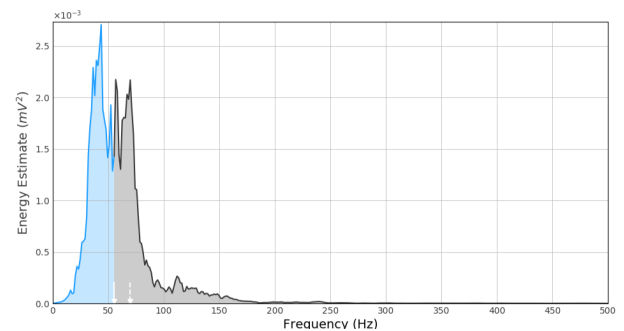
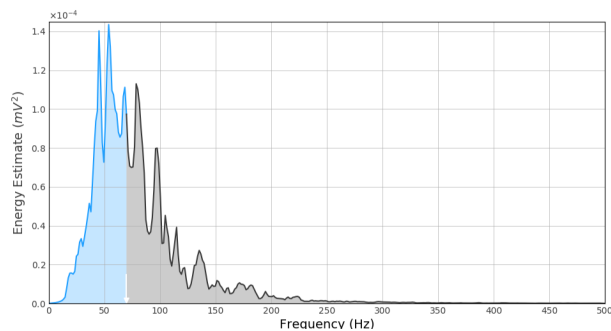
A2 - CUSTOM/0.5/1.0/V



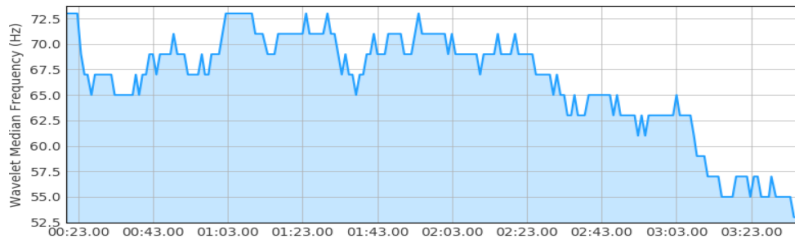
## Median Frequency Analysis [1]



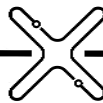
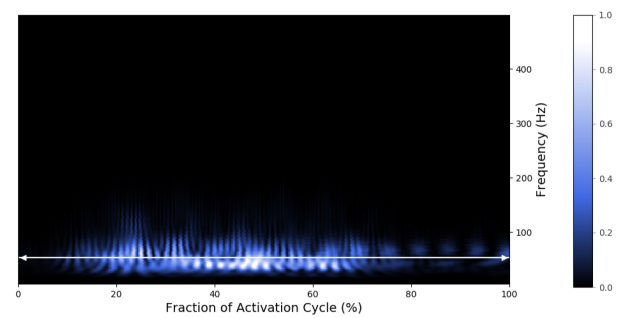
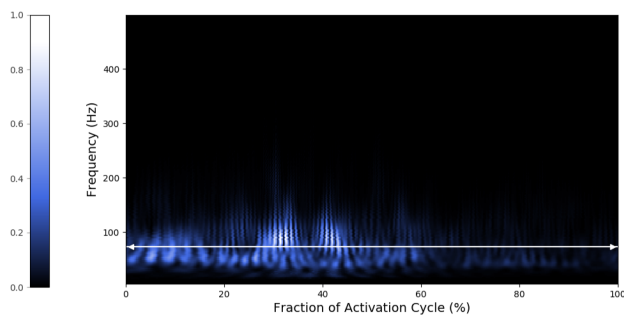
Change Percentage	-20.83	%
Average Value	65.13	Hz
Average Change Rate	-0.07	Hz/s



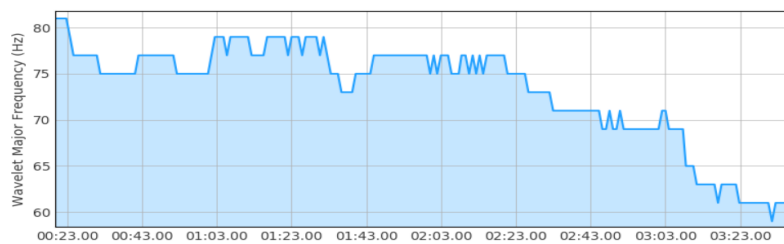
## Wavelet Median Frequency Analysis [2]



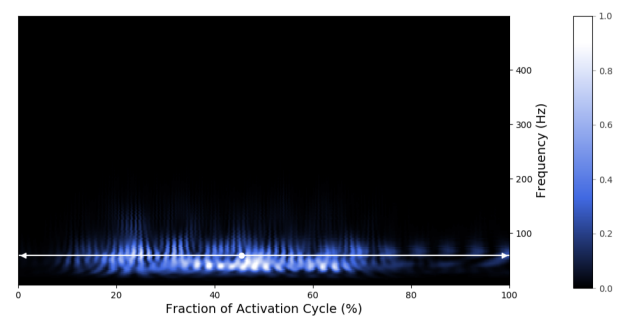
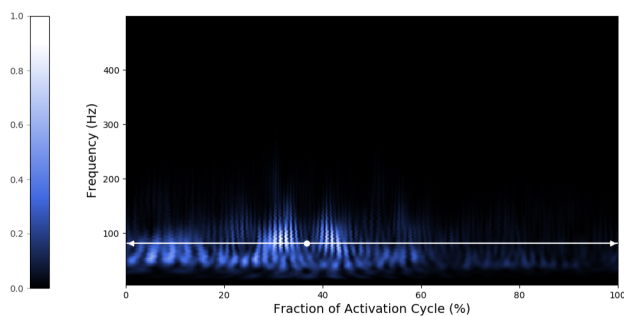
Change Percentage	-27.40	%
Average Value	66.20	Hz
Average Change Rate	-0.10	Hz/s



## Wavelet Major Frequency Analysis [3]



Change Percentage	-27.16	%
Average Value	73.19	Hz
Average Change Rate	-0.11	Hz/s





# Fatigue Analysis

Sun Mar 11 2018 17:18:56 GMT  
OPENSIGNALS VERSION: Public Build 2017-09-20

## Electrocardiographic Component

unit  
Millivolt

session time  
04:04.0

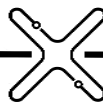
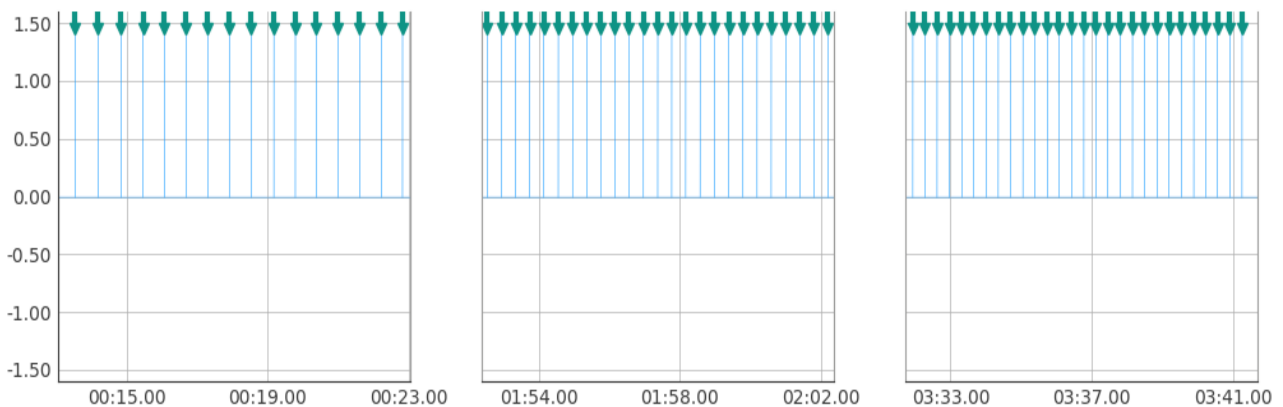
selection start  
00:13.1

selection end  
03:41.7

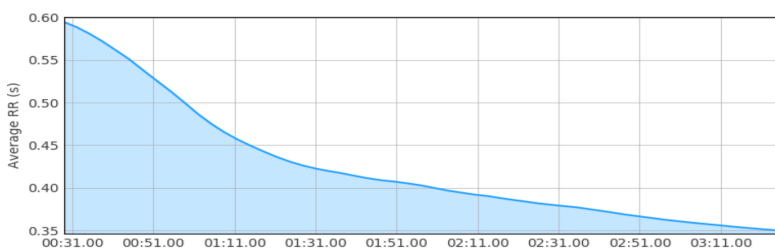
total processed time  
03:28.6

00:07:80:79:6F:D8

A7 - CUSTOM/0.5/1.0/V



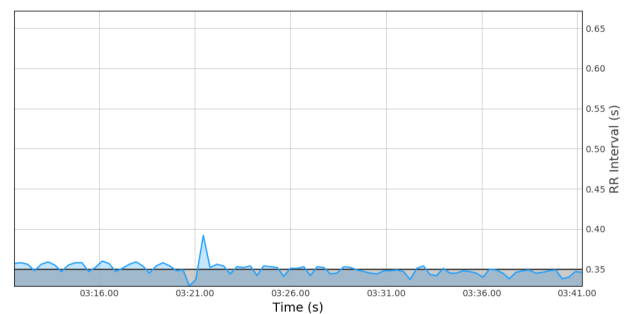
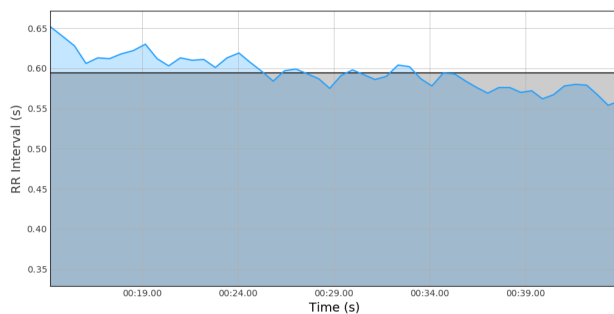
## Average RR Analysis [4]



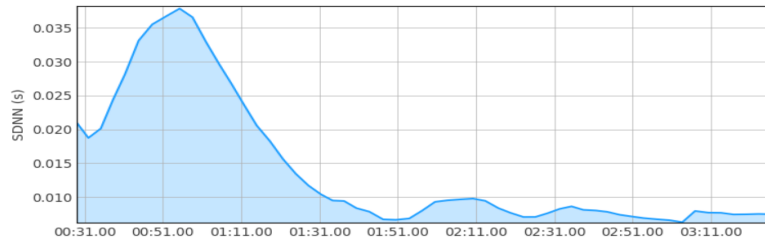
Change Percentage **-41.20** %

Average Value **0.42** s

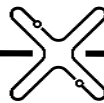
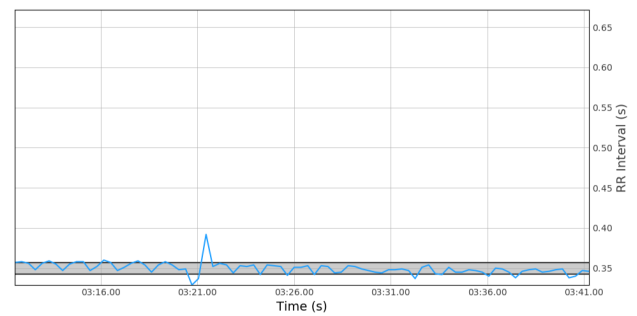
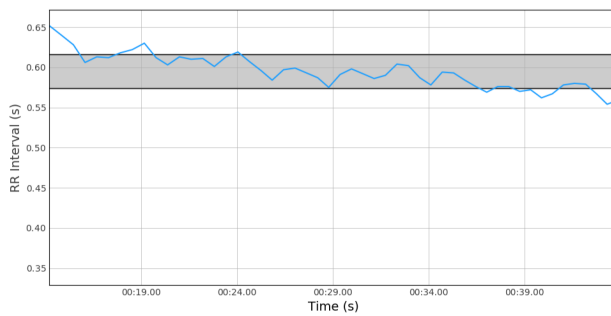
Average Change Rate **-0.00** s/s



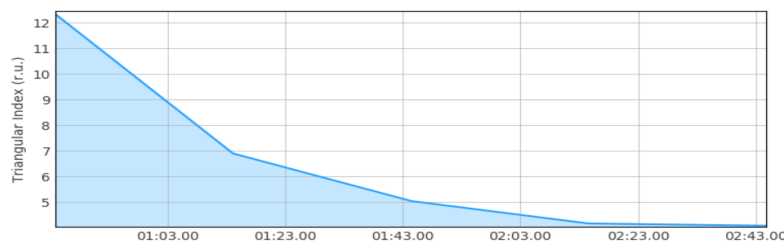
## SDNN Analysis [5]



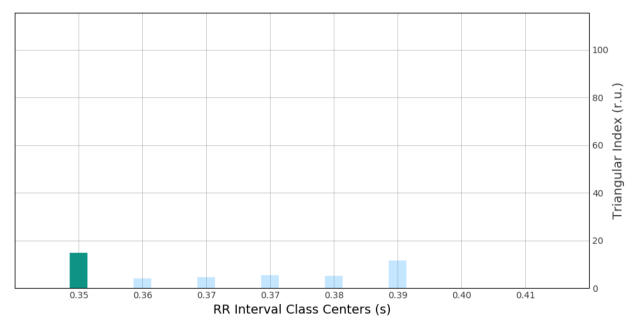
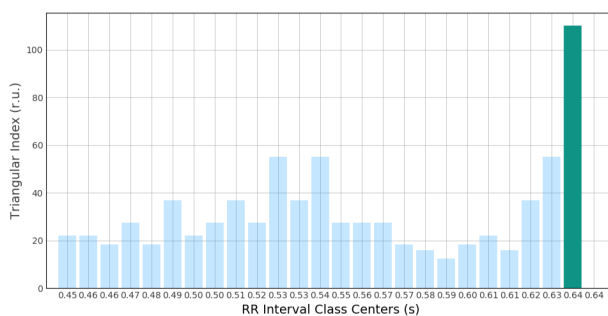
Change Percentage **-64.46** %  
Average Value **0.01** s  
Average Change Rate **-0.00** s/s



## Triangular Index Analysis [6]

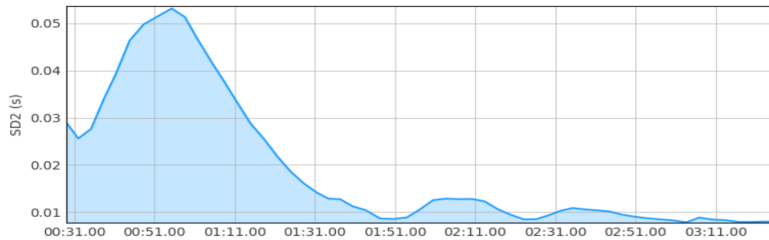


Change Percentage **-66.96** %  
Average Value **6.50** a.u.  
Average Change Rate **-0.07** a.u./s

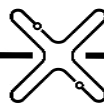
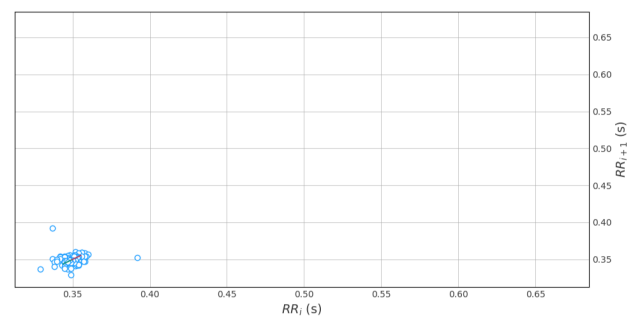
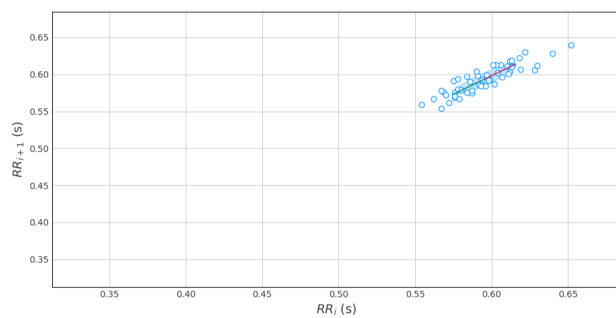




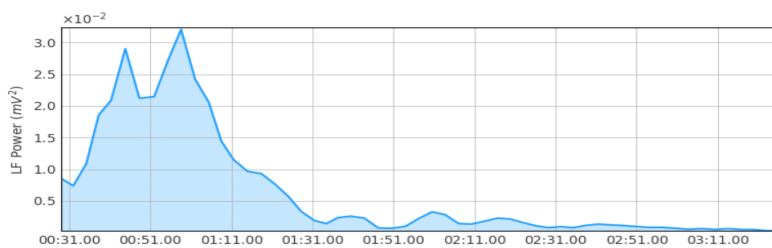
## SD2 Analysis [7]



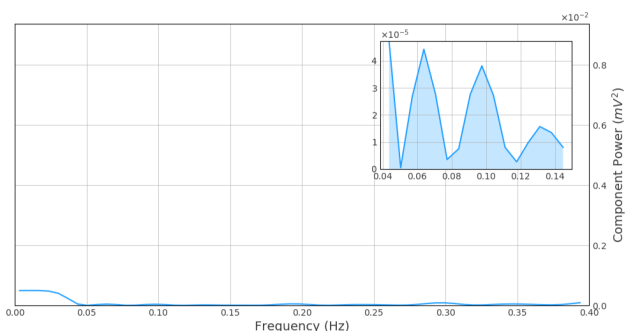
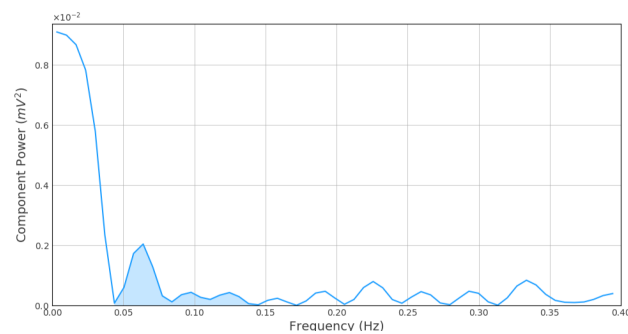
Change Percentage **-72.49** %  
Average Value **0.02** s  
Average Change Rate **-0.00** s/s



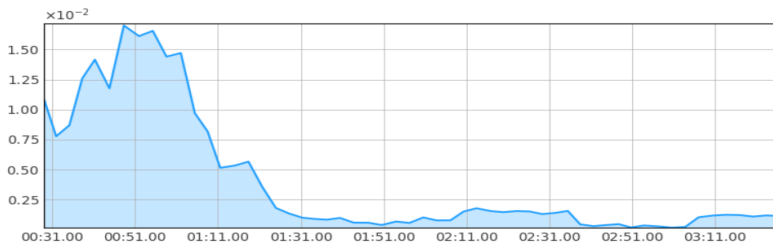
## LF Power Analysis [8]



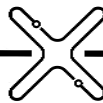
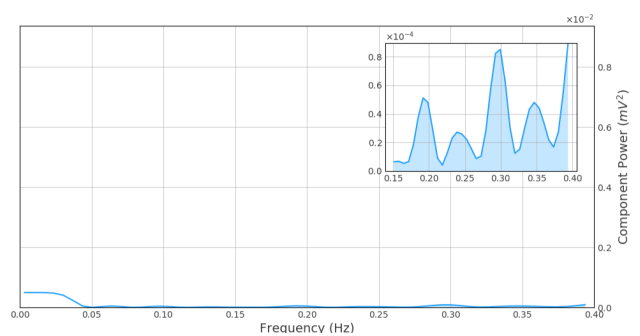
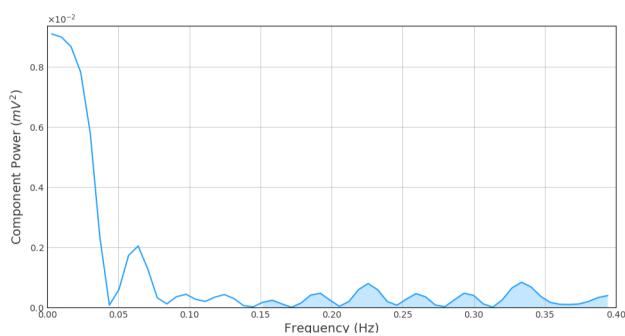
Change Percentage **-96.39** %  
Average Value **0.01**  $s^2$   
Average Change Rate **-0.00**  $s^2/s$



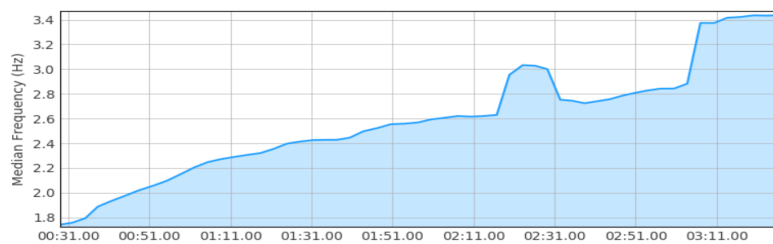
## HF Power Analysis [9]



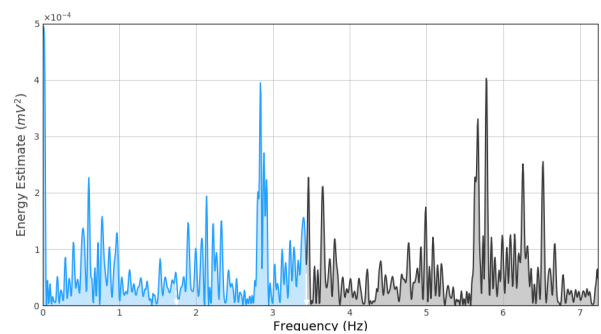
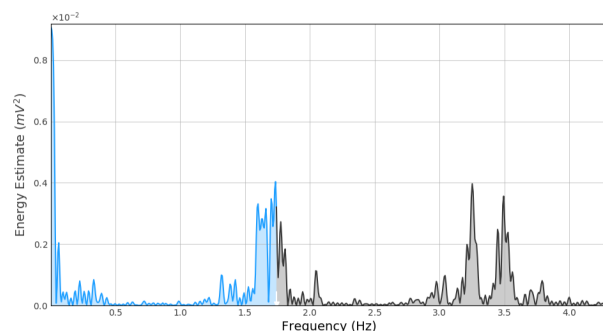
Change Percentage	-89.43	%
Average Value	0.00	s <sup>2</sup>
Average Change Rate	-0.00	s <sup>2</sup> /s



## Median Frequency HRV Analysis [10]



Change Percentage	97.23	%
Average Value	2.59	Hz
Average Change Rate	0.01	Hz/s



## Glossary

1. The median frequency corresponds to a parameter indicative of the way the total energy of the electromyographic (EMG) signal is distributed by the various elementary components, from the signal decomposition procedure based on the Fourier methodology.  
In formal terms the median frequency is the frequency that allows the splitting of the power spectrum into two segments with equal energy (Konrad, 2009).  
Thus, if 50 % of the signal energy is distributed by a number of  $X$  elementary components with low frequency, while the other half is distributed by  $Y$  high frequency elementary components ( $X \ll Y$ ), this means that the spectrum has more information concentrated in lower frequencies and, consequently, the median frequency will have a smaller value, due to the higher weight of the low frequency elementary components 'reaching up' the splitting point of the spectrum into two segments with equal power in a smaller frequency value.  
In fatigue conditions will be expected that this parameter decreases during acquisition, by the fact that the conduction velocity of the nervous impulse on the muscular fibres decreases while the fatigue settles (Cifrek, Medved, Tonkovi and Ostoji, 2009; De Luca, 1984).
2. The present parameter was extracted from the scalogram, obtained by the decomposition of EMG signal using the Wavelet Transform.  
The scalogram is a two-dimensional representation intended to simplify an information with a three-dimensional nature, having dimensions of frequency, time and colour, revealing the energy distribution of the signal over the time-frequency plane. Each point of the plane has a characteristic temporal and frequency resolution, considering the Wavelet Transform base methodology of using multiple scales for decomposing the time series (Rioul and Vetterli, 1991).  
The colour will be the dimensional simplification term, allowing the representation of the wavelet coefficients values in the 2D space, which in normal conditions would originate a new visual dimension, requiring a 3D coordinate system.  
Comparatively to the Fourier Transform, this methodology has the advantage that the results present a better commitment between time and frequency resolution, bypassing the problem of non-stationarity of EMG signals in dynamic contractions conditions, something that affects the reliability of the Fourier Analysis (Cifrek et al., 2009).  
The followed approach, for extracting this parameter, is based on the generation of an average power spectrum in the direction of the frequency dimension (losing the temporal information), considering that the scalogram corresponds to an image where each row is representative of a frequency component/scale and each column of a specific time interval.  
The average spectrum is formed by a number of samples coincident with the number of scalogram rows, having each sample a value given from the mean value of all wavelet coefficients/energy across the correspondent row.  
Such as the median frequency, taken from the Fourier domain, the present feature tends to decrease with the emergence of fatigue (Graham, Wachowiak and Gurd, 2015).
3. Corresponds to the frequency associated to informative centroid, that is, the major frequency will be the y-coordinate of the centroid, correspondent to the frequency axis of the scalogram, after the segmentation stage.  
The segmentation is carried out using the Otsu methodology. After this step only remain the pixels with a high informative content (Otsu, 1979)  
From these remaining pixels will be determined the centroid position, conceptually equivalent to the centre of mass used in mechanical/physical studies, representing an image point where the information is concentrated.  
It will be a positional weighted average, in which the coordinates and the value of each pixel are used, giving a weight (value) to each coordinate, so, more informative pixels contribute with a bigger weight in the definition of the centroid position.  
The determination of this parameter will be more propitious when the Otsu segmentation is used, because, if this step is skipped, the centroid determination 'collects' information from all image pixels rather than contemplating only the pixels with a higher informative content.  
Thus, in simplistic terms, as the centroid corresponds to an object abstraction, where a great set of pixels will be summarized in a single pixel and the major frequency, like said before, will be the frequency of this global point, giving an indication of the direction of the spectrum compression.  
So, the purpose of this feature will be the same as for the Wavelet Median Frequency, producing fatigue an identical tendency of decreasing (Graham et al., 2015).
4. Is an indicator of the way heart-rate changes along the acquisition (inversely proportional to the heart-rate), defining the average duration of RR intervals contained in the processing window.  
In exercise conditions and due to higher energetic needs, the heart-rate will increase, and, consequently, the Average RR decreases, but this effect is not exclusively caused by the emergence of muscular or neurological fatigue, reason why it should be considered as an auxiliary index for fatigue evaluation, that is, analysing only this index does not allow by itself to infer objectively that the fatigue is being acquired.
5. The acronym SDNN means standard-deviation of NN-Tachogram (RR interval evolution without ectopic beats), revealing itself as a measure of variability/dispersion of RR interval duration in relation to the mean value.  
The samples (RR intervals) will be all beats contained in a predefined processing window. This feature constitutes a simple statistical approach but the advantage of simplicity also brings a problematic consequence that is the dependency of the SDNN value in relation to the processing window size, making it difficult or even impossible to compare values taken from heart-rate variability studies with different experimental conditions (Task Force of The European Society of Cardiology and the North American Society of Pacing and Electrophysiology, 1996).  
The average duration of RR interval works as a reference of null heart-rate variability, so the bigger/smaller the dispersion of RR interval around this point of 'null' variability, defined in quantitative terms by SDNN, means that the heart-rate variability increases/decreases (Acharya, Joseph, Kannathal, Lim and Suri, 2006).  
In conditions of fatigue induction the heart-rate variability tends to decrease (Tran, Wijesuriya, Tarvainen, Karjalainen and Craig, 2009) and so SDNN will denote a decrease along acquisition.
6. This feature transmits information identical to SDNN, constituting an alternative for work around some constraints. In terms of evolution should be the same as SDNN (so when SDNN decreases the triangular index also decreases), but in this case the approach is based on a geometrical point of view, that is, the histogram of RR interval duration (during all acquisition or in a specific processing window) will be generated and then the modal bin is identified.  
The triangular index value is determined as the quotient between the total number of RR intervals covered by the processing window and the number of RR intervals inside the modal bin (Acharya et al., 2006).  
But the results of this analysis only have a good statistical significance when a great number of RR intervals (samples) are contained in the processing window, in some studies is recommended a minimum of 20 minutes of ECG data . (Task Force of The European Society of Cardiology and the North American Society of Pacing and Electrophysiology, 1996)  
Considering that the outlier samples remain out of modal bin, this mean that not take any effect in the triangular index determination, which makes this feature more robust than SDNN (Acharya et al., 2006).  
The more intervals are inside de modal bin then the smaller the heart-rate variability is and consequently by definition the lower the triangular index will be, this is a logical result because a bigger number of samples in the modal bin is equivalent to say that a great fraction of RR intervals is in a single class, that is, the variability in RR intervals is small.

7. Is one of the features extracted from the Poincaré plot (non-linear analysis) but before determining the index some concepts need to be presented. In a first stage a Poincaré plot is generated, this cartesian space is populated by two-dimensional samples  $S[i]$ . Each Poincaré sample  $S[i]$  has as coordinates the duration of the RR interval number  $i$  ( $RR[i]$ ) and the next ( $RR[i+1]$ ), that is, two consecutive RR intervals form a point on the Poincaré Plot.

There are two reference lines  $RR[i+1] = RR[i]$  e  $RR[i+1] = -RR[i] + 2 \text{ avg}(RR)$ , defining the geometrical reference of null heart-rate variability, so a sample localized near these lines constitute an event that contributes to a state of small heart-rate variability.

The bigger the dispersion of the samples around the reference lines the bigger the heart-rate variability will be (GoliDska, 2013).

To quantify the level of dispersion SD1 and SD2 are the two available indexes, corresponding to the standard-deviation of the Poincaré samples around each of the two reference lines.

SD1 and SD2 are estimators of short-term and long-term heart-rate variability, respectively (Acharya et al., 2006).

8. The LF acronym means Low-Frequency, so this is one of the three indexes taken from the frequency domain. Before determining his value is necessary to transpose the time series describing the RR interval duration along time (Tachogram) to the new domain.

In normal conditions the typical approach will be the use of Fourier Transform, but Tachogram has samples not evenly spaced which is problematic, so an adaptation is necessary and the Lomb-Scargle method is the chosen solution for the fatigue analysis system (Chou et al., 2011; VanderPlas, 2017).

The alternative approach is based on the interpolation of Tachogram to obtain a time series with a constant sampling frequency and after this step will be applied the conventional Fourier Transform methodology (Clifford and College, 2002).

The LF Power (Low-Frequency Band Power) corresponds to the energy inside the frequency band ranging between 0.04 and 0.15 Hz, establishing themselves as an indicator of sympathetic activity/modulation of heart-rate variability by the autonomous nervous system (Swapna, Ghista, Martis, Ang and Sree, 2012).

However, some cares are needed during the processing stage, namely the choice of the processing window size, considering that shorter time-windows can prevent the generation of a power spectrum with enough resolution for determination of the energy inside this frequency band. It is advised to have a processing window with duration of at least 2 minutes of data (Task Force of The European Society of Cardiology and the North American Society of Pacing and Electrophysiology, 1996).

There are evidences that the energy inside this frequency band tend to decrease with the fatigue emergence, like shown in a particular study on a sports context (Schmitt, Regnard, Auguin and Millet, 2016).

9. The extraction of this feature is similar to the LF Power, but focusing on the frequency band between 0.15 and 0.40 Hz (High-Frequency Band), relating this quantitative measure with vagal/parasympathetic modulation of heart-rate variability.

Like LF Power, the energy inside HF band also tends to decrease with the emergence of fatigue (Schmitt et al., 2016).

10. It is verified an increase of this indicator with fatigue and it is suspected that this behaviour is related with the decrease of the energy in the LF and HF bands, considering that the signal energy 'transits' to higher frequencies 'abandoning' the LF and HF bands, causing his decrease and 'populating' higher frequencies whose character may not be totally related with heart-rate variability.

## Bibliography

- Acharya, U. R., Joseph, K. P., Kannathal, N., Lim, C. M. and Suri, J. S. (2006). Heart rate variability: A review. *Medical and Biological Engineering and Computing*, 44(12), 1031 1051. <https://doi.org/10.1007/s11517-006-0119-0>
- Riou, O. and Vetterli, M. (1991). Wavelets and Signal Processing. *IEEE Signal Processing Magazine*, 8(4), 14 38. <https://doi.org/10.1109/79.91217>
- Schmitt, L., Regnard, J., Auguin, D. and Millet, G. P. (2016). Monitoring training and fatigue status with heart rate variability: case study in a swimming Olympic champion. *Journal of Fitness Research*, 5(3), 38 45. <https://doi.org/10.1089/tmj.2014.0052>
- Swapna, G., Ghista, D. N., Martis, R. J., Ang, A. P. C. and Sree, S. V. (2012). Ecg Signal Generation and Heart Rate Variability Signal Extraction: Signal Processing, Features Detection, and Their Correlation With Cardiac Diseases. *Journal of Mechanics in Medicine and Biology*, 12(4), 1 26. <https://doi.org/10.1142/S021951941240012X>
- Task Force of The European Society of Cardiology and the North American Society of Pacing and Electrophysiology. (1996). Heart Rate Variability Guidelines. *European Heart Journal*, 17, 354 381. <https://doi.org/10.1161/01.CIR.93.5.1043>
- Tran, Y., Wijesuriya, N., Tarvainen, M., Karjalainen, P. and Craig, A. (2009). The relationship between spectral changes in heart rate variability and fatigue. *Journal of Psychophysiology*, 23(3), 143 151. <https://doi.org/10.1027/0269-8803.23.3.143>
- VanderPlas, J. T. (2017). Understanding the Lomb-Scargle Periodogram. Retrieved from <http://arxiv.org/abs/1703.09824>
- Chou, C. C., Tseng, S. Y., Chua, E., Lee, Y. C., Fang, W. C. and Huang, H. C. (2011). Advanced ECG processor with HRV analysis for real-time portable health monitoring. *Digest of Technical Papers - IEEE International Conference on Consumer Electronics*, 172 175. <https://doi.org/10.1109/ICCE-Berlin.2011.6031850>
- Cifrek, M., Medved, V., Tonkovi, S. and Ostojic, S. (2009). Surface EMG based muscle fatigue evaluation in biomechanics. *Clinical Biomechanics*, 24(4), 327 340. <https://doi.org/10.1016/j.clinbiomech.2009.01.010>
- Clifford, G. D. and College, S. C. (2002). *Signal Processing Methods for Heart Rate Variability*.
- De Luca, C. J. (1984). Myoelectrical manifestations of localized muscular fatigue in humans. *Critical Reviews in Biomedical Engineering*, 11(4), 251 279. Retrieved from <http://www.ncbi.nlm.nih.gov/pubmed/6391814>
- GoliDska, A. K. (2013). Poincaré plots in analysis of selected biomedical signals. *Studies in Logic, Grammar and Rhetoric*, 35(48), 117 127. <https://doi.org/10.2478/slgr-2013-0031>
- Graham, R. B., Wachowiak, M. P. and Gurd, B. J. (2015). The assessment of muscular effort, fatigue, and physiological adaptation using EMG and wavelet analysis. *PLoS ONE*, 10(8). <https://doi.org/10.1371/journal.pone.0135069>
- Konrad, P. (2009). The ABC of EMG - A Practical Introduction to Kinesiological Electromyography. *Journal of the American College of Cardiology*. <https://doi.org/10.1016/j.jacc.2008.05.066>
- Otsu, N. (1979). A Threshold Selection Method from Gray-Level Histograms, 9(1), 62 66. <https://doi.org/10.1109/TSMC.1979.4310076>



## Publications and Other Initiatives

During the period of the dissertation work there were some initiatives that provided the dissemination of the project and of some steps that preceded the final result, contained in this document.

In an embryonic phase, we participated in the *Nova Biomedical Engineering Workshop* (NBEW), organized by the Department of Physics of the Faculty of Sciences and Technologies of the Nova University of Lisbon and destined to the exhibition of some of the work in the area of Biomedical Engineering.

Subsequently, after transposing the *offline* algorithm of heart-rate variability analysis to the *real-time* strand, we submitted a *Position Paper* that describe this process for disclosure at a conference.

The document, after some corrections, was accepted and allowed us to present the results achieved at the 11<sup>th</sup> *International Joint Conference on Biomedical Engineering Systems and Technologies* (BIOSTEC 2018).

Framed in the previous initiatives, this appendix contains the poster affixed during NBEW and the *Position Paper* published during the BIOSTEC Conference.

## Introduction

Sport reveals a growing preponderance in today's society, not only in professional but also recreational terms.

Technology can often be considered as a barrier for people to achieve a healthy lifestyle, but increasingly this conception is being refuted, revealing technology as an important ally for example in sport.

The monitoring systems of signals with a physiological origin have undergone an intense dissemination in the last decades, a tendency that also occurs in the sporting context.

Currently platforms such as *Garmin Connect™* or *Xert™* are quite powerful, providing to athletes and cyclists, in particular, an exhaustive analysis of multiple indexes related to the evolution of parameters such as heart rate or power output.

Despite the benefits of a physical activity, there are also problematic consequences, such as an increase in the probability of injury occurrence, with muscle fatigue in the background.

It is at this point where most of the existing systems fail, because their analysis and functioning is focused on the performance of the athlete and their progression, but ignore the quantification of fatigue, which may be extremely useful for injury prevention.

One exception is the *BSXinsight™* device that uses the concept of a lactic threshold for evaluating muscle fatigue.

The present work attempts to validate some of the fatigue indexes established in the scientific environment but that don't have an application in the daily life of the populations or in the commercial segment.

## Purposes of the Work

- Implementation of an algorithm for extraction of fatigue indexes in different signals of physiological origin;
- Identification/Classification of Fatigue State in real-time;
- Creation of a global fatigue index that combines information from different types of indexes.

## Fatigue Evaluation Methods

The literature about fatigue evaluation methods is very wide, and at this stage we emphasize the methods that use the ECG (Electrocardiographic) and EMG (Electromyographic) signals.

In the case of ECG the main parameter to be extracted corresponds to the heart rate variability, and some studies prove that the long-term variability tends to increase with fatigue. [1]

The objective perception of this fact will be attainable by indexes such as SD1 and SD2 of the Poincaré analysis, where each point in the Poincaré graph corresponds to the combination of two consecutive RR intervals duration.

$$SD1 = \frac{\sqrt{2}}{2} SD(x_n - x_{n+1}) \quad (1) \quad SD2 = \sqrt{2SD(x_n)^2 - \frac{1}{2}SD(x_n - x_{n+1})^2} \quad (2)$$

With  $x_n$  denoting the tachogram (evolution of RR intervals),  $x_n - x_{n+1}$  it's derivative and SD the standard deviation

The point dispersion in relation to the reference lines  $RR_{i+1} = RR_i$  and  $RR_{i+1} = -RR_i + 2 \text{ avg}(RR)$ , described by the SD1 and SD2 indexes, respectively, tends to increase, reflecting an increment in heart rate variability. [2] [3]

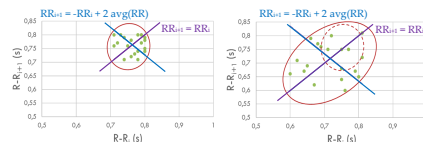


Figure 1 - Comparison between two hypothetical examples where cardiac variability increases when point dispersion is bigger

Concerning to the EMG signal, its relevance for the evaluation of fatigue lies essentially in the frequency domain, namely through the evolution of parameters such as the median frequency, that describes the trend of variation in the composition of the EMG signal.

Under fatigue conditions the median frequency tends to decrease, with the EMG signal being dominated by the low frequency components. [4]

$$\int_0^{f_{\text{median}}} P(f) df = \frac{1}{2} \int_0^{f_s} P(f) df \quad (3)$$

$P(f)$  denotes the power of elementary component with frequency  $f$ , at EMG spectrum and  $f_s$  the sampling frequency.

## Bibliography

- [1] J. Ryu and P. Kim, *Journal of Korean Living Environment System*, vol. 21, no. 6, pp. 897-903 (2014)
- [2] A. K. Golińska, *Studies in Logic, Grammar and Rhetoric*, vol. 35, no. 48, pp. 117-127 (2013)
- [3] U. R. Acharya, K. P. Joseph, N. Kannathal, C. M. Lim, and J. S. Suri, *Medical and Biological Engineering and Computing*, vol. 44, no. 12, pp. 1031-1051 (2006)
- [4] C. J. De Luca, *Critical reviews in biomedical engineering*, vol. 11, no. 4, pp. 251-279 (1984)

## Processing Methods

Data processing will take place in the time domain and also in the frequency domain, with the analysis of time series amplitude evolution, using estimators such as RMS.

Considering that it is intended to implement a real-time fatigue monitoring system, it means that even the frequency domain processing methods need to preserve part of the temporal information, using a system of sliding windows, as shown in Figure 2.

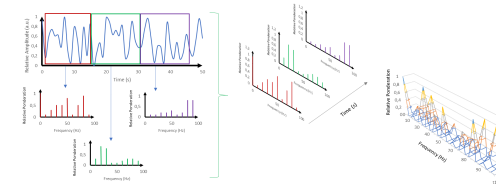


Figure 2 - Sliding Window System for temporal information preservation

## Primordial Results

Until now, the analysis performed was limited to the validation of the results denoted in previous studies, namely the decrease of the median frequency under fatigue conditions. The first results were promising (Figure 3).

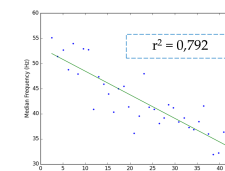


Figure 3 - Primordial results of median frequency evolution under fatigue conditions

## Conclusions/Expectations

Despite the interesting results, at this embryonic stage of the study, it is evident that the adjustment shown in Figure 3 does not always occur, so in the next phase of the project, other indexes will have to be analyzed and combined, permitting the creation of a more robust global fatigue index.

# Real-Time Approach to HRV Analysis

Guilherme Ramos<sup>1,2</sup>, Miquel Alfaras<sup>1</sup> and Hugo Gamboa<sup>2,3</sup>

<sup>1</sup>Plux Wireless Biosignals S.A, Avenida 5 Outubro 70, 1050-59, Lisboa, Portugal

<sup>2</sup>Department of Physics, Faculdade de Ciências e Tecnologia da Universidade Nova de Lisboa, Monte da Caparica, 2892-516, Caparica, Portugal

<sup>3</sup>Laboratório de Instrumentação, Engenharia Biomédica e Física da Radiação (LIBPhys-UNL), Faculdade de Ciências e Tecnologia da Universidade Nova de Lisboa, Monte da Caparica, 2892-516, Caparica, Portugal

**Keywords:** HRV Analysis, Real-Time Processing, Sliding Window, Biomedical Signal Processing.

**Abstract:** In this paper, we present the assessment of heart rate variability (HRV) applied to real-time processing of electrocardiographic (ECG) signals. A general approach for R-peak detection is described based on the computational implementation of Pan and Tompkins algorithm, used in the *offline* version. Besides feature extraction (from temporal and frequency domain), the paper presents the development steps taken towards *online* real-time biosignal processing. The functional basis of the *online* approach consists in the implementation of a simple adaptive double-threshold algorithm for peak detection and a sliding window mechanism along acquisition that provides a dynamically generated tachogram for the features to be successively extracted, highlighting the new application opportunities for continuous observation of HRV parameters.

## 1 INTRODUCTION AND MOTIVATION

Technology has become, specially in recent years, an essential part of life in western societies. With the aim of answering individual and collective needs, digital technologies play nowadays an indisputable role.

Traditionally, humankind has tried to understand human physiology in order to work towards the appropriate corrections when medical conditions arise. Experts are trained for years to access pathologies and prescribe treatment when needed.

In recent times, though, the way society approaches medical conditions has completely changed. While corrective medical attention has always been at the base of the medical practice, preventive healthcare and technology applications boast nowadays a huge interest worldwide.

The fast developments in biosensing and the unstoppable increase of data availability have fostered research in biomedical engineering, which is currently counting on a wide range of tools that enable the acquisition and processing of information from the human body.

In this position paper, we describe a module for a signal processing platform, *OpenSignals*. In line with our data-driven society needs and the ease to access

processing capabilities through mobile phone devices, we present *OpenSignals* extension towards a real-time Heart Rate Variability (HRV) processing approach.

*OpenSignals* software platform allows the study and development of data post-processing tools. This platform is integrated with signal acquisition systems from Plux, such as *Biosignalsplux* (Plux, 2012; Chorão et al., 2012) and *BITalino* (Plux, 2013; Alves et al., 2013), which enable various sensor combinations and easy acquisition of biosignals, like Electrocardiogram (ECG) and Electromyogram (EMG).

The assessment of HRV through ECG signals is at the core of Plux goals, both for the potential impact and for cost reduction in early diagnose of heart conditions. Having a reliable and working HRV platform has allowed the exploration of changes that enable real-time HRV assessment.

While *offline* analyses have proved to be an efficient tool to assess HRV-related conditions, we believe that our approach could constitute one of the first steps towards a better exploitation of the computational resources and device capabilities present nowadays in our society.

Moreover, the real-time monitoring of HRV may play a crucial role in disciplines such as high-performance sports that could benefit from real-time detection of threatening heart conditions.



## 2 MATERIALS AND METHODS

In this section the ECG data signals, features extracted and processing steps are described.

*Biosignalsplux* platform is used as the device for easy ECG acquisitions. This device allows a high sampling rate in signal acquisition, which is fixed to  $F_s = 1000$  Hz in the case of our study.

The user can specify the processing filters applied to the ECG signals. The predefined filter is basically a band-pass filter ( $F_{low} = 0.5$  Hz,  $F_{high} = 40.0$  Hz). This procedure allows for the removal of the baseline and the avoidance of high frequency noise and artefacts.

Electrocardiographic and electromyographic signals share frequency bands. EMG signals can vary from  $F = 5$  Hz to  $F = 400$  Hz. The applied filters help in reducing the cross-talk caused by undesired muscular activity that could appear during ECG acquisition.

The voltage signals are segmented and annotated to the P, Q, R, S, T points widely used in electrocardiography (see fig.1). These points correspond to different stages of atrial/ventricular depolarisation/repolarisation and are used to identify waves and intervals that are relevant for ECG analysis.

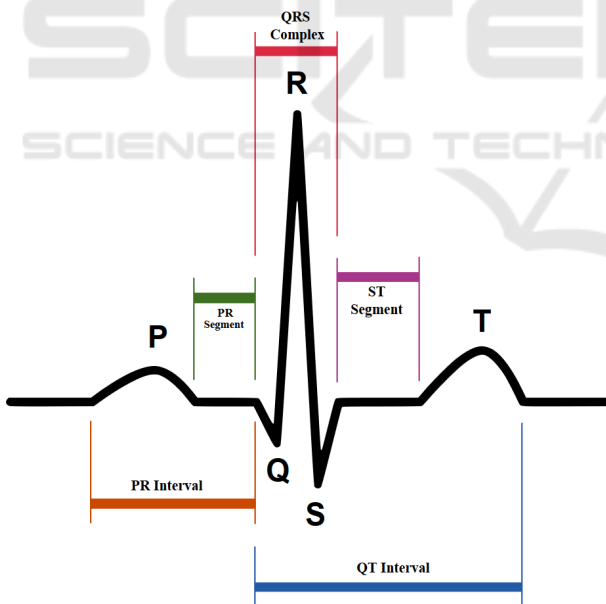


Figure 1: ECG PQRST points.

HRV assessment has traditionally relied on the analysis of the tachogram, giving potential information captured by the time series. The tachogram is the temporal series of RR heartbeat intervals, which contains the most relevant structural information of the HRV.

The first step for HRV assessment consists in R-peak detection. When using the *offline* analysis, our

algorithm is based on the widely used QRS complex detection algorithm (Pan and Tompkins, 1985).

Once the R peaks are located, the tachogram is built in order to proceed to feature extraction. An ectopic heartbeat removal criterion can also be specified. By using two limit values, e.g.  $R_{min} = 0.4$  s and  $R_{max} = 2.0$  s, heartbeats from abnormal origin can be easily discarded.

Our implementation contains the following features:

### Statistical Analysis

**minRR (s).** Minimum RR interval duration.

**maxRR (s).** Maximum RR interval duration.

**avgRR (s).** Average RR interval duration.

**SDNN (s).** Standard Deviation of RR intervals. Null variance would indicate identical consecutive RR intervals (Acharya et al., 2006).

**rmsSD (s).** Root mean square of the successive *tachDiff* differences, an approximation to the dispersion on the tachogram's derivative.

$$rmsSD = \sqrt{\frac{\sum_{i=0}^K tachDiff^2[i]}{K}} \quad (1)$$

$K$  represents the number of points in the differential tachogram.

**NN20 (# intervals).** Number of RR intervals between non-ectopic beats where the difference of duration with respect to the previous RR interval is greater than 20 ms.

**pNN20 (dimensionless).** Ratio between *NN20* and the total number of RR intervals on the processing window. This represents the fraction of RR intervals that verifies the condition of difference of duration greater than 20 ms with respect to the adjacent RR interval.

**NN50 (# intervals) and pNN50 (dimensionless).** Number of RR intervals and ratio between non-ectopic beats where the difference of duration with respect to the previous RR interval is greater than 50 ms.

**avg IHR (bpm).** Average of the instantaneous heart rate (IHR). Instantaneous heart rates are computed via the inverse of every single Tachogram interval, which indicates the number of beats per minute (bpm).

**STD IHR (bpm).** Standard Deviation of the instantaneous heart rate.

### Poincaré Analysis

**SD1 (s) e SD2 (s)** ellipse sub-axes estimators: Non-linear features derived from the Poincaré plot. In the Poincaré plot, each point is formed by the coordinates ( $RR_i$  and  $RR_{i+1}$ ). In other words, the nonlinear trajectory is represented by consecutive RR intervals (two consecutive RR values constitute a point in the plot, fig.2).



$SD1$  and  $SD2$  are estimators for the axes' size of the ellipse that covers all Poincaré samples, directly linked to long-term HRV ( $SD2$ ) and short-term HRV ( $SD1$ ).

A greater value of these indices indicates a wider heart rate variability. These are measures of the standard deviation with respect to reference lines  $RR_{i+1} = RR_i$  and  $RR_{i+1} = -RR_i + 2avgRR$  (Golińska, 2013):

$$SD1 = \sqrt{\frac{SDSD^2}{2}} \quad (2)$$

$$SD2 = \sqrt{2 \times SDNN^2 - SD1^2} \quad (3)$$

where  $SDSD$  is the standard deviation of *tachDiff* (equivalent to *rmsSD*) and  $SDNN$  is the standard deviation of the tachogram, as defined previously.

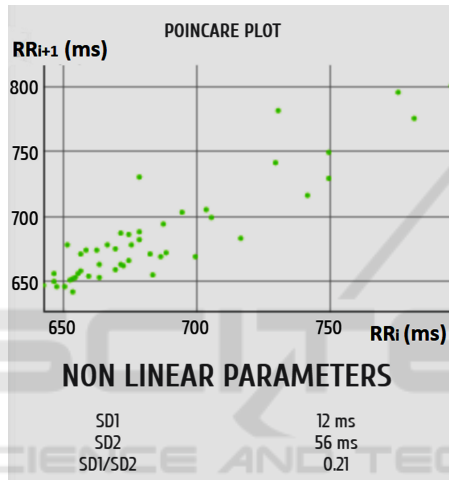


Figure 2: HRV Poincaré plot.

### Frequency Analysis

To take HRV signals to the frequency domain some care is needed, because we deal with time series with irregular sampling period (i.e. the time between two heart rate samples is dependent of the RR interval duration). Under these conditions it is strongly recommended to use the Lomb-Scargle Method, which generates a “Fourier-like power spectrum estimator” (VanderPlas, 2017), based on *Least Squares Method* where for each elementary frequency component (independent variable of Periodogram) the sinusoid that best fits the data is determined, based on *chi-squared* testing (Chou et al., 2011). To achieve an efficient analysis with Lomb-Scargle Methodology, Python *astropy*'s library is used. The frequency scales are automatically defined by the *autopower* property, based on a heuristic approach.

**Power of Components in HRV Informative Bands.** They provide access to information related to the effect of sympathetic and parasympathetic components in the heart rate variability control, which are difficult

to analyse in the temporal domain. The elementary components inside the Low-Frequency (LF - 0.04 to 0.15 Hz) and High-Frequency (HF - 0.15 to 0.40 Hz) bands refer to autonomic segments of heart rate variability. In bands containing Ultra-Low-Frequencies (ULF - 0 to 0.003 Hz) and Very-Low-Frequencies (VLF - 0.003 to 0.04 Hz) data is in most cases inconclusive and is frequently associated with harmonic and incoherent signal components.

The information of *HF Band Power* is correlated with  $SDNN$ ,  $rmsSD$  and  $SDSD$  features. It is expected that when the heart rate variability increases the power value of this component is also increased (Task Force of The European Society of Cardiology and The North American Society of Pacing and Electrophysiology, 1996).

The information that  $SDNN$  feature provides is equivalent to the *Total Power* of the Frequency Spectrum and  $rmsSD$  is linked with the power of HF band of tachogram spectrum.

This correspondence has the advantage of presenting a reduced computational cost with respect to frequency domain analysis methods.

One disadvantage, though, is related to the fact that  $SDNN$  values depend on the window size. Therefore, the comparison between trials is only possible when similar acquisition conditions are guaranteed.

## 2.1 OpenSignals Platform Plugins

*OpenSignals* is a software compatible with multiple platforms and operating systems. It provides a solution to the fast-growing research community using Plux devices. Its design targets the representation of the biosignals captured and transmitted through *Bluetooth* in real-time allowing the subsequent storage on the computer. Devices are easily paired to the software via the MAC address.

*OpenSignals* can be described as a framework that uses the web-based architecture (Pimentel et al., 2015), based on three programming languages (*HTML*, *JavaScript* and *Python*). With this triad it is possible to “combine high-performance data management and computational capacity with an intuitive and user-friendly interface” (Plux, 2016).

The modular structure of *OpenSignals* allows the simple implementation of new functionalities through *plugins* or *add-ons*. The developer needs to generate the interface structure in *HTML*, set the events triggered by the interaction between the user and interface objects with *JavaScript* programming, and finally construct the *Python* processing algorithm.

The development logic is applied in the extension of the *HRV plugin* towards real-time implementation.

### 3 ONLINE HRV MONITORING IMPLEMENTATION

The implementation of *Online HRV plugin* comes from the native *offline* processing steps described below.

#### 3.1 Offline Processing Steps

The majority of the HRV features can be directly implemented into the *online* version. However, some key features of the *offline* processing algorithm were not implemented in the first version of the *Online HRV plugin*, namely the *Pan-Tompkins R-Peak Detection Method*. This algorithm proves to be robust and efficient, with correct detection rates higher than 90% (Pan and Tompkins, 1985). For simplicity, an R-peak detection algorithm has been developed using a two-threshold system that yields an acceptable level of detection with simplicity of implementation.

A description of the *Offline HRV plugin* processing steps, upon which future developments are based, is provided below:

In a first phase, the system reads the file containing the acquisition. The loaded array enters the *Pan-Tompkins R-peak detection function*.

Once the peaks are detected, the ECG signal proceeds to the steps of filtering, differentiation, integration and erroneous R-peak exclusion.

In the filtering step the signal is applied to the input of a second order *Butterworth* band-pass filter (bandwidth  $F_{BW} = [5, 15]$  Hz). The differentiation of the filtered signal is a simple sequential subtraction of consecutive inputs. Differentiated values are squared to avoid negative elements in the series (rectified differences).

At this point, the integration of the signal takes place using a sliding window of dimension  $N = 0.080 \times \text{sampleFrequency}$  (s) and adding up the values. This value is chosen in order to approximate the integration window size to the maximum duration (in physiological terms) that QRS complex can present, e.g.  $t \sim 0.080$ s, half of the suggested value in the Pan and Tompkins work.

As an alternative to an iterative sliding window approach, a cumulative signal is determined by simple iterations:

$$s_{cum}[i] = \sum_{j=0}^i s_{rect}[j] \quad (4)$$

Subsequently, an array with the dimension of the rectified signal ( $M$ ) is filled with the integrated values.

For  $i > N$ :

$$\begin{aligned} s_{int}[i] &= s_{cum}[i] - s_{cum}[i - N] \\ \Leftrightarrow s_{int}[i] &= \sum_{j=0}^i s_{rect}[j] - \sum_{j=0}^{i-N} s_{rect}[j] \end{aligned} \quad (5)$$

At the end of the previous steps, the initialisation of the R-peak detection threshold occurs, according to the characteristics of the integrated signal, selecting a segment of 1 second of  $s_{int}$  (typically this duration is sufficient to guarantee that the segment contains a R peak).

The threshold is initialised using the maximum value of the integrated signal ( $s_{int}^{peak}$ ) in this segment and a noise peak ( $n_{peak}$ ) is set to a null value, using the reference formula:

$$\text{threshold} = n_{peak} + 0.25(s_{int}^{peak} - n_{peak}) \quad (6)$$

Once the initialisation phase of the thresholds is completed, the integrated signal scan is triggered with the detection of all possible peaks (array *PossiblePeaks*). A peak (maximum) is placed at any point  $s_{int}[i]$  where  $s_{int}[i - 1] < s_{int}[i]$  and  $s_{int}[i] > s_{int}[i + 1]$ . In this scan, a maximum is considered a candidate to be a R peak if its amplitude is higher than the active candidate peak (*ActCandPeak*).

*ActCandPeak* is updated whenever a maximum with higher amplitude is detected. When a value found in *PossiblePeaks* is separated from *ActCandPeak* by at least 200 ms, the present peak will be stored in the array containing the probable R peaks (*ProbPeaks*), becoming the new *ActCandPeak*.

The procedure takes place until the end of the list of *PossiblePeaks* is reached. Finally, peaks stored in *ProbPeaks* are compared against the threshold in order to be included into the definitive list of R peaks (*RpeaksList*).

For each peak in *ProbPeaks* where this criterion is true the noise peak  $n_{peak}$  update is triggered, changing the threshold value accordingly (adaptive logic of algorithm).

The noise peak is determined with the expression  $n_{peak} = 0.125 \text{Voltage}_{peak} + 0.875 n_{peak}$ , using the digital value/voltage associated with the probable peak analysed and the old value of  $n_{peak}$ .

Having the definitive list of R peaks, the algorithm can proceed to the generation of the tachogram (RR intervals).

However, prior to this step, the tachogram must pass through ectopic beat removal process. This removal is performed based on the user's specifications. If the tachogram contains RR intervals lasting less/more time than the user-defined lower/greater threshold, they are excluded.

In addition to this, the user can also include an additional level of filtering using an average sliding window, that is, each sample of the tachogram is scanned and the mean value of the tachogram samples contained in the user-defined window is determined. If the sample of present iteration has a duration exceeding the defined interval  $[avgValue + x\% \times avgValue; avgValue - x\% \times avgValue]$  it is excluded from tachogram.

Finally, with the tachogram ready to be explored, the HRV extraction begins.

### 3.2 Online Processing

In this subsection, we present several algorithm modifications towards the real-time HRV assessment. One of our main concerns when thinking of HRV monitoring in real-time is the change of the physical activity regime of the subject of study (e.g. walking, supine resting, standing, etc.).

Along these lines, one of the key modifications consists in an adaptive threshold for R-peak detection.

As opposed to the *offline* study, a threshold is used and computed iteratively as the data is collected. In order to set the initial values, the first few seconds of the signal are taken and only used to compute the first thresholds to apply in R-peak detection before being discarded.

Consequently, a lag on the adaptation of the aforementioned threshold is always present. By taking five-seconds segments of the signal, the thresholds for heartbeat (R-peak) detection are adapted from iteration to iteration. At the acquisition of every segment, ECG signal maximum and minimum values ( $V_{max}, V_{min}$ ) are computed to update the thresholds.

The *triangular index*, a geometric feature of the tachogram, has also been included. This is described here:

#### Geometrical Analysis

**Triangular Index.** A geometrical feature (not subject to outliers) taken from the RR intervals histogram analysis. It is defined as the ratio between the total number of samples (RR intervals) in the histogram and the number of RR intervals on dominant bin. The size of each temporal bin needs to be  $t_s = 1/128s$  (Vanderlei et al., 2010).

$$tIndex = \frac{\#TotalRRIntervals}{\#RRIntervalinModalBin} \quad (7)$$

A greater triangular index indicates that a greater proportion of RR intervals is concentrated inside a single bin. Consequently, the heart rate variability is low. Following reference guidelines, we know that in order to obtain reliable results the time window

lengths of the ECG should be at least equal to 20 minutes (Task Force of The European Society of Cardiology and The North American Society of Pacing and Electrophysiology, 1996).

### 3.3 Online HRV Plugin Presentation Methods

Implementing existing *HRV Offline plugin* algorithms into the *Online* variant is not a straightforward procedure, since the user's access to understandable and reliable information in real-time must be taken into consideration.

In the *offline* version, regardless of acquisition duration, the user only has access to one value for each HRV index. This approach is not adequate in real-time analysis, since a value, even if updated periodically, is difficult to interpret when separately viewed.

Thus, the chosen methodology aims to provide the user with the possibility of monitoring the evolution of the different HRV indices throughout the acquisition, highlighting the trends and variations.

This dynamic approach is possible using a sliding window mechanism, as presented in fig. 5. For each window, a value is extracted for the multiple features in the segment of the ECG signal contained within its boundaries.

The windows should overlap, which becomes more practical for the user since the existence of common information between windows makes the index variation more gradual and, at the same time, allows the sampling rate of new values for the indices to be higher as compared to a non-overlapping sliding window.

The above specifications are important in a system/interface interactivity perspective. We emphasise the *online* algorithm characteristics to guarantee the rigour and the statistical or physical meaning of the extracted indices.

To ensure that the measurements are reliable, the sliding window size is the key factor. In the bibliographical research, it is noticed that feature extraction in the temporal domain uses windows that should contain a segment with at least 30 seconds of the ECG signal (Acharya et al., 2006), although longer duration windows provide increased statistical relevance, since more RR intervals are used.

However, it is necessary to understand that extremely large windows translate into a lower temporal resolution. Hence, a compromise must be reached between the statistical perspective and temporal uncertainty.

As for the features extracted from the frequency domain, the time window should have a minimum du-

ration of 2 minutes, enabling the computation of the power values of the VLF, LF and HF bands. Shorter windows translate into insufficient frequency resolutions to distinguish the elementary components of the spectrum in the different bands.

With a window of 2 minutes, however, information about the ULF band is lost, which denotes some importance in clinical terms. The user should increase the duration of the window if the extraction of information from this band is desired.

A simple presentation of the real-time HRV assessment *plugin* interface is provided in this section (*HTML* and *JavaScript* functionalities), from the user's point of view. The graphical interface is introduced in order to facilitate the access to the different functionalities of the platform.

In the case of HRV monitoring, parameter configuration for the algorithm is enabled through *OpenSignals*. One of the key parameters is the filter choice and configuration (high-pass, band-pass, cut-off frequencies, etc.) (see fig. 3).

Furthermore, time domain characteristics such as sliding window length and window overlapping can also be set.

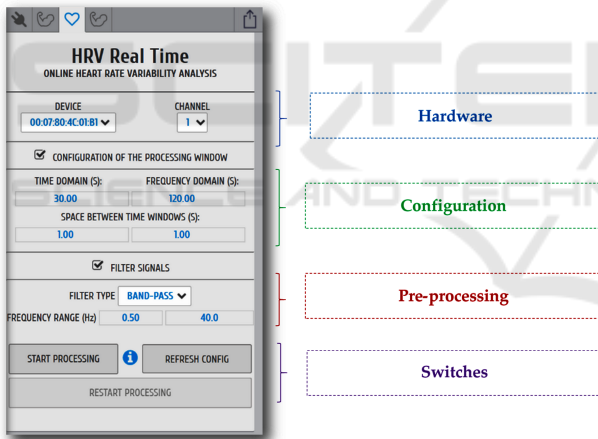


Figure 3: OpenSignals HRV configuration.

In order to start the processing of the signal, several samples are required. Hence, some warm-up time is necessary before presenting the first visualisation plots (fig. 4).

Right after the obtention of the first plots, the user can choose which are the features of interest for the HRV study. The real-time HRV analysis *plugin* is based on a sliding window approach. Every consecutive window is responsible for the computation of single values that make up the temporal series of features.

The sliding window concept is illustrated in fig. 5 example. Window duration values in the example are merely illustrative. When processing HRV data, the

window duration is always set to values greater than  $t = 30$ s.

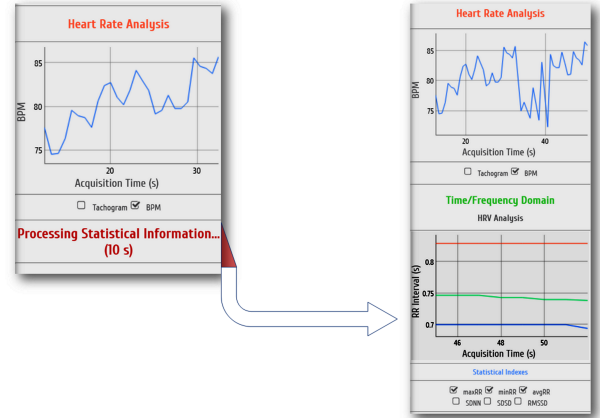


Figure 4: OpenSignals HRV warm-up.

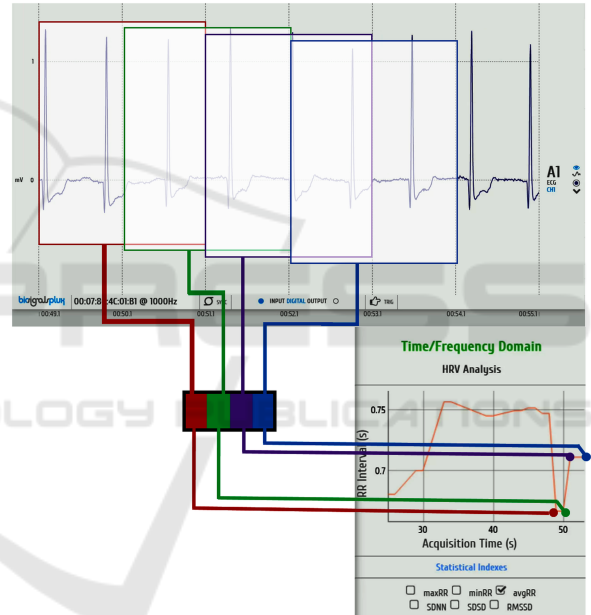


Figure 5: OpenSignals HRV sliding window.

The signal acquisition and analysis can be interrupted or reset at any time, changing the configuration when needed. The software allows the generation of report files that summarise the signal features of interest.

## 4 DISCUSSION

The *online* access to features allows to set further detection mechanisms and thresholding to detect predefined conditions directly during acquisition. Tracking of the features and their evolution is possible, as plots are built and shown dynamically through the interface.



Regarding features obtained in real-time, some remarks are needed. On the one hand, there is an important limitation on the window sizes. Frequency related features pose the question of the need for a minimal warm-up phase (so that spectral representation is relevant). Features such as nonlinear Poincaré measures can be remarkably affected when values below 5 minutes are used as window lengths. Further research is needed to support the idea that low values do not compromise nonlinear features. There is no reason to think that feasibility of the online procedure is further compromised once these requirements are met.

On the other hand, our preliminary tests on acquired data show relevant differences between the tachograms generated by the two methods (*online/offline*). This is solely a consequence of working with a simpler peak detection algorithm. Our priority for further development is, hence, the implementation of the robust R-peak detection algorithm (J. Pan and W. Tompkins) providing not only a more precise detection but also fewer false R peaks.

In order to guarantee that the *online* approach provides meaningful information, a validation step against *offline* treatment is needed. Once peak detection is updated, the procedure consists in the application of both processing methods (*online* and *offline*) to the same collected data samples. Each of the two methods provides a set of peaks and features that are to be compared. Taking *offline* peak detection as a reference, comparison of the two algorithms is achieved by computing the amount of wrongly placed peaks. Once tachograms are generated, an aligning process takes place by the use of standard cross-correlation procedures. Tools such as Bland-Altman plots, which are frequently used in new ECG acquisition approaches against well-established reference procedures, provide statistical insight to analyse our implementation.

Into this regard, frequencies ( $F_s \geq 1000$  Hz) guarantee the best peak detection. The need for validation with sufficiently large ECG databases has already been identified. Widely used Physionet databases with healthy ECG recordings such as the MIT-BIH Normal Sinus Rhythm (Goldberger et al., 2000) are possible candidates for this task. In accordance with frequency requirements, interpolation preprocessing of signals may be necessary.

In the first line of implementation, measures of cardiac variability studied were essentially linear, with the exception of Poincaré Analysis. This is done considering that some non-linear parameters could be incompatible with a real-time analysis methodology due to their greater computational complexity.

Further developments could include the exploration of more complex and robust parameters, namely the determination of the approximate entropy of the HRV signal, provided it can be realised in an *online* system. This would allow to identify objectively which is the degree of complexity of the tachogram through a quantitative result (higher values denote a greater complexity and irregularity of the time series, that is, a greater cardiac variability). The interest of this measure lies on the capability to overcome the limitations of the linear measurements. Considering that the heart rate modulation is the result of the interaction of several physiological systems and mechanisms, there is an intrinsic underlying non-linear behaviour, only accessible by these means (Singh and Kaur, 2016).

## 5 CONCLUSION

HRV continues to trigger the interest of the scientific community nowadays. This is particularly relevant in the context of sports research, considering the central role of the cardiovascular system in athlete performance and establishing cardiac variability as an indicator of the adaptive capabilities of the organism.

Recent studies, such as (Paliwal et al., 2016; Schmitt et al., 2015; Schmitt et al., 2016), illustrate the potential of HRV assessment. Real-time analysis research, e.g. (Lv et al., 2015) and (Tsunoda et al., 2016), present sliding window based approaches more in line with our contribution. The works of Lv and Tsunoda are two examples of the informative potential of the HRV, leading to the identification of cardiac pathologies and the measurement of the cognitive efficiency.

The processing functionalities described in our work provide a quick and adjustable real-time analysis of HRV. This allows the information contained in the acquired signals to become meaningful. Our test implementation shows that feedback during the acquisition can be achieved with real-time processing, offering additional information that complements HRV monitoring towards a prognosis focused view.

The *HRV online plugin* is an initial approach on translating information processed by an *offline plugin* into real-time logic. Despite the limitations arisen throughout our study and the further developments needed, the structure of the presented approach is already well established, namely the system of user-defined sliding windows.

Due to the fact that this is an ongoing research, many future modifications are envisioned, as discussed in the previous section. A following direc-

tion could be the application of the same development guidelines to other types of signals, such as the implementation of the EMG *plugin* for real-time processing. As discussed before, this opens a wide range of application development in areas like high-performance sports and the detection of threatening heart conditions.

## ACKNOWLEDGEMENTS

The authors acknowledge the support received from ITN AffecTech under the Marie Skłodowska Curie Actions (ERC H2020 Project ID: 722022).

## REFERENCES

- Acharya, U. R., Joseph, K. P., Kannathal, N., Lim, C. M., and Suri, J. S. (2006). Heart rate variability: a review. *Medical & Biological Engineering & Computing*, 44(12):1031–1051.
- Alves, A. P., Silva, H., Lourenço, A., and Fred, A. (2013). BITalino: A biosignal acquisition system based on the arduino. In *Proceedings of the International Conference on Biomedical Electronics and Devices*. SciTePress - Science and Technology Publications.
- Chorão, R., Sousa, J., Araújo, T., and Gamboa, H. (2012). A new tool for the analysis of heart rate variability of long duration records. In *Proceedings of the International Conference on Signal Processing and Multimedia Applications and Wireless Information Networks and Systems*. SciTePress - Science and Technology Publications.
- Chou, C. C., Tseng, S. Y., Chua, E., Lee, Y. C., Fang, W. C., and Huang, H. C. (2011). Advanced ECG processor with HRV analysis for real-time portable health monitoring. *Digest of Technical Papers - IEEE International Conference on Consumer Electronics*, pages 172–175.
- Goldberger, A. L., Amaral, L. A. N., Glass, L., Hausdorff, J. M., Ivanov, P. C., Mark, R. G., Mietus, J. E., Moody, G. B., Peng, C.-K., and Stanley, H. E. (2000). PhysioBank, PhysioToolkit, and PhysioNet : Components of a New Research Resource for Complex Physiologic Signals. *Circulation*, 101(23):e215–e220.
- Golińska, A. K. (2013). Poincaré plots in analysis of selected biomedical signals. *Studies in Logic, Grammar and Rhetoric*, 35(1).
- Ly, T., Ko, M., Stark, B., and Chen, Y. (2015). An On-line Heart Rate Variability Analysis Method Based on Sliding Window Hurst Series. *Journal of Fiber Bioengineering and Informatics*, 8(2):391–400.
- Paliwal, S., Lakshmi, C. V., and Patvardhan, C. (2016). Real time heart rate detection and heart rate variability calculation. In *2016 IEEE Region 10 Humanitarian Technology Conference (R10-HTC)*, pages 1–4. IEEE.
- Pan, J. and Tompkins, W. J. (1985). A real-time QRS detection algorithm. *IEEE Transactions on Biomedical Engineering*, BME-32(3):230–236.
- Pimentel, A., Gomes, R., Olstad, B. H., and Gamboa, H. (2015). A new tool for the automatic detection of muscular voluntary contractions in the analysis of electromyographic signals. *Interacting with Computers*, 27(5):492–499.
- Plux (2012). Biosignalsplux. <http://biosignalsplux.com/en/>.
- Plux (2013). Bitalino. <http://www.bitalino.com/en/>.
- Plux (2016). Opensignals datasheet. [http://bitalino.com/datasheets/OpenSignals\\_Datasheet.pdf](http://bitalino.com/datasheets/OpenSignals_Datasheet.pdf).
- Schmitt, L., Regnard, J., Auguin, D., and Millet, G. P. (2016). Monitoring training and fatigue status with heart rate variability: case study in a swimming Olympic champion. *Journal of Fitness Research*, 5(3):38–45.
- Schmitt, L., Regnard, J., Parmentier, A. L., Mauny, F., Mourot, L., Coulmy, N., and Millet, G. P. (2015). Typology of Fatigue by Heart Rate Variability Analysis in Elite Nordic-skiers. *International Journal of Sports Medicine*, 36(12):999–1007.
- Singh, A. and Kaur, J. (2016). Approximate Entropy (ApEn) based Heart Rate Variability Analysis. *Indian Journal of Science and Technology ISSN*, 9(947):974–6846.
- Task Force of The European Society of Cardiology and The North American Society of Pacing and Electrophysiology (1996). Heart rate variability : Standards of measurement, physiological interpretation, and clinical use. *Circulation*, 93(5):1043–1065.
- Tsunoda, K., Chiba, A., Chigira, H., Yoshida, K., Watanabe, T., and Mizuno, O. (2016). Online Estimation of a Cognitive Performance using Heart Rate Variability. *IEEE 38th Annual International Conference of the Engineering in Medicine and Biology Society (EMBC), 2016*, pages 761–765.
- Vanderlei, L. C. M., Pastre, C. M., Júnior, I. F. F., and de Godoy, M. F. (2010). Índices geométricos de variabilidade da frequência cardíaca em crianças obesas e eutróficas. *Arquivos Brasileiros de Cardiologia*, 95(1):35–40.
- VanderPlas, J. T. (2017). Understanding the Lomb-Scargle Periodogram.

